APPENDIX DATA TABLES FROM

EXPERIMENTAL TECHNIQUES FOR LOW-TEMPERATURE MEASUREMENTS:

Cryostat Design, Material Properties, and Superconductor Critical-Current Testing

JACK W. EKIN
National Institute of Standards and Technology
Boulder, Colorado

Published by Oxford University Press
First Printing 2006, Second Printing 2007, Third Printing 2007, Fourth Printing 2011

Appendix Table of Contents

Data Handbook of Material Properties and Cryostat Design

Each section is keyed to the chapter of the corresponding number.
Use “Control F” to rapidly find material

PREFACE

Der Teufel liegt im Detail

When I started low-temperature experimental work in graduate school and wanted to know "how to do it," I was struck by the abbreviated "experimental detail section" of most publications that simply stated the sample was mounted in the test apparatus, leads were attached, and the measurement made. But try to "simply" do that. The details are everything. Somehow the vital bits of experimental know-how do not get into print, the specifics of how to do it yourself. This book starts to answer some of the detailed questions about the design and construction of cryogenic probes in general, and superconductor measurements in particular. Simply put, these are the things I wish I had been told when I began.

This text is not about how to perform the vast array of cryogenic measurements; that is an extensive topic covered in many specialized references. Rather, it is about *design* techniques *common* to most measurement cryostats; the appendixes provide materials-property data for carrying out that design.

The mantra for this book is that it be *useful*. Topics include, for example, thermal techniques for designing a cryogenic apparatus that works (instead of one whose temperature is impossible to control), selecting appropriate materials (that do not thermally contract and rip the rig apart, or embrittle and snap), making high-quality electrical contacts to a superconductor (that avoid thermal runaway), and making a critical-current measurement that is believable (and does not vaporize your sample).

No one book can do it all; to really learn, we have to get into the lab and try it out. A wise man once said that the only way to become an expert is to make all the mistakes; it is my hope that this book will shorten that learning curve. In this spirit, I occasionally share a few of my own mistakes, because I think a lot can be learned from what does *not* work.

Audience: The main text is written for specialists, but it also includes introductory material. Thus, it would be useful for a wide range of experimentalists —graduate students, industry measurement engineers, materials scientists, and experienced researchers. In short, the book is intended for anyone interested in techniques for designing and operating effective low-temperature (1 K to 300 K) measurement systems, with special emphasis on superconductor critical-current measurements.

Data-handbook: The extensive appendix is a data handbook for cryostat design and measurements. It was written for specialists in the field of cryogenic measurements who want to save time by having much of the information for designing a new measurement probe collected in one place. These tables have been compiled from information supplied by colleagues and from over fifty years of literature. Appendix contents are listed on the inside back cover and include:

- Electrical, thermal, magnetic, thermoelectric, expansion, specific heat, mechanical, and vacuum properties of cryostat materials

- Data on cryogenic liquids
- Thermometer properties and standard calibration tables
- Properties of construction parts and materials: pipes, tubing, bolts, wire, brazing compounds, solders, fluxes, and sticky stuff
- Suppliers of hard-to-find parts and materials

Up front, I want to emphasize that this is not a review of the literature. It is a compendium of information that I have freely edited and reduced to the bare bones. On most subjects, I have also taken the license to express my opinion of what I like, along with the ideas of trusted associates. When I start learning a new area, I do not want to know all the possibilities in great detail; rather, I would like a road map based on the subjective thoughts of someone who has been there, so I can get started. On the other hand, I do want complete, easy-to-find reference tables and figures so I can return to other possibilities after I have had some experience. The book has been written with this approach in mind. So, for example, a comprehensive table of cryogenic thermometer properties is given in Appendix A5.2, but in the main text (Chapter 5) I recommend which thermometer I would typically use in practical situations. This represents only my opinion, and no doubt others may have different ideas as to what is best. But at least it is a place to start. And the other possible choices are there, tabulated in the appendix for later reference.

Cryogenic measurements are basically a matter of: (1) designing and building a measurement apparatus, (2) mounting samples, and (3) making measurements and analyzing the data. The three main parts to this book are organized along these simple guidelines.

I hope this step-by-step integrated approach, the examples, and the collection of appendix data on technical materials will take some of the devil out of the details.

J.W.E.
Sydney, Australia
Boulder, Colorado

DEDICATION

For my dear family: Sharon, Lindy, and Lisa;

and in memory of my close colleague and friend, Steve Bray.

About the author:

Jack Ekin is a research physicist at the National Institute of Standards and Technology in Boulder, Colorado, where his contributions have spanned a wide range of topics in low-temperature physics, including studies of fundamental conduction processes in normal metals, electro-mechanical properties of both high- and low-T_c superconductors, and interface conduction in thin films and nanostructures. His discoveries include the first quantitative understanding of Umklapp processes in normal metals, the formulation of the strain and unified scaling laws used to engineer superconducting magnets, the analytic treatment of current-transfer effects in multifilamentary superconductors, and the offset criterion for defining critical current. His early work with high-T_c superconductors led to the first four patents for making practical electrical contacts to these oxide materials. At present, he is engaged in extensive collaborations to measure and understand the physics of strain effects in high-T_c superconductors and advanced conductor designs.

After completing a B.S. degree at the University of Michigan, Dr. Ekin conducted his early graduate work in physics at the University of Heidelberg as a Fulbright Scholar, and received M.S. and Ph.D. degrees from Cornell University. Currently, he holds an appointment as a Senior Research Scientist at the University of Colorado. Outside of his research interests, he serves as a professional fine-art photographer collaborating with numerous open-space organizations. He is a Fellow of the American Physical Society and a member of the Institute of Electrical and Electronics Engineers. He has published over 160 cryogenic research articles, textbook chapters, and patents, and has lectured and consulted internationally in the field of low-temperature measurements.

DISCLAIMER

Trade names, products, and companies named here are cited only in the interest of scientific description, and do not constitute or imply endorsement by NIST or by the U. S. government. Other products may be found to serve just as well.

CONTACT INFORMATION

Enlarged figures, table updates, and additional information are available at www.ResearchMeasurements.com Comments, suggestions, or consultation enquiries can be sent to Dr. Jack Ekin at JackEkin@ResearchMeasurements.com.

EXCERPT FROM INTRODUCTION: ORGANIZATION OF BOOK

1. INTRODUCTION TO MEASUREMENT CRYOSTATS AND COOLING METHODS

Everything should be made as simple as possible, but not simpler.
–ALBERT EINSTEIN

1.1 Introduction

No single multitask measurement apparatus exists that is adequate for many different types of measurements over a wide temperature range. Once, I tried to design one—it turned into a "camel" (a camel has been defined as a "horse put together by a committee"). Measurement cryostats can range anywhere from a simple stainless-steel tube (or even a wooden stick) for dipping a sample in liquid helium, to complex systems with multiple vacuum jackets, internal variable temperature control, and radiation windows. In general, the *simpler* the cryostat to do the job, the better; however, always keep in mind that sometimes a little extra complexity makes a cryostat more flexible for a wider range of measurements.

The design and construction process for measurement apparatus is unlike that used for commercial manufacturing. It would probably make most good production engineers shake their heads in disbelief. Measurement requirements change all the time and so the rigs, which evolve, are usually one-of-a-kind affairs. There just is not enough time or return on investment to perform a full-fledged production-line engineering design. So, a lot of it ends up being "seat-of-the-pants" design. In the true experimental spirit, we sometimes have to make an educated guess and simply try it out. Usually a lot of designs will work, and often it just does not matter which you use. But it is essential to do *some* design, especially heat-transfer calculations. "…as simple as possible, but not simpler." The process is a compromise. (Generally, we physicists need to do more engineering than we usually do. We waste too much time fixing stuff that could have been designed better in the first place.)

Also, there is no substitute for selecting construction materials appropriate to the task. Once a rig is build, it is usually an onerous task to replace the main structural supports with a material having a lower susceptibility, better strength, or different thermal contraction coefficient. So, some up-front thinking about material properties can preclude a lot of problems down the road. The text includes an extensive appendix of tabulated heat-transfer data, materials-selection data, and construction information needed for cryostat design. I've also made

some effort to supply the *reference sources* for each material's data, so you can go back to the sources for more information.

This book is about the design process and construction techniques that are *common* to most measurement apparatus, not an exhaustive handbook of highly specialized cryostat designs. That we learn mostly from others in our field of specialization and their instrumentation literature. The emphasis is on those aspects of cryostat design and construction that are nearly universal—the challenge of cooling samples and accurately controlling their temperature throughout the cryogenic range under a wide variety of current, magnetic-field, and mechanical conditions. Additional reading on related subjects is given in the *Further-reading* section at the end of each chapter.

1.1.1 Organization of the book

Contents of this book proceed from *general to specific.* The first six chapters (Part I) present experimental techniques that apply generally to *cryostat design* and *materials selection.* The next two chapters (Part II) focus on mounting and making electrical connections to samples for *transport* measurements. The last two chapters (Part III) narrow the focus still further and apply the information in the early chapters to one specific transport measurement, *critical current,* perhaps the most widely measured property of superconductors.

Throughout this book, concepts are illustrated with figures directly in the chapters, backed up by detailed tables of data in the *appendix.* (The data tables are collected in the appendix for easy look-up later). Appendixes 1 through 10 parallel Chapters 1 through 10 and represent the information I have always wanted assembled in one place when designing a new test rig. In some sense, the appendixes represent a *formalized lab wall;* that is, an assemblage of material that in many cases I have literally taken off the walls of our laboratories, since they were hanging there for good reason (usually).

Part I: Cryostat Design and Materials Selection

Chapter 1 is mainly an *example* chapter, presented at the beginning so you can picture where we are headed. Here, we give an overview of useful types of measurement cryostats for the temperature range from 300 K to about 1 K. We also introduce cooling options and the properties of the most common cryogenic liquids and their powerful cooling capability.

Chapters 2 through 5 focus on practical cryogenic *techniques*. The order of presentation is that of the four steps I usually follow to design and build a measurement rig, or to attach a sample to the cold stage of a cryocooler. First, heat-transfer calculation is the single most important factor in cryostat design (Chapter 2). This is followed by materials selection and construction (Chapter 3), wiring (Chapter 4), and thermometer installation (Chapter 5).

Along the way, a few suggestions are included on how to make a cryostat work. The ultimate success of a rig results more from attitude than technique; it reminds me of a saying on a sign in a factory where a friend worked, and I have never forgotten it: *"Cut to fit, bend to shape, paint to cover."* It simply implies that in the end you have to take time and be creative to "make

it work," to do all the adjusting, fitting, and retooling it takes to get good data. It also means running reality checks to build confidence in the rig's data, as amplified at the end of this section.

Chapter 6 and the accompanying appendix tables describe *material properties* at cryogenic temperatures. Whereas Chapter 3 presents *guidelines* for choosing construction materials, Chapter 6 looks at the *physics* of material properties at low temperatures, giving detailed graphs of properties and tables of data (*thermal, electrical*, *magnetic*, and *mechanical* handbook values).

Part II: Electrical Transport Measurements – Sample Holders and Contacts

Chapters 7 and 8 focus on *transport* measurements of both bulk and thin-film samples. These measurements are given special emphasis because of the challenge of *sample mounting* and *connections* when electrical current needs to be introduced into the test sample. The details of sample holders and contacts are the Achilles heel of such measurements as Hall-coefficients, critical current, or thermo-electric coefficients. Poor sample-holder design and contact techniques have led to more "unusual" effects and scuttled more transport measurements than any other factor I know.

Part III: Critical-Current Measurements and Data Analysis

Finally, in Chapters 9 and 10, we look specifically at superconductor critical-current measurements, which serve to illustrate in a practical way the application of Parts I and II. Although we focus in detail on the measurement of critical current, many of the topics in Chapters 9 and 10 have application to a wide variety of other cryogenic measurements. This measurement provides a rich example of problem solving, including procedures for initial equipment checkout, troubleshooting, automatic data acquisition, reality checks, and detailed data analysis.

So, that is the organization of the book—general cryostat design and construction techniques in the first half, followed by a focus on transport measurements and critical-current testing in the second half. The material *within each chapter* is also organized to proceed from general topics in the first part of each chapter to more specialized techniques in the last part.

In approaching this, or any other book, it is sometimes useful to skip less relevant subjects and look at the parts that best suit your specific requirements at the moment, noting the other material and coming back to read it in detail later when it is needed. To guide you to pertinent sections of the text, I have included in this introductory chapter a *checklist* of questions intended (Sec. 1.3.1) to lead you quickly to information about your specific apparatus. A detailed index and tables of contents for both the main text and appendixes are provided for quick navigation. (The latter is located on the inside of the back cover.)

1.1.2 The last step

Since it is usually not emphasized in textbooks, let me underscore at the outset the main

difference between a good measurement apparatus and anathema. The last step in the cryostat design-and-construction process is running experimental *reality checks* on a new test rig. No book and no one else can do that for us; it is a matter of personal integrity.

Sometimes it is so tempting to rush to publish a new effect from a new rig, just to be first (but ignoring some flaw in the apparatus or measurement technique). Too often, the "new effect" has to be dealt with, wastes everybody's time and money, and contributes to "literature pollution." It is our responsibility to *check the apparatus using (standard) test samples with known properties*. Any new apparatus should yield not only approximately the right results, but *exactly* the right results. It's incumbent on us to trace down every little foible, jump in value, hysteresis, and so on, before it hurts us in a more difficult situation.

My experience is that theoreticians usually take published experimental data at face value and, given enough time and desire, they can find models to explain experimental artifacts. We know our apparatus and experimental procedure like no one else. So it pays to think about simple alternative explanations, especially for "unusual" data.

A reputation is a fragile thing. The more unusual the results, the greater the caution needed. As Carl Sagan often said, "Extraordinary claims require extraordinary evidence."

1.1.3 Extra items

Experimental tips: From time to time, I have included a few specific suggestions that do not exactly fit the main flow of text, but are, nevertheless, helpful items appropriate to the subject matter. These are indented and flagged by a little pointer (→).

Two *addenda* are included at the end of Chapter 1:

- *Safety (Sec. 1.6.1)*: This list is a genuine sharing of a few cryogenic situations where we have gotten into trouble. You might as well know up front what does *not* work. "Those who do not learn from history are doomed to repeat it."
- *Transferring cryogenic liquids (Sec. 1.6.2)*: This essential skill is nontrivial; it usually takes many mistakes to become proficient. There is no substitute for having someone knowledgeable *watch* you as you initially learn, but these tips may shorten the learning curve.

Equations: Where there are many equations, a box has been drawn around some of them to distinguish the more important relations and, especially in Chapter 10, to indicate sets of interconnected equations.

Definitions: Often when starting in a new field, it is helpful to decode a few of the terms we throw around all too glibly. A listing of common terms and ubiquitous acronyms is given in the first appendix (Appendix A1.1).

In this vein, let me mention that I have used the word "cryostat" throughout this book to describe the apparatus or insert that holds samples for measurements. More generally, the term

cryostat can also refer to the insert *plus* the vacuum-insulated container, or "dewar," that holds cryogenic liquids. However, dewars are not the focus of the book, because efficient, well designed dewars are available commercially. Other more colloquial terms I have used to describe the measurement cryostat are: "probe, rig, jig, ...".

APPENDIXES

DATA HANDBOOK OF MATERIAL PROPERTIES AND CRYOSTAT DESIGN

The following tables provide handbook data for cryostat design and measurements. In many cases the tables serve as a ready collection of *general design information* for quick reference, including SI conversion factors sorted by function, cooling power data, suppliers of specialty parts, heat conduction down stainless-steel tubing, strengths of bolts, metric equivalents, vacuum-design data, wire properties, magnetic-correction factors for thermometers, and so on. In other cases, the tables provide a convenient aid in *material selection*, presenting, at a glance, a condensed overview of the temperature dependence of the properties of many materials (sorted by type of material and property). Once a material is selected, more detailed information can then be obtained for that particular material by referring to the extensive references accompanying each table or to the Internet data sources given in Sec. 6.7.2.

The appendix tables are divided into categories corresponding to each chapter, starting with general information and properties of cryogenic fluids, continuing with heat transfer, construction, wiring, thermometers, properties of solids, sample holders, contacts, and ending with information useful for critical-current analysis. The text sections indicated in parentheses with each appendix table contain specific information on the application and interpretation of the data in that table.

A1. General information and cryogen properties (ref. Chapter 1)

A1.1 Term-abbreviation-acronym decoder

When starting in a new field, the jargon can sometimes be daunting. The following is only an brief introductory list, given in rractical terms, but it may be useful to help clarify a few of the more commonly used terms, abbreviations, and acronyms.

An accessible multilingual website containing introductory information on *polymers* and their designations is http://www.pslc.ws/macrog/index.htm.

Default nomenclature: Alloy compositions in this book are given in *weight* percent (for example: 2wt%Al or 2%Al) unless specifically indicated as *atomic* percent (e.g., 2at%Al).

AISI: American Iron and Steel Institute, a designation system for steel alloys (Appendix A6.9)

Alumel: A high electrical-resistivity nickel alloy used for thermocouples consisting of Ni–2%Al–2%Mn–1%Si.

ASTM: Formerly known as the American Society for Testing and Materials, ASTM International provides a global forum for consensus standards for materials, products, systems, and services.

AWG: American Wire Gauge, a designation system for wire size. Appendix A4.1a lists physical information by AWG wire size. Corresponding *metric* wire sizes are given in Appendix A4.1b.

Bi-2212: A common abbreviation for the high-T_c superconductor material $Bi_2Sr_2CaCu_2O_{8+\delta}$ (where, typically, $\delta << 1$). The name is derived from the subscripts of the first four elements in the compound formula. This superconductor is also sometimes referred to as BSCCO (pronounced "bisco"). ($T_c \approx 90$ K)

Bi-2223: A common abbreviation for the high-T_c superconductor $(Bi,Pb)_2Sr_2Ca_2Cu_3O_{10-\delta}$; also sometimes referred to as BSCCO. ($T_c \approx 110$ K)

Chromel: A high electrical-resistivity nickel alloy commonly used for resistive wiring and thermocouples, consisting of Ni–10%Ni.

Constantan: Another high electrical-resistivity alloy commonly used for resistive wiring and thermocouples, consisting of Cu–45%Ni.

Critical current I_c: The maximum amount of current that can be carried by a superconductor before it starts to become resistive. Good commercial superconductors can carry over 1000 A/mm^2 in the presence of a 12 T magnetic field applied perpendicular to the wire.

Critical magnetic field: There are several definitions of critical magnetic field, described in Sec. 10.3.1. Generally, the so-called *upper critical field* H_{c2} is the practical quantityfor low-T_c superconductors, corresponding to the magnetic field above which all superconductivity is suppressed. H_{c2} values at 0 K for low-T_c materials range up to about 30 T, and for high-T_c materials to over 100 T. Typical values are tabulated for practical superconductors in Appendix A6.6 and plotted vs. temperature in Fig. 10.15. The so-

called *irreversibility* or *depinning field* H_{irr} is the practical quantity for high-T_c superconductors, plotted vs. temperature in Fig. 10.16.

Critical temperature T_c: The temperature below which a superconductor must be cooled before it becomes superconducting. Typical values for practical low-T_c materials range from about 10 K to 40 K; for high-T_c materials, from about 90 K to 130 K. Values are tabulated for the most common superconductors in Appendix A6.6.

Cryocooler: A cryogenic refrigerator.

Cryogen: Another name for a *cryogenic liquid*, such as liquid helium (T_{boil} = 4.2 K), liquid neon (T_{boil} = 27 K), or liquid nitrogen (T_{boil} = 77 K). The physical properties of common cryogens are given in Appendix A1.5.

CTFE: Polychlorotrifluoroethylene, a type of Teflon™.

ELI Ti–6Al–4V: Extra Low Interstitial form of Ti–6Al–4V. The mechanical properties of titanium strongly depend on interstitial elements (especially oxygen, nitrogen, and carbon), which affect particularly the fracture toughness. ELI grade is a purer form of titanium with a greater fracture toughness.

Ethylene glycol dimethyl terepthalate: Mylar™

ETP copper: Electrolytic-Tough-Pitch copper [designated by the Unified Numbering System (UNS) as C10300]. This is the copper commonly used to make ordinary copper wire.

Eutectic mixture: The alloy composition with the lowest melting-temperature; eutectic compositions are particularly useful as solder materials.

FEP: Fluorinated ethylene propylene, a type of Teflon™

G-10, G-11: Designations for fiberglass-epoxy composites (commonly used as commercial electronic circuit boards) made from layers of fiberglass cloth filled with epoxy.

Hastelloy C: A corrosion-resistant nickel alloy consisting of 54%Ni–17%Mo–15%Cr–5%Fe–4%W.

HTS: High-T_c (high-critical-temperature) superconductors. Copper-oxide materials having critical temperatures ranging to over 100 K. Also referred to as *oxide* superconductors or *ceramic* superconductors. Examples are: $YBa_2Cu_3O_{7-x}$ (T_c = 92 K), $Bi_2Sr_2CaCu_2O_{8+x}$ (T_c = 85 K), $(Bi,Pb)_2Sr_2Ca_2Cu_3O_{10-x}$ (T_c = 110 K), $(Tl,Pb)_1(Ba,Sr)_2Ca_2Cu_3O_{10+x}$ (T_c = 115 K), and $HgBa_2Ca_2Cu_3O_{8+x}$ (T_c = 135 K).

ISO: International Standards Organization.

ITS-90: The International Temperature Scale of 1990.

KF flange: *Klein Flange*, meaning "small flange;" a flexible O-ring vacuum coupling.

LTS: Low-T_c (low-critical-temperature) superconductors. These materials (usually with niobium as the core element) have critical temperatures up to about 40 K and are based on a phonon-coupling mechanism between superconducting pairs of electrons. Common examples are: Nb–Ti (T_c = 9.5 K), Nb_3Al (T_c = 15 K), Nb–N (T_c = 16 K), Nb_3Sn (T_c = 18 K), Nb_3Ge (T_c = 23 K), and MgB_2 (T_c = 39 K).

Lambda point: The temperature (2.177 K) where normal ^{4}He (also designated as He I)

transforms into superfluid helium ^{4}He (also designated as He II); see Sec. 1.2.2.

Manganin: An alloy commonly used for cryostat wiring and heaters in nonmagnetic applications, consisting of Cu–13%Mn–4%Ni.

Martensitic phase transformation: A change in the atomic structure of a metal to a new crystalline phase that is usually harder and more brittle. In stainless steels commonly used in cryogenic apparatus, such as AISI 304, 310, and 316, the martensitic phase transformation is precipitated by cooling to low temperatures or by applied stress (Sec. 6.6.5). The martensitic phase of the metal has a lower fracture toughness and is usually ferromagnetic.

Monel: A high-strength, corrosion-resistant, nickel alloy consisting of Ni–30%Cu.

n value: An index of the nonlinearity or sharpness of the voltage–current (V–I) curve near the critical current of a superconductor. It is defined by the relation $V = \mathrm{c}\, I^n$ (Sec. 10.1.3). Good superconductors have n values above 20 to 30.

Nichrome: A highly resistive alloy commonly used for heater wiring, consisting of Ni–20%Cr.

OFHC™ copper: A type of oxygen-free copper [designated by the Unified Numbering System (UNS) as C10200; a higher-purity type is designated as C10100].

PCTFE: Polychlorotrifluoroethylene.

PET: Polyethylene terephthalate, Mylar™.

Phosphor bronze: An alloy commonly used for cryostat and thermometer instrumentation wiring composed of Cu–5%Sn–0.2%P (Grade A).

PMMA: Polymethyl methacrylate, Plexiglas™.

Polyamide: Nylon™.

Polyimide: Kapton™.

Phonon: A wave-like displacement of the atoms from their equilibrium positions in a solid, usually thermally generated.

Poisson's ratio: A term used in mechanics (Secs. 3.5.3 and 3.5.4) that is the (negative of the) ratio of the *lateral* strain to *longitudinal* strain when a beam is uniformly and elastically stressed along the longitudinal axis. (It simply expresses the fact that the beam becomes narrower as it is stretched, to approximately conserve its volume.) The Poisson's ratio of metals is typically about 1/3, with values ranging from 0.28 to 0.42 for most materials.

PTFE: Polytetrafluoroethylene, a type of Teflon™.

Quench: A colloquial term for a thermal runaway event; see Thermal runaway.

SI: The international system of units (Système International d'Unités).

SQUID: Superconducting Quantum Interference Device. A very sensitive magnetometer able to detect magnetic flux as small as a fraction of magnetic flux quantum Φ_0 ($= 2.0678 \times 10^{-15}$ Wb).

TFE: Tetrafluoroethylene, Teflon™.

Thermal runaway (quench): A process wherein a small part of a superconductor carrying very high current densities is momentarily heated into the resistive state (by sample movement,

friction, or some other disturbance). The resulting electrical (Joule) heating in this portion of the superconductor then heats additional surrounding superconductor material into the resistive state, resulting in a thermal-runaway process with an ever-growing resistive zone and rapidly increasing Joule heating. When measuring the critical current of a superconducting strand, the Joule heating typically locally melts the superconductor unless the current is shut off quickly (in less than a second). More information is given in Sec. 7.5.1.

Type I superconductors: Superconducting materials where magnetic field uniformly penetrates the material, suppressing superconductivity at relatively low magnetic fields (typically much less than 1 T). This is the original type of superconductivity discovered in 1911 by Onnes. It was not until nearly fifty years later that practical (high-field) Type II superconductivity was discovered.

Type II superconductors: Superconductors wherein magnetic field is localized by circulating supercurrents, confining the field to small regions (vortices) and thereby leaving most of the superconductor free of magnetic field; see Fig. 10.7. This second type of superconductivity, which was discovered half a century after Type I superconductors, allows superconductivity to persist to much higher magnetic fields and comprises the practical superconducting materials from which most of today's applications are fabricated. Paradoxically, Type II superconductors have a much lower electrical conductivity in the normal (nonsuperconducting) state than that of Type I superconductors (which are typically pure metallic elements).

YBCO: The term commonly used for the high-T_c material $YBa_2Cu_3O_{7-\delta}$ ($T_c \approx 92$ K), also sometimes referred to as simply *123* because of the subscripts of the first three elements in the compound.

A1.2 Fundamental constants

Fundamental Physical Constants [a]

Quantity	Symbol	Value
Avogadro constant	N_A	$6.022\ 141\ 99 \times 10^{23}$ mol^{-1}
Boltzmann constant	$k_B = R/N_A$	$1.380\ 650\ 3 \times 10^{-23}$ J·K^{-1}
electric constant	$\varepsilon_0 = 1/\mu_0 c^2$	$8.854\ 187\ 817 \times 10^{-12}$ F·m^{-1}
electron volt	eV	$1.602\ 176\ 463 \times 10^{-19}$ J
elementary charge	e	$1.602\ 176\ 463 \times 10^{-19}$ C
Lorenz constant (Sec. 6.4.2)	$L_N = (\pi^2/3)\,(k_B/e)^2$	2.443×10^{-8} V^2·K^{-2}
magnetic flux quantum	$\Phi_0 = h/2e$	$2.067\ 833\ 637 \times 10^{-15}$ Wb
molar gas constant	R	$8.314\ 472$ J·mol^{-1}·K^{-1} = $8.314\ 472$ Pa·m^3·mol^{-1}·K^{-1}
magnetic constant	μ_0	$4\pi \times 10^{-7} = 1.2566 \times 10^{-6}$ N·A^{-2} = 1.2566 μV·s·A^{-1}·m^{-1} = 1.2566 μWb·A^{-1}·m^{-1} = 1.2566 μH·m^{-1}
Newtonian constant of gravitation	G	6.673×10^{-11} m^3·kg^{-1}·s^{-2}
Planck's constant	h	$6.626\ 068\ 76 \times 10^{-34}$ J·s
speed of light in vacuum	c	$2.997\ 924\ 58 \times 10^{8}$ m·s^{-1}
Stefan–Boltzmann constant (Sec. 2.4)	$\sigma = (\pi^2/60)k_B^4/(h/2\pi)^3 c^2$	$5.670\ 400 \times 10^{-8}$ W·m^{-2}·K^{-4}

[a] From *CRC Handbook of Chemistry and Physics* (2002), 83rd edition, CRC Press LLC, Boca Raton, Florida.

Useful approximate equivalents:

Pressure: 1 atm (≡ 760 torr) → ~10^5 Pa

Temperature: 11 000 K → ~1 eV

Wavelength: 12 000 Å → ~1 eV

A1.3 SI conversion factors

SI: Système International d'Unités (International System of Units)

To convert from	to	multiply by
	ACCELERATION	
ft/s^2	meter per second^2 (m/s^2)	3.048 000 E–01
free fall, standard	meter per second^2 (m/s^2)	9.806 650 E+00
in/s^2	meter per second^2 (m/s^2)	2.540 000 E–02
	AREA	
acre	meter^2 (m^2)	4.046 873 E+03
barn	meter^2 (m^2)	1.000 000 E–28
circular mil	meter^2 (m^2)	5.067 075 E–10
ft^2	meter^2 (m^2)	9.290 304 E–02
in^2	meter^2 (m^2)	6.451 600 E–04
mi^2 (U.S. statute mile)	meter^2 (m^2)	2.589 988 E+06
section	meter^2 (m^2)	2.589 988 E+06
township	meter^2 (m^2)	9.323 957 E+07
yd^2	meter^2 (m^2)	8.361 274 E–01
	BENDING MOMENT OR TORQUE	
dyne·centimeter	newton·meter (N·m)	1.000 000 E–07
kgf·m	newton·meter (N·m)	9.806 650 E+00
ozf·in	newton·meter (N·m)	7.061 552 E–03
lbf·in	newton·meter (N·m)	1.129 848 E–01
lbf·ft	newton·meter (N·m)	1.355 818 E+00
	CAPACITY (*see* VOLUME)	
	DENSITY (*see* MASS PER UNIT VOLUME)	
	ELECTRICITY AND MAGNETISM [a]	
ampere hour	coulomb (C)	3.600 000 E+01
EMU of capacitance	farad (F)	1.000 000 E+09
EMU of current	ampere (A)	1.000 000 E+01
EMU of electric potential	volt (V)	1.000 000 E–08
EMU of inductance	henry (H)	1.000 000 E–09
EMU of resistance	ohm (Ω)	1.000 000 E–09
ESU of capacitance	farad (F)	1.112 650 E–12
ESU of current	ampere (A)	3.335 6 E–10
ESU of electric potential	volt (V)	2.997 9 E+02

[a] ESU means electrostatic cgs unit. EMU means electromagnetic cgs unit.

To convert from	to	multiply by
ESU of inductance	henry (H)	8.987 554 E+11
ESU of resistance	ohm (Ω)	8.987 554 E+11
gauss	tesla (T)	1.000 000 E–04
gilbert	ampere (A)	7.957 747 E–01
maxwell	weber (Wb)	1.000 000 E–08
oersted	ampere per meter (A/m)	7.957 747 E+01

ENERGY (includes WORK)

British thermal unit (thermochemical)	joule (J)	1.054 350 E+03
calorie (thermochemical)	joule (J)	4.184 000 E+00
electron volt	joule (J)	1.602 176 E–19
erg	joule (J)	1.000 000 E–07
ft·lbf	joule (J)	1.355 818 E+00
kilocalorie (thermochemical)	joule (J)	4.184 000 E+03
kW·h	joule (J)	3.600 000 E+06
W·h	joule (J)	3.600 000 E+03
W·s	joule (J)	1.000 000 E+00

FLOW (*see* MASS PER UNIT TIME or VOLUME PER UNIT TIME)

FORCE

dyne	newton (N)	1.000 000 E–05
kilogram-force (kgf)	newton (N)	9.806 650 E+00
kilopond-force	newton (N)	9.806 650 E+00
kip (1000 lbf)	newton (N)	4.448 222 E+03
ounce-force (avoirdupois)	newton (N)	2.780 139 E–01
pound-force (lbf)	newton (N)	4.448 222 E+00
poundal	newton (N)	1.382 550 E–01

FORCE PER UNIT AREA (*see* Pressure)

FORCE PER UNIT LENGTH

lbf/in	newton per meter (N/m)	1.751 268 E+02
lbf/ft	newton per meter (N/m)	1.459 390 E+01

HEAT

Btu (thermochemical)·in/s·ft^2·°F (*k*, thermal conductivity)	watt per meter kelvin (W/m·K)	5.188 732 E+02
Btu (thermochemical)·in/h·ft^2·°F (*k*, thermal conductivity)	watt per meter kelvin (W/m·K)	1.441 314 E–01
Btu (thermochemical)/ft^2	joule per meter^2 (J/m^2)	1.134 893 E+04
Btu (thermochemical)/h·ft^2·°F (*C*, thermal conductance)	watt per meter^2 kelvin (W/m^2·K)	5.674 466 E+00
Btu (thermochemical)/lb	joule per kilogram (J/kg)	2.324 444 E+03
Btu (thermochemical)/lb·°F (*c*, specific capacity)	joule per kilogram kelvin (J/kg·K)	4.184 000 E+03

To convert from	to	multiply by
Btu (thermochemical)/s·ft^2·°F	watt per meter^2 kelvin (W/m^2·K)	2.042 808 E+04
cal (thermochemical)/cm^2	joule per meter^2 (J/m^2)	4.184 000 E+04
cal (thermochemical)/cm^2·s	watt per meter^2 (W/m^2)	4.184 000 E+04
cal (thermochemical)/cm·s·°C	watt per meter kelvin (W/m·K)	4.184 000 E+02
cal (thermochemical)/g	joule per kilogram (J/kg)	4.184 000 E+03
cal (thermochemical)/g·°C	joule per kilogram kelvin (J/kg·K)	4.184 000 E+03
°F·h·ft^2/Btu (thermochemical) (*R,* thermal resistance)	Kelvin meter^2 per watt (K·m^2/W)	1.761 102 E–01
ft^2/h (thermal diffusivity)	meter^2 per second (m^2/s)	2.580 640 E–05

LENGTH

angstrom	meter (m)	1.000 000 E–10
astronomical unit	meter (m)	1.495 98 E+11
fermi (femtometer)	meter (m)	1.000 000 E–15
foot (ft)	meter (m)	3.048 000 E–01
inch (in)	meter (m)	2.540 000 E–02
light year	meter (m)	9.460 528 E+15
micron	meter (m)	1.000 000 E–06
mil	meter (m)	2.540 000 E–05
mile (U.S. statute)	meter (m)	1.609 347 E+03
pica (printer's)	meter (m)	4.217 518 E–03
point (printer's)	meter (m)	3.514 598 E–04
rod	meter (m)	5.029 210 E+00
yard (yd)	meter (m)	9.144 000 E–01

LIGHT

footcandle	lumen per meter^2 (lm/m^2)	1.076 391 E+01
footcandle	lux (lx)	1.076 391 E+01

MASS

grain	kilogram (kg)	6.479 891 E–05
gram	kilogram (kg)	1.000 000 E–03
hundredweight (long)	kilogram (kg)	5.080 235 E+01
hundredweight (short)	kilogram (kg)	4.535 924 E+01
ounce (avoirdupois)	kilogram (kg)	2.834 952 E–02
pound (lb) (avoirdupois)	kilogram (kg)	4.535 924 E–01
slug	kilogram (kg)	1.459 390 E+01
ton (assay)	kilogram (kg)	2.916 667 E–02
ton (long, 2240 lb)	kilogram (kg)	1.016 047 E+03
ton (metric)	kilogram (kg)	1.000 000 E+03
ton (short, 2000 lb)	kilogram (kg)	9.071 847 E+02

MASS PER UNIT VOLUME (includes DENSITY and MASS CAPACITY)

g/cm^3	kilogram per meter^3 (kg/m^3)	1.000 000 E+03
oz (avoirdupois)/gal (U.K. liquid)	kilogram per meter^3 (kg/m^3)	6.236 027 E+00
oz (avoirdupois)/gal (U.S. liquid)	kilogram per meter^3 (kg/m^3)	7.489 152 E+00
oz (avoirdupois)/in^3	kilogram per meter^3 (kg/m^3)	1.729 994 E+03
lb/ft^3	kilogram per meter^3 (kg/m^3)	1.601 846 E+01

To convert from	to	multiply by
lb/in^3	kilogram per meter^3 (kg/m^3)	2.767 990 E+04
lb/gal (U.K. liquid)	kilogram per meter^3 (kg/m^3)	9.977 644 E+01.
lb/gal (U.S. liquid)	kilogram per meter^3 (kg/m^3)	1.198 264 E+02
ton(long, mass)/yd^3	kilogram per meter^3 (kg/m^3)	1.328 939 E+03
	POWER	
Btu (thermochemical)/s	watt (W)	1.054 350 E+03
Btu (thermochemical)/min	watt (W)	1.757 250 E+01
Btu (thermochemical)/h	watt (W)	2.928 751 E–01
cal (thermochemical)/s	watt (W)	4.184 000 E+00
cal (thermochemical)/min	watt (W)	6.973 333 E–02
erg/s	watt (W)	1.000 000 E–07
ft·lbf/h	watt (W)	3.766 161 E–04
ft·lbf/min	watt (W)	2.259 697 E–02
ft·lbf/s	watt (W)	1.355 818 E+00
horsepower (550 ft·lbf/s)	watt (W)	7.456 999 E+02
kilocalorie (thermochemical)/min	watt (W)	6.973 333 E+01
kilocalorie (thermochemical)/s	watt (W)	4.184 000 E+03
	PRESSURE OR STRESS (FORCE PER UNIT AREA)	
atmosphere (normal = 760 torr)	pascal (Pa)	1.013 25 E+05
atmosphere (technical = 1 kgf/cm^2	pascal (Pa)	9.806 650 E+04
bar	pascal (Pa)	1.000 000 E+05
centimeter of mercury (0 °C)	pascal (Pa)	1.333 22 E+03
centimeter of water (4 °C)	pascal (Pa)	9.806 65 E+01
dyne/cm^2	pascal (Pa)	1.000 000 E–01
foot of water (39.2 °F)	pascal (Pa)	2.989 070 E+03
gram-force/cm^2	pascal (Pa)	9.806 650 E+01
inch of mercury (32 °F)	pascal (Pa)	3.386 389 E+03
inch of mercury (60 °F)	pascal (Pa)	3.376 85 E+03
inch of water (39.2 °F)	pascal (Pa	2.490 82 E+02
inch of water (60 °F)	pascal (Pa)	2.488 4 E+02
kgf/cm^2	pascal (Pa)	9.806 650 E+04
kgf/m^2	pascal (Pa)	9.806 650 E+00
kgf/mm^2	pascal (Pa)	9.806 650 E+06
kip/in^2 (ksi)	pascal (Pa)	6.894 757 E+06
millibar	pascal (Pa)	1.000 000 E+02
millimeter of mercury (0 °C)	pascal (Pa)	1.333 224 E+02
poundal/foot^2	pascal (Pa)	1.488 164 E+00
lbf/ft^2	pascal (Pa)	4.788 026 E+01
lbf/in^2 (psi)	pascal (Pa)	6.894 757 E+03
psi	pascal (Pa)	6.894 757 E+03
torr (mm Hg, 0 °C)	pascal (Pa)	1.333 22 E+02
	SPEED (*see* VELOCITY)	
	STRESS (*see* PRESSURE)	
	TEMPERATURE	
degree Celsius (^{o}C)	kelvin (K)	$t_K = t_C + 273.15$

To convert from	to	multiply by
degree Fahrenheit (^{o}F)	kelvin (K)	$t_K = (t_F + 459.67)/1.8$
degree Rankine	kelvin (K)	$t_K = t_R/1.8$
degree Fahrenheit (^{o}F)	degree Celsius (°C)	$t_C = (t_F - 32)/1.8$
kelvin (K)	degree Celsius (°C)	$t_C = t_K - 273.15$

TIME

day (mean solar)	second (s)	8.640 000 E+04
day (sidereal)	second (s)	8.616 409 E+04
hour (mean solar)	second (s)	3.600 000 E+03
minute (mean solar)	second (s)	6.000 000 E+01
year (calendar)	second (s)	3.153 600 E+07

TORQUE (*see* BENDING MOMENT)

VELOCITY (includes SPEED)

ft/h	meter per second (m/s)	8.466 667 E–05
ft/min	meter per second (m/s)	5.080 000 E–03
ft/s	meter per second (m/s)	3.048 000 E–01
in/s	meter per second (m/s)	2.540 000 E–02
km/h	meter per second (m/s)	2.777 778 E–01
knot (international)	meter per second (m/s)	5.144 444 E–01
mi/h (U.S. statute)	meter per second (m/s)	4.470 400 E–01
mi/min (U.S. statute)	meter per second (m/s)	2.682 240 E+01
mi/s (U.S. statute)	meter per second (m/s)	1.609 344 E+03
mi/h (U.S. statute)	km/h	1.609 344 E+00

VISCOSITY

centipoise	pascal-second (Pa·s)	1.000 000 E–03
centistokes	meter^2 per second (m^2/s)	1.000 000 E–06
ft^2/s	meter^2 per second (m^2/s)	9.290 304 E–02
poise	pascal-second (Pa·s)	1.000 000 E–01
poundal·s/ft^2	pascal-second (Pa·s)	1.488 164 E+00
lb/ft·s	pascal-second (Pa·s)	1.488 164 E+00
lbf·s/ft^2	pascal-second (Pa·s)	4.788 026 E+01
slug/ft·s	pascal-second (Pa·s)	4.788 026 E+01
stoke	meter^2 per second (m^2/s)	1.000 000 E–04

VOLUME (includes CAPACITY)

acre-foot	meter^3 (m^3)	1.233 489 E+03
barrel (oil, 42 gal)	meter^3 (m^3)	1.589 873 E–01
board foot	meter^3 (m^3)	2.359 737 E–03
bushel (U.S.)	meter^3 (m^3)	3.523 907 E–02
cup	meter^3 (m^3)	2.365 882 E–04
fluid ounce (U.S.)	meter^3 (m^3)	2.957 353 E–05
foot^3	meter^3 (m^3)	2.831 685 E–02
gallon (Canadian liquid)	meter^3 (m^3)	4.546 090 E–03
gallon (U.K. liquid)	meter^3 (m^3)	4.546 092 E–03
gallon (U.S. dry)	meter^3 (m^3)	4.404 884 E–03

To convert from	to	multiply by
gallon (U.S. liquid)	meter^3 (m^3)	3.785 412 E–03
inch^3	meter^3 (m^3)	1.638 706 E–05
liter	meter^3 (m^3)	1.000 000 E–03
ounce (U.K. fluid)	meter^3 (m^3)	2.841 307 E–05
ounce (U.S. fluid)	meter^3 (m^3)	2.957 353 E–05
peck (U.S.)	meter^3 (m^3)	8.809 768 E–03
pint (U.S. liquid)	meter^3 (m^3)	4.731 765 E–05
quart (U.S. liquid)	meter^3 (m^3)	9.463 529 E–04
tablespoon	meter^3 (m^3)	1.479 000 E–05
teaspoon	meter^3 (m^3)	4.929 000 E–06
ton (register)	meter^3 (m^3)	2.831 685 E+00
yard^3	meter^3 (m^3)	7.645 549 E–01
VOLUME PER UNIT TIME (includes FLOW)		
ft^3/min	meter^3 per second (m^3/s)	4.719 474 E–04
ft^3/s	meter^3 per second (m^3/s)	2.831 685 E–02
in^3/min	meter^3 per second (m^3/s)	2.731 177 E–07
yd^3/min	meter^3 per second (m^3/s)	1.274 258 E–02
gal (U.S. liquid)/day	meter^3 per second (m^3/s)	4.381 264 E–08
gal (U.S. liquid)/min	meter^3 per second (m^3/s)	6.309 020 E–05
WORK (*see* ENERGY)		

Source: Selected excerpts from *Metric Practice Guide,* Designation: E 380 – 74 (1974), American Society for Testing and Materials, 100 Barr Harbor Drive, West Conshocken, PA 19428-2959; updated with data from Sl10-02 IEEE/ASTM SI 10 *American National Standard for Use of the International System of Units (SI): The Modern Metric System* (2002), SI10-02 IEEE/ASTM SI 10, 100 Barr Harbor Drive, West Conshocken, PA 19428-2959.

A1.4 Magnetic units: Equivalency table [a]

Symbol	Quantity	Conversion from Gaussian and cgs emu to SI [b]
Φ	magnetic flux	1 Mx = 1 G·cm^2 $\rightarrow$ 10^{-8} Wb = 10^{-8} V·s
B	magnetic flux density, magnetic induction	1 G $\rightarrow$ 10^{-4} T = 10^{-4} Wb/m^2
H	magnetic field strength	1 Oe $\rightarrow$ $10^3/(4\pi)$ A/m
m	magnetic moment	1 erg/G = 1 emu $\rightarrow$ 10^{-3} A·m^2 = 10^{-3} J/T
M	magnetization	1 erg/(G·cm^3) = 1 emu/cm^3 $\rightarrow$ 10^3 A/m
$4\pi M$	magnetization	1 G $\rightarrow$ $10^3/(4\pi)$ A/m
σ	mass magnetization, specific magnetization	1 erg/(G·g) = 1 emu/g $\rightarrow$ 1 A·m^2/kg
j	magnetic dipole moment	1 erg/G = 1 emu $\rightarrow$ $4\pi \times 10^{-10}$ Wb·m
J	magnetic polarization	1 erg/(G·cm^3) = 1 emu/cm^3 $\rightarrow$ $4\pi \times 10^{-4}$ T
χ, κ	volume susceptibility [c]	1 $\rightarrow$ 4π
χ_ρ, χ/ρ	mass susceptibility [d]	1 cm^3/g $\rightarrow$ $4\pi \times 10^{-3}$ m^3/kg
μ	permeability	1 $\rightarrow$ $4\pi \times 10^{-7}$ H/m = $4\pi \times 10^{-7}$ Wb/(A·m)
μ_r	relative permeability	$\mu \rightarrow \mu_r$
w, W	energy density	1 erg/cm^3 $\rightarrow$ 10^{-1} J/m^3
N, D	demagnetizing factor	1 $\rightarrow$ $1/(4\pi)$

[a] Table based on R. B. Goldfarb and F. R. Fickett (1985), NBS STP 696, National Bureau of Standards. U.S. Government Printing Office, Washington, D.C.

[b] Gaussian units are the same as cgs emu for magnetostatics; Mx = maxwell, G = gauss, Oe = oersted; Wb = weber, V = volt, s = second, T = tesla, m = meter, A = ampere, J = joule, kg = kilogram, H = henry.

[c] Volume susceptibility is dimensionless but is sometimes expressed in cgs units as emu/cm^3 or emu/(cm^3·Oe).

[d] Mass susceptibility is sometimes expressed in cgs units as emu/g or emu/(g·Oe).

A1.5 Properties of common cryogenic fluids. (Sec. 1.2)

Additional data on the vapor-pressure vs. temperature dependence of these cryogenic fluids are given in Appendix A5.1.

Fluid: Property:	^{3}He	^{4}He	H_2 * (Para)	H_2 * (Normal)	Ne	N_2	Ar	O_2	CH_4 (Methane)
Molecular Weight	3.0160	4.0026	2.0159	2.0159	20.179	28.013	39.948	31.999	16.043
Critical Temp. [K]	3.324	5.195	32.93	33.18	44.49	126.2	150.7	154.6	190.6
Critical Pressure [atm]	1.145	2.245	12.67	12.98	26.44	33.51	47.99	49.77	45.39
Boiling Point [K]	3.191	4.230	20.27	20.27	27.10	77.35	87.30	90.20	111.7
Melting Point [K]		4.2 (at 140 atm)	13.80	13.95	24.56	63.15	83.81	54.36	90.72
Liquid Density at B.P. [g/mL]	0.05722	0.1247	0.07080	0.07080	1.207	0.8061	1.395	1.141	0.4224
Gas Density at 0°C and 1 atm [g/L]	0.1345	0.1785	0.08988	0.08988	0.8998	1.250	1.784	1.429	0.7175
Vapor Density at B.P. [g/L]	24.51	16.76	1.339	1.339	9.577	4.612	5.774	4.467	1.816
Liquid Thermal Conductivity at B.P. [mW/(m•K)]	—	18.66	103.4	103.4	155.0	145.8	125.6	151.6	183.9
Liquid Isobaric Specific Heat at B.P. [J/(g•K)]	24.80	5.299	9.659	9.667	1.862	2.041	1.117	1.699	3.481
Latent Heat of Vaporization at B. P.	7.976 J/g	20.75	445.4	445.4	85.75	199.2	161.1	213.1	510.8
	(0.4564 J/mL)	(2.589)	(31.54)	(31.54)	(103.5)	(160.6)	(224.9)	(243.1)	(215.8)
Latent heat of Fusion at M.P. [J/g]	—	30.5	—	58.2	16.6	25.5	27.8	13.8	58.7

Fluid: Property:	^{3}He	^{4}He	H_2 * (Para)	H_2 * (Normal)	Ne	N_2	Ar	O_2	CH_4 (Methane)
Vap. Pres. of Solid at M. P. [kPa]	—	—	7.04	7.20	43.46	12.52	68.89	0.146	11.5
Magnetic Susceptibility [10^{-6} cm^3/mol] [a] (+ ≡ paramagnetic)		–2.02 (gas)	–5.44 (liq., 20.3K)	–3.99 (gas, $\gtrsim$ 293K)	–6.96 (gas)	–12.0 (gas)	–19.32 (gas)	+3 449 (gas) +7 699 (liq., 90K) +10 200 (sol., 54K)	–17.4

B.P. ≡ boiling point; M.P. ≡ melting point.

Principal source of data: E.W. Lemmon, NIST, evaluated from equations of state referenced in Appendix A5.1.

Data on solids:

V. Johnson (1960), NBS, Wright Air Development Div. (WADD) Technical Report 60-56, Part II. U.S. Government Printing Office, Washington, D.C.

D. H. J. Goodall (1970), A.P.T. Division, Culham, Culham Science Center, Abingdon, Oxfordshire, UK.

K. Timmerhaus and T. Flynn (1989), *Cryogenic Process Engineering,* Plenum Press, New York.

* Hydrogen can exist in two different molecular forms: higher-energy *ortho*hydrogen (nuclear spins aligned) and lower-energy *para*hydrogen (nuclear spins opposed). The equilibrium ratio is determined by temperature: at room temperature and above, hydrogen consists of about 25 % para and 75 % ortho (so-called *normal* hydrogen), but at the atmospheric boiling temperature of liquid hydrogen (20.27 K) and below, the equilibrium shifts almost completely to parahydrogen (99.79 % para and 0.21 % ortho at 20.27 K).

[a] *CRC Handbook of Chemistry and Physics* (2002), 83rd edition, CRC Press, Boca Raton, Florida.

A1.6a Cooling power data for ^4He, H_2, and N_2 (Sec. 1.2)

Tabulated values are consumption rates resulting from 1 W dissipated directly in the indicated cryogenic liquid at atmospheric pressure.

Cryogenic liquid	Volume of liquid boiled off from 1 W [L/h]	Flow of gas at 0°C, 1 atm from 1 W [L/min]	Enthalpy change at 1 atm pressure [J/g]
^4He	1.377	16.05	87 (4.2 K–20 K)
			384 (4.2 K–77 K)
			1542 (4.2 K–300 K)
H_2	0.1145	1.505	590 (20 K–77 K)
			3490 (20 K–300 K)
N_2	0.0225	0.243	233.5 (77 K–300 K)

Data compiled from:

V. Johnson (1960), NBS, Wright Air Development Div. (WADD) Technical Report 60-56, Part II, U.S. Government Printing Office, Washington, D.C.

D. H. J. Goodall (1970), A.P.T. Division, Culham Science Center, Abingdon, Oxfordshire, UK.

A1.6b Cooling power data: Amount of cryogenic fluid needed to cool common metals [a,b] (Sec. 1.2)

Cryogenic Fluid:		^{4}He (T_b = 4.2 K)		H_2 (T_b = 20.3 K)		N_2 (T_b = 77.3 K)
Initial Temp. of Metal:		300 K [L/kg]	77 K [L/kg]	300 K [L/kg]	77 K [L/kg]	300 K [L/kg]
Using the latent heat of vaporization only	Aluminum	58	2.6	5.4	0.25	1.01
	Copper	27	1.8	2.4	0.17	0.46
	Stainless Steel	30	1.2	2.8	0.12	0.54
Using both the latent heat and the enthalpy of the gas	Aluminum	1.60	0.22	1.03	0.14	0.64
	Copper	0.80	0.15	0.51	0.092	0.29
	Stainless Steel	0.80	0.10	0.52	0.064	0.34

T_b is the boiling temperature at atmospheric pressure.

[a] Determined from data by J. B. Jacobs (1962), *Adv. Cryog. Eng.* **8**, 529.

[b] For temperature combinations other than those given in this table, see Jacobs (1962, reference above).

A1.7 Suppliers of specialty parts and materials

The following is a list of suppliers of specialty parts and materials for constructing measurement cryostats. It is provided as a convenience to save time locating less-common items. These are not complete listings of suppliers and information can change over time, but at least they are a place to start. They may also serve as points of reference if contact information has changed.

Updated supplier information is listed for *cryogenic* instrumentation annually each December in the *Cold Facts Buyer's Guide*, Cryogenic Society of America, http://www.cryogenicsociety.org/. Suppliers for *general physics* instrumentation are updated each August in the *Physics Today Buyers Guide,* American Institute of Physics, http://www.physicstoday.org/guide/.

Trade names, products, and companies cited here do not constitute or imply endorsement by NIST or by the U. S. government, and do not imply that they are the best available for the purpose.

Adhesives (see Appendix A3.10)

Coaxial cables for cryogenic applications (Secs. 4.7.1, 4.8)

Solid dielectric coaxial cables for lower frequency applications (< 1 GHz) where dimensional stability of the terminations on thermal cycling is not needed (see Sec. 4.8):

Axon Cable Inc., 390 E. Higgins Rd., Suite 101, Elk Grove Village, IL 60007, Tel. 708-806-6629, Fax. 708-806-6639, http://www.axon-cable.com/. Supplier of miniature coaxial cable; stock number SM50 comes standard with Teflon™ dielectric and jacket; PXC47K08 can also be supplied with a Teflon™ jacket.

Lake Shore Cryotronics, Westerville, OH 43081, Tel. 614-891-2244, Fax. 614-818-1600, http://www.lakeshore.com/.

Micro-Coax, 206 Jones Blvd., Pottstown, PA 19464-3465, Tel. 610-495-0110, 800-223-2629, Fax. 610-495-6656, http://www.micro-coax.com/.

Oxford Instruments–Cryospares, Witney, Oxfordshire, UK OX294TL, Tel. +44(0)1865 881437, Fax. +44(0)1865 884045, http://www.oxinst.com/cryospares/.

Precision Tube, Coaxitube Div., 620 Naylor Mill Road, Salisbury, MD 21801, Tel. 410-546-3911, Fax. 410-546-3913, http://www.precisiontube.com/. Catalog contains helpful information on the electrical selection of coaxial cables.

RS, United Kingdom, Tel. +44-1536-201201, Fax. +44-1536-201-501, http://www.rs-components.com. Supplier of miniature coaxial cable with Teflon™ dielectric and jacket; "RF cable MCX" stock numbers: 388-530 (50 Ω), 388-546 (75 Ω).; (for low frequencies, where impedance matching is not a concern, the 75 Ω might be better since the capacitance is a bit lower).

Storm Products Co., Microwave Sales Office, 10221 Werch Drive, Woodridge, IL 60517, Tel. 630-754-3300, 888-347-8676, Fax. 630–754-3500, http://www.stormproducts.com/.

Expanded dielectric coaxial cables for higher frequency applications (> 1 GHz) where dimensional stability of the terminations on thermal cycling is needed (see Sec. 4.8):

Storm Products Co., Microwave Sales Office, 10221 Werch Drive, Woodridge, IL 60517, Tel. 630-754-3300, 888-347-8676, Fax. 630–754-3500, http://www.stormproducts.com/; expanded dielectric coaxial cables, for example cable #421-193.

Connectors (Secs. 4.1, 4.6, 4.7, 4.8)

Alligator clips: smooth, flat jaws; 7/32" jaw opening, #20 wire or smaller; crimp connection:

Mueller Electric Co., part number (PN) BU-34C, http://www.muellerelectric.com/ (distributed by Allied Electronics, Inc., PN 860-4340, Tel. 800-433-5700, http://www.alliedelec.com/ or Newark Electronics, PN 28F497, Tel. 800-263-9275, http://www.newark.com/.

Rf connectors:

Fischer Connectors, Tel. 1-800-551-0121, http://www.fischerconnectors.com/

Lemo Connectors, http://www.lemousa.com/.

Vacuum lead-throughs (room temperature):

Cerama-Seal, 1033 State Route 20, New Lebanon, NY 12125, Tel. 10518-794-7800, Fax 518-794-8080, http://www.ceramaseal.com/.

Detoronics Corp., 10660 East Rush St., So. El Monte, CA 91733-3432, Tel. 818-579-7130, Fax 818-579-1936, http://www.detoronics.com/.

Contacts (springy devices) (Sec. 7.4.3)

Beryllium–copper clad circuit board for making microsprings:

Specialty order from Q-Flex, 1220 S. Lyon St., Santa Ana, CA 92705, Tel. 714-835-2868, Fax. 714-835-4772, http://www.q-flex.com/.

Fuzz Buttons:

Techknit, Cranford, NJ, http://www.fuzzbuttons.com/.

Pogo Pins:

Emulation Technology, Inc., Santa Clara, CA, http://www.emulation.com/pogo/.

Cryogenic accessories and consumables

Lake Shore Cryotronics, Westerville, OH 43081, Tel. 614-891-2244, Fax. 614-818-1600, http://www.lakeshore.com/.

Oxford Instruments–Cryospares, Witney, Oxfordshire, UK OX294TL, Tel. +44(0)1865 881437, Fax. +44(0)1865 884045, http://www.oxinst.com/cryospares/.

Cryogenic measurement systems – Complete (Sec. 1.4)

Cryo Industries; 11124 S. Willow St., Manchester, NH 03103; Tel. 603-621-9957; cryo@cryoindustries.com; http://www.cryoindustries.com/.

Janis Research Co.; 2 Jewel Dr. P. O. Box 696, Wilmington, MA 01887-0696; Tel. 978-657-8750, http://www.janis.com/.

Oxford Instruments, Witney, Oxfordshire, UK OX294TL, Tel. +44(0)1865 881437, Fax. +44(0)1865 884045, http://www.oxinst.com/.

Precision Cryogenic Systems, Inc.; 1171 West Rockville Rd., Indianapolis, Indiana 46234; Tel. 317-272-0880, http://www.precisioncryo.com/.

Quantum Design; 6325 Lusk Glvd., San Diego, CA 92121–3733; Tel. 858-481-4400, Fax. 858-481-7410, http://www.qduse.com/.

Current leads (Secs. 4.9, 4.10)

Flexible superconducting braid:

Supercon Inc., 830 Boston Turnpike, Shrewsbury, MA 01545, http://www.supercon-wire.com/ (by special order).

Low-T_c and high-T_c superconductors – see Superconducting wire

Vapor-cooled leads:

American Magnetics Inc., P.O. Box 2509, 112 Flint Road, Oak Ridge, TN 37831-2509, USA, http://www.americanmagnetics.com/.

Cryomagnetics Inc., 1006 Alvin Weinberg Drive, Oak Ridge, TN 37830, USA, http://www.cryomagnetics.com/.

Current power supplies; low-ripple, series-transistor regulated (Sec. 9.2)

Alpha Scientific Electronics, Hayward, CA, 510-782-4747, http://www.alphascientific.com/.

Inverpower Controls Ltd., Burlington, Ontario, Canada, 905-639-4692, http://www.inverpower.com/.

Walker LDJ Scientific Inc., Worcester, MA 01606, 508-852-3674, http://www.walkerscientific.com/ (current ≤ 500 A).

Dewars for measurement systems—metal and fiberglass–epoxy

American Magnetics Inc., P.O. Box 2509, 112 Flint Road, Oak Ridge, TN 37831-2509, USA, http://www.americanmagnetics.com/.

Cryomagnetics Inc., 1006 Alvin Weinberg Drive, Oak Ridge, TN 37830, USA, http://www.cryomagnetics.com/.

International Cryogenics, 4040 Championship Drive, Indianapolis, IN 46268, Tel. 317-297-4777, Fax. 317-297-7988, http://www.intlcryo.com/.

Janis Research Co.; 2 Jewel Dr. P. O. Box 696, Wilmington, MA 01887-0696; Tel. 978-657-8750, http://www.janis.com/.

Oxford Instruments, Witney, Oxfordshire, UK OX294TL, Tel. +44(0)1865 881437, Fax. +44(0)1865 884045, http://www.oxinst.com/.

Precision Cryogenic Systems, Inc., 7804 Rockville Road, Indianapolis, Indiana 46214, Tel. 317–273-2800, Fax. 317-273-2802, prcry@iquest.net, http://www.precisioncryo.com/.

Tristan Technologies, Inc., 6185 Cornerstone Court East, Suite 106, San Diego, CA 92121, Tel. 877-436-1389, http://www.tristantech.com/.

Epoxies and pastes -- Conductive (Secs. 7.4.1 and 8.3.2)

Silver-based epoxy:

Ted Pella, Inc., P.O. Box 492477, Redding, CA 96049-2477, Tel. 800-237-3526; Fax. 530-243-3761, http://www.TedPella.com/.

Silver paste:

Ted Pella, Inc., P.O. Box 492477, Redding, CA 96049-2477, Tel. 800-237-3526; Fax. 530-243-3761, http://www.TedPella.com/.

Heaters, thin film (Secs. 1.4, 5.4, 7.3.1, and 7.4.1)

Minco Products, Inc., 7300 Commerce Lane, Minneapolis, MN 55432-3177, Tel. 763-571-3121, Fax. 763-571-0927, Info@minco.com, http://www.minco.com/ .

Liquid-level monitors (Sec. 1.6.2)

Janis Research Co.; 2 Jewel Dr. P. O. Box 696, Wilmington, MA 01887-0696; Tel. 978-657-8750, http://www.janis.com/.

Lake Shore Cryotronics, Westerville, OH 43081, Tel. 614-891-2244, Fax. 614-818-1600, http://www.lakeshore.com/.

Oxford Instruments, Witney, Oxfordshire, UK OX294TL, Tel. +44(0)1865 881437, Fax. +44(0)1865 884045, http://www.oxinst.com/.

Lubricants (see Appendix A3.11)

Magnets, superconducting (Secs. 1.4, 1.5, 9.1.4, 9.2.1)

American Magnetics Inc., P.O. Box 2509, 112 Flint Road, Oak Ridge, TN 37831-2509, USA, http://www.americanmagnetics.com/.

American Superconductor Corp., Two Technology Dr., Westborough, MA 01581, Tel. 508-836-4200, Fax. 508-836-4248, http://www.amsuper.com/ (high-T_c magnets).

Cryomagnetics Inc., 1006 Alvin Weinberg Drive, Oak Ridge, TN 37830, http://www.cryomagnetics.com/.

Oxford Instruments, Witney, Oxfordshire, UK OX294TL, Tel. +44(0)1865 881437, Fax. +44(0)1865 884045, http://www.oxinst.com/.

SuperPower, Inc., 450 Duane Ave., Schenectady, NY 12304, Tel. 518-346-1414, Fax. 518-346-6080, http://www.igc.com/superpower/ (high-T_c magnets).

Materials, less common and specialty sizes (Secs. 3.2, 3.4, 6.5.2, 7.3, 7.4)

Metals – general supplier of high purity metals and metallic compounds:

ESPI, 1050 Benson Way, Ashland, OR 97520, Tel. 800-638-2581, Fax. 800-488-0060, http://www.espimetals.com/.

Aluminum – high conductivity wires:

Alcoa Technical Center, 100 Technical Drive, Alcoa Center, PA 15069, http://www.alcoa.com/

Sumitomo Chemical, Japan, http://www.sumitomo-chem.co.jp/english/

Swiss Federal Institute of Technology, Zurich, Switzerland, Tel. +41 44 632 1111, Fax. +41 44 632 1010, http://www.ethz.ch

Copper – high conductivity, oxygen free; (see Appendix A3.1 for a listing of the various types)**:**

Copper & Brass Sales, Tel. 800-926-2600, Fax. 888-926-2600, http://www.copperandbrass.com/ (OFHC™ copper tubes).

Farmer's Copper & Industrial Supply 800-231-9450, Fax. 409-765-7115, http://www.farmerscopper.com/ (OFHC™ copper tubes).

McMaster–Carr, http://www.mcmaster.com/.

Fiberglass–epoxy composite tubes; custom sizes (made from G-10, G-11, G-13):

A & M Composites, P.O. Box 3281, Big Spring, TX 79721, Tel. 432-267-6525, Fax. 432-267-6599, http://www.amcctx.com/.

Microwave circuit board (TMM™) (with a thermal-expansion coefficient less than that of G-10 circuit board, so as to give better dimensional stability):

Rogers Corp., One Technology Dr., P.O. Box 188, Rogers, CT 06263-0188, Tel. 860-774-9605, Fax. 860-779-5509, http://www.rogers-corp.com/ .

Titanium tubes – less common sizes:

Titanium Sports Technologies (TST), 1426 E. Third Ave., Kennewick, WA 99336, Tel. 509-586-6117, http://www.titaniumsports.com/.

Mechanical actuators and linear motors (Sec. 3.6)

Energen, Inc., 650 Suffolk St., Lowell, MA 01854, http://www.energeninc.com/index.htm.

Soldering materials (Secs. 3.3.4, 4.5, 4.6, 8.3.2, 8.3.3)

Indium-alloy solders:

Indium Corp. of America, Indalloy® solders, Tel. 315-853-4900 or 800-4-INDIUM, askus@indium.com, http://www.indium.com/.

Lake Shore Cryotronics, Ostalloy® solders, Westerville, OH 43081, Tel. 614-891-2244, Fax. 614-818-1600, http://www.lakeshore.com/ .

Umicore Indium Products, Ostalloy® solders, http://www.thinfilmproducts.umicore.com/.

Solder flux:

• Combined solder and flux paste:

Fusion Automation, Inc., http://www.fusion-inc.com/ Model SSX-430-830.

Multicore Kester 135, http://www.kester.com/.

• Mild flux:

Alpha HF260, http://www.alphametals.com/distributors/pdfs/2001134214.pdf.

Litton ESF33, http://www.amsuper.com/products/library/003-TechNote_Soldering.pdf.

• Unactivated rosin flux:

Kester, Tel. 800-253-7837, Fax. 847-390-9338, technicalservice@kester.com, http://www.kester.com/ designated "Plastic core" RNA (rosin non-activated).

Solder with antimony to minimize embrittlement and cracking at cryogenic temperatures:

Kester, Tel. 800-253-7837, Fax. 847-390-9338, technicalservice@kester.com, http://www.kester.com/.

Strain gauges, accessories, and gauge adhesives for cryogenic service (Sec. 9.4.4)

Vishay Intertechnology, Inc., Vishay Micro-Measurements Division, http://www.vishay.com/.

Sticky stuff: (see Appendix A3.10)

Superconducting wire (Secs. 4.9, 4.10, Chapters 9 and 10)

Updated links to superconductor suppliers are available at http://superconductors.org/Links.htm.

Low-T_c (Nb–Ti and Nb_3Sn):

Alstom Magnets & Superconductors, 90018 Belfort Cedex, France, Tel. +33 (0)3 84 55 32 26, Fax. +33 (0)3 84 55 70 93, http://www.powerconv.alstom.com/.

Bochvar, 5 ulitsa Rogova, Moscow 123060, Tel. (095) 190-49-93[1], 190-82-97[2], Fax. (095) 196-41-68, e-mail**:** post@bochvar.ru, http://www.bochvar.ru.

European Advanced Superconductor (EAS), Ehrichstraße 10, 63450 Hanau, Germany, Tel. (+49) (6181) 43 84-41 00, Fax. (+49) (6181) 43 84-44 00, http://www.advancedsupercon.com/.

Furukawa Electric, 6-1, Marunouchi 2-chome, Chiyoda-ku, Tokyo 100, Japan, Tel. 81-3-3286-3001, Fax. 81-3-3286-3747,3748, http://www.furukawa.co.jp/english.

Kobe Steel, Ltd., Shinko Building, 10-26, Wakinohamacho, 2-chome, Chuo-ku, Kobe, Hyogo 651-8585, Japan, Tel. 81-78-261-511, Fax. 81-78-261-4123, http://www.kobelco.co.jp/english.

Outokumpu**,** http://www.outokumpu.com/.

Oxford Superconducting Technology, 600 Milik St., P.O. Box 429, Carteret, NJ 07008-0429, Tel. 732 541 1300, Fax. 732 541 7769, http://www.oxford-instruments.com/.

Shape Metal Innovations (SMI); Nb_3Sn powder-in-tube (PIT) process, Tel. +31 53 4340704, JLSMI@worldonline.nl.

Sumitomo, One North Lexington Ave., White Plains, NY 10601, Tel. 914-467-6001, Fax. 914-467-6081, http://www.sumitomoelectricusa.com/.

Supercon Inc., 830 Boston Turnpike, Shrewsbury, MA 01545, http://www.supercon-wire.com/.

Western Superconducting Material Technology Corp., P.O. Box 51 Xi'an Shaanxi, 710016 P.R. China.

Low-T_c (MgB_2):

Columbus Superconductor S.R.L., Corso F. Perrone 24, 16152 Genova, Italy, Tel. +39 (0)10 65 98 784, Fax. +39 (0)10 65 98 732.

Diboride Conductors, http://www.diboride.biz/.

Hyper Tech Research, Inc., 110 E. Canal St., Troy, OH 45373-3581, Tel. 937-332-0348, http://www.hypertechresearch.com/.

High-T_c (Bi-2212):

Oxford Superconducting Technology, 600 Milik St., P.O. Box 429, Carteret, NJ 07008-0429, Tel. 732 541 1300, Fax. 732 541 7769, http://www.oxford-instruments.com/.

Showa Electric Wire and Cable Co., Ltd., http://www.swcc.co.jp/eng/index.htm.

High-T_c (Bi-2223):

American Superconductor Corp., Two Technology Drive, Westborough, MA 01581, Tel. 508.836.4200, Fax. 508.836.4248, http://www.amsuper.com/.

European Advanced Superconductor (EAS), Ehrichstraße 10, 63450 Hanau, Germany, Tel. (+49) (6181) 43 84-41 00, Fax. (+49) (6181) 43 84-44 00, http://www.advancedsupercon.com/.

Innova Superconductor Technology Co. Ltd, 7 Rongchang Dongjie, Longsheng Industrial Park, Beijing 100176, People's Republic of China.

Sumitomo, One North Lexington Ave., White Plains, NY 10601, Tel. 914-467-6001, Fax. 914-467-6081, http://www.sumitomoelectricusa.com/.

Trithor GmbH, Heisenbergstrasse 16, D-53359 Rheinbach, Germany, Tel.: +49 (0) 2226 - 90 60 – 0, Fax. +49 (0) 2226 - 90 60 – 900, http://www.trithor.com/.

High-T_c (YBCO):

American Superconductor Corp., Two Technology Drive, Westborough, MA 01581, Tel. 508.836.4200, Fax 508.836.4248, http://www.amsuper.com/.

Fujikura, http://www.fujikura.co.jp/ie_e.html.

SuperPower, 450 Duane Avenue, Schenectady, NY 12304, Tel.: 518/346-1414, Fax. 518/346-6080, http://www.igc.com/superpower/.

Theva GmbH, Rote-Kreuz-Str. 8, D-85737 Ismaning Germany, Tel. +49 89 923346-0, Fax. +49 89 923346-10, info@theva.com, http://www.theva.com/.

Thermometers and accessories (Chapter 5)

Beryllium-oxide high-thermal-conductivity chips:

Lake Shore Cryotronics, Westerville, OH 43081, Tel. 614-891-2244, Fax. 614-818-1600, http://www.lakeshore.com/.

Capacitance bridges:

Automatic bridges—Andeen–Hagerling Inc., Cleveland, OH, Tel. 440-349-0370, Fax. 440-349-0359, http://www.andeen-hagerling.com/.

Capacitance controller card—Lake Shore Cryotronics, Westerville, OH 43081, Tel. 614-891-2244, Fax. 614-818-1600, http://www.lakeshore.com/.

General Radio capacitance bridges (5 digit) available from IET Labs Inc., Westbury, NY, Tel. 800-899-8438, Fax. 516-334-5988, http://www.ietlabs.com/ or Tucker Electronics, Dallas TX, Tel. 800-527-4642, Fax. 214-348-0367, http://www.tucker.com/.

Grease – thermally conducting:

Apiezon N™ grease – Apiezon Products, M & I Materials Ltd., Manchester, UK, Tel. +44 (0)161 864 5419, Fax. +44 (0)161 864 5444, http://www.apiezon.com/.

Cry-Con™ grease – available, for example, from Janis Research Co., Accessories and Ancillary Equipment, http://www.janis.com/.

Thermometers for cryogenic temperatures and calibration services:

Lake Shore Cryotronics, Westerville, OH 43081, Tel. 614-891-2244, Fax. 614-818-1600, http://www.lakeshore.com/.

Oxford Instruments–Cryospares, Witney, Oxfordshire, UK OX294TL, Tel. +44(0)1865 881437, Fax. +44(0)1865 884045, http://www.oxinst.com/cryospares/.

Scientific Instruments, Inc., West Palm Beach FL 33407, Tel. 561-881-8500, Fax. 561-881-8556, http://www.scientificinstruments.com/.

Tinsley Manufacturing, supplier of rhodium–iron resistance thermometers in wire form.

Temperature controllers:

Lake Shore Cryotronics, Westerville, OH 43081, Tel. 614-891-2244, Fax. 614-818-1600, http://www.lakeshore.com/.

Oxford Instruments, Witney, Oxfordshire, UK OX294TL, Tel. +44(0)1865 881437, Fax. +44(0)1865 884045, http://www.oxinst.com/.

Thermocouple wire (Secs. 5.1.1, 5.1.2, 5.1.4, 5.1.6, and 5.5.9)

Omega Engineering, P.O. Box 4047, Stamford, Connecticut 06907-0047, 800-848-4286 or 203-359-1660, Fax. 203-359-7700, http://www.omega.com/.

River Bend Technology Centre, Northbank, Irlam, Manchester M44 5BD, United Kingdom, http://www.omega.co.uk/.

Vacuum accessories (Secs. 3.3.1, 3.7)

C-ring metal seals:

American Seal & Engineering Co., P.O. Box 1038, Orange, CT 06477, 800-878-2442, http://www.ameriseal.com.

Garlock–Helicoflex, P.O. Box 9889, Columbia, SC 20290, Tel. 800-713-1880, http://www.helicoflex.com.

Hydrodyne, 325 Damon Way, Burbank, CA 91505, Tel. 818-841-9667, http://www.hydrodyne.com.

Nicholsons Sealing Technologies Ltd., Hamsterley, Newcastle upon Tyne, UK, NE17 7 SX, Tel. +44 (0)1207 560505, http://www.nicholsons.com.

Dynamic seals: O-rings, spring-loaded PTFE:

Bal Seal Engineering Co., Inc., 620 West Ave., Santa Ana, CA 92707-3398, Tel. 714-557-5192.

Vacuum flanges and fixtures: Ladish Tri-Clover, and ISO KF; available from general vacuum-equipment suppliers such as:

Duniway Stockroom Corp., Tel. 800-446-8811, http://www.duniway.com/.

Kurt J. Lesker Co., Tel. 800-245-1656, http://www.lesker.com/.

O-rings, indium wire:

Indium Corp. of America, 1676 Lincoln Ave., Utica, NY. 13503.

O-rings, metal:

Perkin Elmer, Beltsville, MD, Tel. 301-937-4010.

Screws (silver plated to prevent galling, precleaned, and optionally vented for vacuum systems):

McMaster–Carr, http://www.mcmaster.com/.

U-C Components, Morgan Hill, CA, http://www.uc-components.com/.

Wire (Sec. 4.1, 4.2, and 4.3)

Phosphor-bronze twisted-wire pairs for thermometer leads:

Lake Shore Cryotronics, Westerville, OH 43081, Tel. 614-891-2244, Fax. 614-818-1600, http://www.lakeshore.com/ Quad-Twist™ cryogenic wire.

Pure indium wire for indium O-rings:

Indium Corp. of America, Tel. 315-853-4900 or 800-4-INDIUM, askus@indium.com, http://www.indium.com/.

Stripper (chemical) for polyimide (Kapton™) wire insulation:

Miller–Stephenson chemical, George Washington Hwy., Danbury, CT 06810, Tel. 203-743-4447, Fax. 203-791-8702, support@miller-stephenson.com, MS-111 stripping agent.

A2. Heat-transfer (ref. Chapter 2)

A2.1 Thermal conductivity integrals for technical cryostat materials [a] (see also Fig. 2.1 in Sec. 2.2)

The thermal conductivity integrals tabulated below are referenced to 4 K. Steady-state heat conduction $\dot{q}_{\rm cond}$ through a solid member of uniform cross section A and length L may be determined between two arbitrary temperatures T_1 and T_2 by taking the difference between the two corresponding 4 K integral values:

$$\dot{q}_{\rm cond} \equiv A/L \int_{T1}^{T2} \lambda(T)\, {\rm d}T \;\; = \;\; A/L \, \{ \int_{4K}^{T2} \lambda(T)\, {\rm d}T - \int_{4K}^{T1} \lambda(T)\, {\rm d}T \},$$

where $\lambda(T)$ is the temperature-dependent thermal conductivity.

Data for materials other than those tabulated may be estimated well enough for cryostat-design purposes by using data for similar materials, especially if they have a low thermal conductivity and do not contribute much to the total heat influx. For example, most commercial glasses, as well as many plastics and disordered polymers can be represented (within a factor of about two) by the integral values given for Pyrex™. Values for Manganin can be approximated by those given for Constantan, and values for Inconel and Monel alloys are between those of stainless steel and Constantan.

Greater care must be given to the highly conducting materials. Phosphorus deoxidized copper is the type of copper used most often in pipe, rods, and bars. Electrolytic tough pitch copper is the material from which copper electrical wires are usually made.

The temperature dependence of the thermal conductivity of additional cryostat construction materials is given in Appendix A6.7.

Thermal Conductivity Integrals

	$\int_{4K}^{T} \lambda \, dT$ [kW/m]									[W/m]			
	COPPER		COPPER ALLOYS		ALUMINUM			STAINLESS STEEL	CONST-ANTAN	GLASS	POLYMERS		
T(K)	Elect. Tough Pitch [b]	Phos. Deox.	Be/Cu 98 Cu 2 Be	German Silver 60 Cu 25 Zn 15 Ni	Com-mon Pure 99 Al [b]	Mn/Al 98.5 Al 1.2 Mn plus traces	Mg/Al 96 Al 3.5 Mg plus traces	Average Types 303,304, 316, 347		Average Pyrex™ Quartz Boro-Silicate	Teflon™	Perspex™	Nylon™
6	0.80	0.0176	0.0047	0.00196	0.138	0.0275	0.0103	0.00063	0.0024	0.211	0.113	0.118	0.0321
8	1.91	0.0437	0.0113	0.00524	0.342	0.0670	0.025	0.00159	0.0066	0.443	0.262	0.238	0.0807
10	3.32	0.0785	0.0189	0.010	0.607	0.117	0.0443	0.00293	0.0128	0.681	0.44	0.359	0.148
15	8.02	0.208	0.0499	0.030	1.52	0.290	0.112	0.00816	0.0375	1.31	0.985	0.669	0.410
20	14.0	0.395	0.0954	0.0613	2.76	0.534	0.210	0.0163	0.0753	2.00	1.64	1.01	0.823
25	20.8	0.635	0.155	0.102	4.24	0.850	0.338	0.0277	0.124	2.79	2.39	1.44	1.39
30	27.8	0.925	0.229	0.153	5.92	1.23	0.490	0.0424	0.181	3.68	3.23	1.96	2.08
35	34.5	1.26	0.316	0.211	7.73	1.67	0.668	0.0607	0.244	4.71	4.13	2.59	2.90
40	40.6	1.64	0.415	0.275	9.62	2.17	0.770	0.0824	0.312	5.86	5.08	3.30	3.85
50	50.8	2.53	0.650	0.415	13.4	3.30	1.24	0.135	0.457	8.46	7.16	4.95	6.04
60	58.7	3.55	0.930	0.568	17.0	4.55	1.79	0.198	0.612	11.5	9.36	6.83	8.59
70	65.1	4.68	1.25	0.728	20.2	5.89	2.42	0.270	0.775	15.1	11.6	8.85	11.3
76	68.6	5.39	1.46	0.826	22.0	6.72	2.82	0.317	0.875	17.5	13.0	10.1	13.1
80	70.7	5.89	1.60	0.893	23.2	7.28	3.09	0.349	0.943	19.4	13.9	11.0	14.2
90	75.6	7.20	1.99	1.060	25.8	8.71	3.82	0.436	1.11	24.0	16.3	13.2	17.3
100	80.2	8.58	2.40	1.23	28.4	10.2	4.59	0.528	1.28	29.2	18.7	15.5	20.4
120	89.1	11.5	3.30	1.57	33.0	13.2	6.27	0.726	1.62	40.8	23.7	20.0	26.9

	$\int_{4K}^{T} \lambda \, dT$ [kW/m]									[W/m]			
	COPPER		COPPER ALLOYS		ALUMINUM			STAINLESS STEEL	CONST-ANTAN	GLASS	POLYMERS		
T(K)	Elect. Tough Pitch [b]	Phos. Deox.	Be/Cu 98 Cu 2 Be	German Silver 60 Cu 25 Zn 15 Ni	Com-mon Pure 99 Al [b]	Mn/Al 98.5 Al 1.2 Mn plus traces	Mg/Al 96 Al 3.5 Mg plus traces	Average Types 303,304, 316, 347		Average Pyrex™ Quartz Boro-Silicate	Teflon™	Perspex™	Nylon™
140	97.6	14.6	4.32	1.92	37.6	16.2	8.11	0.939	1.97	54.2	28.7	24.7	33.6
160	106	18.0	5.44	2.29	42.0	19.4	10.1	1.17	2.32	69.4	33.8	29.4	40.5
180	114	21.5	6.64	2.66	46.4	22.5	12.2	1.41	2.69	85.8	39.0	34.2	47.5
200	122	25.3	7.91	3.06	50.8	25.7	14.4	1.66	3.06	103.0	44.2	39.0	54.5
250	142	35.3	11.3	4.15	61.8	33.7	20.5	2.34	4.06	150.0	57.2	51.0	72.0
300	162	46.1	15.0	5.32	72.8	41.7	27.1	3.06	5.16	199.0	70.2	63.0	89.5

[a] Data from:

V. Johnson (1960), NBS, Wright Air Development Div. (WADD) Technical Report 60-56, Part II. U.S. Government Printing Office, Washington, D.C.

D. H. J. Goodall (1970), A.P.T. Division, Culham Science Center, Abingdon, Oxfordshire, UK.

[b] The high thermal conductivity of nearly pure metals is variable and strongly depends on their impurity content; see Sec. 6.4.2.

A2.2 Emissivity of technical materials at a wavelength of about 10 μm (room temperature) (Sec. 2.4)

Material	Emissivity		
	polished	highly oxidized	common condition
Metallic:			
Ag	0.01		
Cu	0.02	0.6	
Au	0.02		
Al	0.03	0.3	
Brass	0.03	0.6	
Soft-solder			0.03
Nb, crystalline, bulk			0.04
Lead	0.05		
Ta	0.06		
Ni	0.06		
Cr	0.07		
Stainless Steel			0.07
Ti			0.09
Tin (gray), single crystal			0.6
Nonmetallic:			
IMI 7031 varnish			0.9
Phenolic lacquer			0.9
Plastic tape			0.9
Glass			0.9

Compiled from:

American Institute of Physics Handbook (1972), 3rd edition, Chapter 6, McGraw–Hill, New York.

M. M. Fulk, M. M. Reynolds, and O. E. Park (1955), *Proc 1954 Cryogenic Eng. Conf.,* Nat. Bur. Stands. (U.S.) Report No. 3517, p. 151. U.S. Government Printing Office, Washington, D.C.

W. H. McAdams (1954), *Heat Transmission*, 3rd edition, McGraw–Hill, New York.

W. T. Ziegler and H. Cheung (1957), *Proc 1956 Cryogenic Engineering Conference,* National Bureau of Standards, p. 100. U.S. Government Printing Office, Washington, D.C.

Emissivities of additional materials at room temperature are available in the technical reference section of *The*

Temperature Handbook (2002), p. Z-171. Omega Engineering Inc., Stamford, Connecticut (http://www.omega.com/).

A2.3 Heat conductance across solid interfaces pressed together with 445 N force (45 kgf or 100 lbf) (Sec. 2.6)

Heat conductance at a force level F other than 445 N can be determined by multiplying these data by the ratio F / 445 N. In addition to these data, see Fig. 2.7 for heat conductance values covering a wide range of temperatures (0.1 K to 300 K) for pressed contacts of gold/gold, indium/copper, copper/copper, and stainless/stainless. Data are also given in Fig. 2.7 for solder, grease, and varnish joints.

Interface Materials	4.2 K	77 K	y *
Gold/Gold	2×10^{-1} W/K [a]		1.3 [a]
Copper/Copper	1×10^{-2} W/K [b]	3×10^{-1} W/K [b]	1.3 [a]
Steel/Steel	5×10^{-3} W/K [b]	3×10^{-1} W/K [b]	
Sapphire/Sapphire	7×10^{-4} W/K [a]		3 [a]

* Values of y are for calculating the heat conductance at temperatures below 4.2 K by using Eq. (2.14) in Sec. 2.6.

[a] R. Berman and C. F. Mate (1958), *Nature* **182**, 1661.

[b] R. Berman (1956), *J. Appl. Phys*. **27**, 318.

A3. Cryostat construction (ref. Chapter 3)

A3.1 High-thermal-conductivity construction-metal properties: RRR, thermal conductivity, and electrical resistivity (Sec. 3.2.2)

RRR ≡ ρ_{293K}/ρ_{4K}, the residual resistivity ratio; [a] λ ≡ thermal conductivity; ρ ≡ electrical resistivity

The thermal conductivities of additional construction materials are shown in Fig. 2.1 and tabulated in Appendix A6.7.

Material	RRR [a,f] ($\equiv\rho_{293K}/\rho_{4K}$)	$\lambda_{293\ K}$ [g] [W/(m·K)]	$\lambda_{4.2\ K}$ [f,h] [W/(m·K)]	$\rho_{293\ K}$ [f,g] [μΩ·cm]	$\rho_{77\ K}$ [f] [μΩ·cm]	Use	Comments
Copper							
High purity (99.999 % pure) [c,d]	~2000	394	~11300	1.68	0.19	Very high thermal-cond. parts.	Thermal conductivity can be increased by annealing; see footnotes c and d.
Oxygen-free [c,d,e]						High thermal-cond. foil, rods, plates, and tubes.	Thermal conductivity can be increased by annealing; see footnotes c and d.
Grade C10100 [b,c,d] (99.99 % pure)	~150	394	~850	1.72	0.19		
Electronic grade C10200 [b,c,d] (99.95 % pure)	~100	390	~560	1.72	0.19		
ETP Grade C11000 [b,c]	~100	390	~560	1.71	—	High thermal-cond. rods, plates, wire, and wire braid.	ETP ≡ electrolytic-tough-pitch copper Contains about 0.3 % oxygen—cannot be used for hydrogen brazing Thermal conductivity of cold-worked ETP copper can be increased by annealing; see footnote c.
Phosphorus deoxidized Grade C12200	3 to 5	339	~14 to 24	2.03	—	Tubes	

Material	RRR [a,f] ($\equiv\rho_{293K}/\rho_{4K}$)	$\lambda_{293\ K}$ [g] [W/(m·K)]	$\lambda_{4.2\ K}$ [f,h] [W/(m·K)]	$\rho_{293\ K}$ [f,g] [μΩ·cm]	$\rho_{77\ K}$ [f] [μΩ·cm]	Use	Comments
Brass	~2.5	125	~4.5	7.2	4.7		
Free cutting brass							
Grade C36000							
Beryllium copper, annealed	1.5 to 2.5	~84	~1.8 to 3.0	6.4 to 10.7	4.2 to 8.5		
Grade C17000–C17300		depends on processing		depends on processing	depends on processing		
Aluminum							
99.999 % high purity	~1000	235	~3400	2.76	0.23		
Grade 1100	~14	222	~45		—		
Grade 6063	~7	218	~22		—		
Grade 5052	~1.4	138	~2.8	4.93	—		

[a] The listed RRR values are nominal and can vary by about 50 % from sample to sample for the purer grades, depending on the amount and type of impurities as well as cold-work condition.

[b] Unified Numbering System (UNS) grade numbers for metals and alloys.

[c] The thermal and electrical conductivity of *deformed* and *coldworked* high-purity, oxygen-free, and ETP copper can be increased (depending on the amount of cold work) by annealing. Heat in vacuum ($\lesssim 10^{-4}$ torr) or argon at about 500 °C for about an hour. If vacuum or argon are not readily available, copper can be heated in air, but a surface scale forms, which can be removed afterward with dilute nitric acid.

[d] Although this is not commonly done, further increase in the thermal and electrical conductivity can be obtained by oxidizing the magnetic iron impurities in high-purity and oxygen-free copper (but not in ETP copper, which contains too many impurities other than iron). The RRR of oxygen-free copper is typically increased from ~100 as received, to ~800 after oxidation; the RRR of high purity (99.99 %) copper is typically increased from ~1500 as received, to more than 10 000 after oxidation. Heat the copper part at about 1000 °C in oxygen at about 0.13 Pa to 1.3 Pa (10^{-3} torr to 10^{-2} torr) pressure. About a day of annealing is required for small parts, up to a month for large copper billets [ref. F. R. Fickett (1974), *Mater. Sci. Eng.* **14**, 199–210].

[e] Sources of oxygen-free copper are not as plentiful as ETP copper, especially in tube form. However, if high-thermal-conductivity tubes are needed or if hydrogen brazing is to be done, oxygen-free copper is required. Suppliers of oxygen-free copper are listed in Appendix A1.7 under Material, copper.

[f] From C. A. Thompson, W. M. Manganaro, and F. R. Fickett (1990), *Cryogenic Properties of Copper,* Wall Chart, NIST, and the references cited therein. U.S. Government Printing Office, Washington D.C.

[g] *Metals Handbook* (1961), Vol. 1, *Properties and Selection of Materials,* 8th edition, ASM International, Materials Park, Ohio.

[h] Calculated from the Wiedemann–Franz–Lorenz law, Eq. (2.4): $\lambda = L_N T / \rho$, where L_N is the Lorenz constant; this results in $\lambda(4.2\ K) = \lambda(293\ K)\ (\rho_{293K}/\rho_{4K})\ (4.2\ K/293\ K)$.

A3.2 Heat conduction along thin-walled stainless-steel tubing [a] *(Sec. 3.2.2)*

The heat conduction values tabulated in this table may be simply scaled to lengths other than 10 cm (inversely proportional) and wall thicknesses other than those listed in column 2 (directly proportional).

The tabulated values of conducted heat assume no gas cooling of the tubing. If the gas boiled off by the conducted heat were to cool the tubing with 100 % efficiency, the resultant heat flow would be 1/10 of the values given for T = 77 K and l/32 of those for T = 300 K.

Tube O.D. [inches]	Wall Thickness [inches (mm)]	Cross Sectional Area [cm^2]	Heat conducted [milliwatts] along 10 cm of tubing with one end at 4 K and the other at: T=77 K	T=300 K
1/8	0.004" (0.10 mm)	0.0098	3.1 mW	30 mW
3/16	0.004" (0.10 mm)	0.0149	4.7	45
1/4	0.004" (0.10 mm)	0.020	6.3	61
3/8	0.006" (0.15 mm)	0.045	14	137
1/2	0.006" (0.15 mm)	0.060	19	184
5/8	0.006" (0.15 mm)	0.075	24	230
3/4	0.006" (0.15 mm)	0.091	29	277
1	0.006" (0.15 mm)	0.121	38	370
1 1/4	0.010" (0.25 mm)	0.251	80	770
1 1/2	0.010" (0.25 mm)	0.302	96	924
2	0.015" (0.38 mm)	0.604	191	1847

All dimensions are in inches.

[a] From:

V. Johnson (1960), NBS, Wright Air Development Div. (WADD) Technical Report 60-56, Part II. U.S. Government Printing Office, Washington, D.C.

D. H. J. Goodall (1970), A.P.T. Division, Culham Science Center, Abingdon, Oxfordshire, UK.

A3.3 Pipe and tubing sizes [a,b] (Sec. 3.5)

	Type K Copper Tubing		Brass Pipe		Steel and PVC Pipe, Schedule 40		Soft Copper Refrigeration Tubing	
Nominal Size [inches]	Internal Diameter	External Diameter	Internal Diameter	External Diameter	Internal Diameter	External Diameter	Internal Diameter	External Diameter
1/8	NA [c]	NA	NA	NA	0.269	0.405	0.065	0.125
1/4	0.30	0.375	0.410	0.540	0.364	0.540	0.190	0.250
3/8	0.40	0.500	0.545	0.675	0.493	0.675	0.311	0.375
1/2	0.53	0.625	0.710	0.840	0.622	0.840	0.436	0.500
5/8	0.65	0.750	NA	NA	NA	NA	0.555	0.625
3/4	0.75	0.875	0.920	1.050	0.824	1.050	0.680	0.750
1	1.00	1.125	1.185	1.315	1.049	1.315		
1-1/4	1.25	1.375	1.530	1.660	1.380	1.660		
1-1/2	1.48	1.625	1.770	1.900	1.610	1.900		
2	1.96	2.125	2.245	2.375	2.067	2.375		
2-1/2	2.44	2.625	2.745	2.875	2.469	2.875		
3	2.91	3.125	3.334	3.500	3.068	3.500		
3-1/2	3.39	3.625	3.810	4.000	3.548	4.000		
4	3.86	4.125	4.296	4.500	4.026	4.500		
5	4.81	5.125	5.298	5.562	5.047	5.562		
6	5.74	6.125	6.309	6.625	6.065	6.625		

[a] From B. Brandt (2002), National High-Field Magnet Laboratory, Florida State University, personal communication.

[b] All dimensions are in inches.

[c] NA ≡ Not Available.

A3.4 Screw and bolt sizes, hexagon socket-head sizes, and load limits (Sec. 3.3.1)

Maximum load and minimum engaged thread length are determined for stainless-steel (SS) bolts assuming a yield strength of 414 MPa (60 ksi). Hexagon socket-head diameters and heights are given to facilitate laying out bolt circles on vacuum flanges.

Screw [a] Size – Number of threads per inch	Major Diam. [inches (mm)]	Nearest Standard Metric Size	Maximum [b] load (SS bolts) [lbf (kN)]	Engaged length [c] (SS into SS) [inches (mm)]	Number [c] engaged threads (SS into SS)	Engaged length (SS into Al) [inches (mm)]	Number engaged threads (SS into Al)	Socket head diameter [d] [inches]		Socket head height [d] [inches]		Tap drill size (inch, number, & letter drills)	Clearance drill size (number & inch drills)
								Max	Min	Max	Min		
0-80	0.0600 (1.524)	M1.6 × 0.35	108 (0.48)	0.0328 (0.833)	2.6	0.0654 (1.66)	5.2	0.096	0.091	0.060	0.057	3/64	51
1-64	0.0730 (1.854)	M2 × 0.4	157 (0.70)	0.0396 (1.01)	2.5	0.0786 (2.00)	5.0	0.118	0.112	0.073	0.070	53	47
1-72	"	"	167 (0.74)	0.0407 (1.03)	2.9	0.0831 (2.11)	6.0	"	"	"	"	53	47
2-56	0.0860 (2.184)	"	222 (0.99)	0.0471 (1.20)	2.6	0.0938 (2.38)	5.3	0.140	0.134	0.086	0.083	50	42
2-64	"	"	236 (1.05)	0.0482 (1.22)	3.1	0.0100 (0.25)	6.4	"	"	"	"	50	42
3-48	0.0990 (2.515)	M2.5 × 0.45	292 (1.30)	0.0539 (1.37)	2.6	0.0107 (0.27)	5.2	0.161	0.154	0.099	0.095	47	37
3-56	"	"	314 (1.40)	0.0558 (1.42)	3.1	0.115 (2.93)	6.5	"	"	"	"	46	37
4-40	0.1120 (2.845)	M3 × 0.5	362 (1.61)	0.0602 (1.53)	2.4	0.118 (2.99)	4.7	0.183	0.176	0.112	0.108	43	31
4-48	"	"	396 (1.76)	0.0625 (1.59)	3.0	0.129 (3.27)	6.2	"	"	"	"	3/32	31
5-40	0.1250 (3.175)	"	477 (2.12)	0.0688 (1.75)	2.8	0.139 (3.53)	5.6	0.205	0.198	0.125	0.121	38	29
5-44	"	"	499 (2.22)	0.0703 (1.79)	3.1	0.145 (3.68)	6.4	"	"	"	"	37	29
6-32	0.1380 (3.505)	M4 × 0.7	545 (2.42)	0.0741 (1.88)	2.4	0.144 (3.65)	4.6	0.226	0.218	0.138	0.134	36	27
6-40	"	"	609 (2.71)	0.0775 (1.97)	3.1	0.161 (4.08)	6.4	"	"	"	"	33	27
8-32	0.1640 (4.166)	"	841 (3.74)	0.0914 (2.32)	2.9	0.186 (4.73)	6.0	0.270	0.262	0.164	0.159	29	18

Screw [a] Size – Number of threads per inch	Major Diam. [inches (mm)]	Nearest Standard Metric Size	Maximum [b] load (SS bolts) [lbf (kN)]	Engaged length [c] (SS into SS) [inches (mm)]	Number [c] engaged threads (SS into SS)	Engaged length (SS into Al) [inches (mm)]	Number engaged threads (SS into Al)	Socket head diameter [d] [inches]		Socket head height [d] [inches]		Tap drill size (inch, number, & letter drills)	Clearance drill size (number & inch drills)
								Max	Min	Max	Min		
8-36	"	"	884 (3.93)	0.0932 (2.37)	3.4	0.196 (4.98)	7.1	"	"	"	"	29	18
10-24	0.1900 (4.826)	M5 × 0.8	1 050 (4.68)	0.103 (2.61)	2.5	0.201 (5.11)	4.8	0.312	0.303	0.190	0.185	26	9
10-32	"	"	1 200 (5.34)	0.109 (2.76)	3.5	0.230 (5.83)	7.3	"	"	"	"	21	9
12-24	0.2160 (5.486)	"	1 450 (6.45)	0.120 (3.05)	2.9	0.244 (6.20)	5.9	—	—	—	—	16	2
12-28	"	"	1 550 (6.88)	0.123 (3.13)	3.5	0.261 (6.62)	7.3	—	—	—	—	15	2
1/4-20	0.2500 (6.350)	M6 × 1.0	1 910 (8.49)	0.138 (3.51)	2.8	0.278 (7.05)	5.6	0.375	0.365	0.250	0.244	7	17/64
1/4-28	"	"	2 180 (9.71)	0.146 (3.71)	4.1	0.318 (8.07)	8.9	"	"	"	"	3	17/64
5/16-18	0.3125 (7.938)	M8 × 1.25	3 150 (14.0)	0.177 (4.48)	3.2	0.366 (9.30)	6.6	0.469	0.457	0.312	0.306	F	21/64
5/16-24	"	M8 × 1.0	3 480 (15.5)	0.185 (4.69)	4.4	0.405 (10.3)	9.7	"	"	"	"	I	21/64
3/8-16	0.3750 (9.525)	M10 × 1.5	4 650 (20.7)	0.214 (5.43)	3.4	0.451 (11.5)	7.2	0.562	0.550	0.375	0.368	5/16	25/64
3/8-24	"	M10 × 1.0	5 270 (23.4)	0.226 (5.75)	5.4	0.511 (12.3)	12.3	"	"	"	"	Q	25/64
7/16-14	0.4375 (11.112)	M12 × 1.75	6 380 (28.4)	0.251 (6.37)	3.5	0.530 (13.5)	7.4	0.656	0.642	0.438	0.430	U	29/64
7/16-20	"	M12 × 1.25	7 120 (31.7)	0.263 (6.68)	5.3	0.592 (15.0)	11.8	"	"	"	"	25/64	29/64
1/2-13	0.5000 (12.700)	M12 × 1.75	8 510 (37.9)	0.289 (7.34)	3.8	0.619 (15.7)	8.1	0.750	0.735	0.500	0.492	27/64	33/63
1/2-20	"	M12 × 1.25	9 600 (42.7)	0.305 (7.74)	6.1	0.698 (17.7)	14.0	"	"	"	"	29/64	33/64
9/16-12	0.5625 (14.288)	M16 × 2.0	10 900 (48.6)	0.327 (8.30)	3.9	0.706 (17.9)	8.5	—	—	—	—	31/64	37/64
9/16-18	"	M16 × 1.5	12 200 (54.2)	0.343 (8.72)	6.2	0.788 (20.0)	14.2	—	—	—	—	33/64	37/64
5/8-11	0.6250 (15.875)	M16 × 2.0	13 600 (60.3)	0.364 (9.25)	4.0	0.790 (20.1)	8.7	0.938	0.921	0.625	0.616	17/32	41/64
5/8-18	"	M16 × 1.5	15 400 (68.3)	0.385 (9.78)	6.9	0.894 (22.7)	16.1	"	"	"	"	37/64	41/64

Screw [a] Size – Number of threads per inch	Major Diam. [inches (mm)]	Nearest Standard Metric Size	Maximum [b] load (SS bolts) [lbf (kN)]	Engaged length [c] (SS into SS) [inches (mm)]	Number [c] engaged threads (SS into SS)	Engaged length (SS into Al) [inches (mm)]	Number engaged threads (SS into Al)	Socket head diameter [d] [inches]		Socket head height [d] [inches]		Tap drill size (inch, number, & letter drills)	Clearance drill size (number & inch drills)
								Max	Min	Max	Min		
3/4-10	0.7500 (19.050)	M20 × 2.5	20 100 (89.3)	0.442 (11.2)	4.4	0.973 (24.7)	9.7	1.125	1.107	0.750	0.740	21/32	49/64
3/4-16	"	M20 × 1.5	22 400 (99.5)	0.464 (11.8)	7.4	1.09 (25.6)	17.4	"	"	"	"	11/16	49/64

Al ≡ aluminum, SS ≡ stainless steel

[a] ANSI screw thread standard.

[b] It is good practice to derate these maximum loads by about a factor of 2 safety margin.

[c] To prevent galling and seizing, especially for stainless steel into stainless steel, use silver-plated stainless-steel bolts or coat them with MoS_2. Sources of such screws are listed in Appendix A1.7 under Vacuum accessories, Screws.

[d] From R. O. Parmley, ed. (1997), *Standard Handbook of Fastening and Joining,* McGraw–Hill.

A3.5 Clearances for various types of fits

When machining parts that need to slip or slide over each other, the required gap varies with the type of fit desired and the diameter of the part. The following table can be used as a rough guide. For more critical parts, follow the detailed specifications in the *Machinery's Handbook* (2000), Industrial Press, Inc., New York.

Be sure to adjust the gap for any difference in thermal contractions between the two materials.

The clearance gaps tabulated below are appropriate only for moving parts that are protected from repeated air exposure. Beware of liquid air films that can freeze movable parts (see the tip in Sec. 1.5.1 for preventing this). Also, the gap between a dip probe and the inner wall of a dewar (or the bore of a magnet) must be much larger than the clearances indicated below. A 1 mm to (preferably) 2 mm gap is needed to accommodate frost that can form on surfaces during repeated insertion and removal of probes from a dewar.

Type of Fit	Approximate Gap for a 1/8th inch (3.2 mm) diameter shaft [10^{-3} inch]	Approximate Gap for a 1 inch (25 mm) diameter shaft [10^{-3} inch]	Approximate Gap for a 5 inch (127 mm) diameter shaft [10^{-3} inch]
Running fit	0.3	1	2
Sliding fit	0.15	0.5	1
Push fit	<0.1	<0.3	<0.4

A3.6 Common braze materials [b,c,d] *(Sec. 3.3.3)*

Braze Materials	T_{melt} [^{o}C]	Comments	Materials Commonly Joined
35%Au–65%Cu	990–1010	For the first two braze materials, make gap 0.02 to 0.08 mm (0.001 to 0.003 inch) (Trade name: NIORO) For NIORO, make gap 0.10 to 0.13 mm (0.004 to 0.005 inch)	For any of the braze materials in this group: SS to SS and SS to Cu [a]
50%Au–50%Cu	955–970		
82%Au–18%Ni eutectic	950		
72%Ag–28%Cu	780	Eutectic mixture (Trade name: CUSIL)	For any of the braze materials in this group: Cu to Cu [a]
63%Ag–27%Cu–10%In	685–730	(Trade name: INCUSIL 10)	
61.5%Ag–24%Cu–14.5%In	630–705	(Trade name: INCUSIL 15)	

[a] Be aware that copper melts at about 1083 ^{o}C.
[b] Available in wire, sheet, powder, and preforms.
[c] Braze stop material (STOPYT) can be used to control unwanted flow.
[d] Materials available from WESGO Division, GTE Prod. Corp., 477 Harbor Blvd., Belmont, CA 94022.

A3.7 Solder: Physical properties [a,b] (Sec. 3.3.4)

Solder materials are generally ordered within each tabulated group according to melting temperature. Additional data on the electrical resistivities of selected solders at 295 K, 77 K, and 4 K are given in Appendix A8.4.

To make strong solder joints, hold the parts together with hand pressure while the solder is still molten, until it solidifies. For machined pieces, the gap between the parts should be as noted in the table, generally in the range of about 0.05 mm to 0.13 mm (0.002 inch to 0.005 inch).

Suppliers of specialty solders are given under the heading of Soldering materials in Appendix A1.7.

Solder	Composition [percent by weight]	Melting Temperature	Mass Density [a] [g/cm^3]	Electrical Cond.[a] [% of Cu]	Thermal Cond.[a] @ 85°C [W/m·K]	Thermal Coef. of Expansion[a] @ 20°C [10^{-6}]	Tensile Strength[a] [MPa]	Comments	Flux
Hard (silver) solder group (Ag–Cu alloys)								Gap should be about 0.05 to 0.1 mm (0.002 to 0.004 inch)	Fluoride flux, Borax, or Boric acid mixed to a paste with alcohol (Wash with hot water after soldering; see Sec. 3.3.4)
	56Ag–22Cu–17Zn–5Sn (Safety Silv #56)	618–649 °C 1144–1200 °F	9.21					Flows freely, ductile	
	45Ag–30Cu–25Zn (ASTM Grade 4)	675–745 °C 1247–1373 °F						Strong	
	20Ag–45Cu–35Zn (ASTM Grade 2)	775–815 °C 1427–1499 °F						Flows readily on melting	

Solder	Composition [percent by weight]	Melting Temperature	Mass Density[a] [g/cm^3]	Electrical Cond.[a] [% of Cu]	Thermal Cond.[a] @ 85^{o}C [W/m·K]	Thermal Coef. of Expansion[a] @ 20^{o}C [10^{-6}]	Tensile Strength[a] [MPa]	Comments	Flux
	70Ag–20Cu–10Zn (ASTM Grade 7) Ag	725–755 °C 1337–1391 °F 960 °C 1760 °F						Malleable and ductile	
Soft–solder group (alloys of Sn and Pb)								Gap should be about 0.05 to 0.13 mm (0.002 to 0.005 inch)	See Table 3.8 to match flux and metal: *Mild*: Rosin, rosin in alcohol, paste of petroleum jelly, $ZnCl_2$ & NH_4Cl *Stronger, corrosive*: $ZnCl_2$ (Zn dissolved in HCl) *Stainless-steel flux, highly corrosive*: $ZnCl_2$ with excess HCl, H_3PO_4 (after soldering, neutralize these fluxes with baking soda and wash with water)

Solder	Composition [percent by weight]	Melting Temperature	Mass Density[a] [g/cm^3]	Electrical Cond.[a] [% of Cu]	Thermal Cond.[a] @ 85^{o}C [W/m·K]	Thermal Coef. of Expansion[a] @ 20^{o}C [10^{-6}]	Tensile Strength[a] [MPa]	Comments	Flux
	63Sn–37Pb (60Sn–40Pb)	183 °C 361 °F	8.4	11.5	50	25.0	52	Eutectic mixture, high quality, general-purpose solder used in electronics	Use pure (not "activated") rosin flux for electrical Cu connections, Sec. 3.3.4
	63Sn–36.65Pb–0.35Sb	183 °C 361 °F						Eutectic mixture, general-purpose solder used for *electrical connections* at low temperatures. Sb helps inhibit embrittlement and cracking from cryogenic thermal cycling.	Use pure (not "activated") rosin flux for electrical Cu connections, Sec. 3.3.4
	96.5Sn–3.5Ag	221 ^{o}C 430 ^{o}F	7.50	16.0	33	30.2	39	Eutectic mixture; stronger than Pb–Sn solders (a common trade name is Staybrite™)	

Solder	Composition [percent by weight]	Melting Temperature	Mass Density [a] [g/cm^3]	Electrical Cond.[a] [% of Cu]	Thermal Cond.[a] @ 85^{o}C [W/m·K]	Thermal Coef. of Expansion[a] @ 20^{o}C [10^{-6}]	Tensile Strength[a] [MPa]	Comments	Flux
	93Pb–5.2Sn–1.8Ag	299 °C 570 °F						Used for *electrical connections* when a higher melting temperature is needed. Low Sn helps inhibit embrittlement and cracking from cryogenic thermal cycling.	Use pure (not "activated") rosin flux for electrical copper connections, Sec. 3.3.4
	97.5Pb–1.0Sn–1.5Ag	309 °C 588 °F						Eutectic higher-melting-temperature solder; widely used in semiconductor assembly	
	92.5Pb–5In–2.5Ag	300–310 °C 572–590 °F	11.02	5.5	25	25.0	31	Higher-melting-temperature solder with minimal Au-leaching properties	

Solder	Composition [percent by weight]	Melting Temperature	Mass Density [a] [g/cm^3]	Electrical Cond.[a] [% of Cu]	Thermal Cond.[a] @ 85^{o}C [W/m·K]	Thermal Coef. of Expansion[a] @ 20^{o}C [10^{-6}]	Tensile Strength[a] [MPa]	Comments	Flux
	95Pb–5Sn	308–312 °C 586–593 °F	11.06	8.8	23	30.0	28	Low-cost high-melting temperature solder. Not recommended for Ag- or Au-plated parts because Sn aggressive dissolves Ag and Au films	
Specialty solder group									
Solders compatible with drinking water	95.5Sn–3.5Cu–1Ag [b]	214–228 °C 417–442 °F						Pb-free solder for potable water Cu pipes; flows well	Any of the mild fluxes
Solders for aluminum	10Sn–90Zn	199 °C 390 °F	7.27	15.0	61		55	Solders Al; eutectic with lowest melting temp.	Reaction flux: contains $ZnCl_2$, tin chloride, or both; must be heated to 280–380^{o}C to work.
	60Sn–40Zn	199–340 °C 390–644 °F						Solders Al; low melting temp.	Reaction flux

Solder	Composition [percent by weight]	Melting Temperature	Mass Density [a] [g/cm^3]	Electrical Cond.[a] [% of Cu]	Thermal Cond.[a] @ 85^{o}C [W/m·K]	Thermal Coef. of Expansion[a] @ 20^{o}C [10^{-6}]	Tensile Strength[a] [MPa]	Comments	Flux
	95Zn–5Al	382 °C 720 °F	6.6					Solders Al; high joint strength	Reaction flux; no flux needed for electronic applications
Solders for thin noble-metal films	66.3In–33.7Bi	72 °C 162 °F	7.99					Eutectic; very low melting temperature solder for thin Ag or Au films and contacting high-T_c superconductors; low strength	Mild $ZnCl_2$ solution for soldering to Cu; no flux needed for Ag if surfaces are freshly made and clean
	97In–3Ag	143 °C 290 °F	7.38	23.0	73	22.0	5.5	Eutectic; low leaching solder for thin Ag or Au films and contacting high-T_c superconductors	Mild $ZnCl_2$ solution for Cu; no flux needed for Ag if surfaces are freshly made and clean
Solders for difficult-to-solder materials	52In–48Sn	118 °C 244 °F	7.30	11.7	34	20.0	11.8	Eutectic; low melting temperature; higher yield strength; Sn leaches Ag or Au films	Mild $ZnCl_2$ solution for Cu

Solder	Composition [percent by weight]	Melting Temperature	Mass Density [a] [g/cm^3]	Electrical Cond.[a] [% of Cu]	Thermal Cond.[a] @ 85^{o}C [W/m·K]	Thermal Coef. of Expansion[a] @ 20^{o}C [10^{-6}]	Tensile Strength[a] [MPa]	Comments	Flux
	50In–50Sn	116–126 °C 241–259 °F	7.30	11.7	34	20.0	11.8	Wets glass readily.	
	In	157 °C 315 °F	7.31	24.0	86	29.0	1.9	Low strength; wets glass	No flux needed for wetting glass, but clean surfaces required; mild $ZnCl_2$ flux needed for soldering to Cu-based materials
	62Sn–36Pb–2Ag	179 °C 354 °F	8.41	11.9	50	27.0	44	Eutectic; higher strength, moderate melting-temperature solder	
Solders for low thermoelectric voltage	70.44Cd–29.56Sn							Very low thermo-electric power with respect to copper near room temperature. Contains cadmium, whose fumes are TOXIC.	

Solder	Composition [percent by weight]	Melting Temperature	Mass Density[a] [g/cm^3]	Electrical Cond.[a] [% of Cu]	Thermal Cond.[a] @ 85^{o}C [W/m·K]	Thermal Coef. of Expansion[a] @ 20^{o}C [10^{-6}]	Tensile Strength[a] [MPa]	Comments	Flux
	97In–3Ag	143 °C 290 °F						Eutectic; a NON-TOXIC alternative to low-thermo-electric-voltage Cd-based solder; In and Ag have thermoelectric powers close to Cu; stronger than pure In	Mild $ZnCl_2$ solution for soldering to Cu
Very low melting-temp. solder group (Alloys of Bi with Pb, Sn, Cd, and In)								As a class, Bi-based solders expand on solidification and are weak and brittle.	Corrosive $ZnCl_2$ solution usually required; pre-tin parts at higher temp. ($\gtrsim$ 300 ^{o}C) to activate flux
	49Bi–18Pb–12Sn–21In	58 °C 136 °F	9.01	2.43	10	23.0	43	Eutectic alloy; expands slightly on solidification and then shrinks slowly over several hours.	

Solder	Composition [percent by weight]	Melting Temperature	Mass Density [a] [g/cm^3]	Electrical Cond.[a] [% of Cu]	Thermal Cond.[a] @ 85^{o}C [W/m·K]	Thermal Coef. of Expansion[a] @ 20^{o}C [10^{-6}]	Tensile Strength[a] [MPa]	Comments	Flux
	50Bi–25Pb–12.5Sn–12.5Cd (Wood's metal)	65–70 °C 149–158 °F	9.60	3.1			31	Contains Cd, whose fumes are TOXIC. Similar to Ostalloy® 158	
	50Bi–26.7Pb–13.3Sn–10Cd (Cerrobend)	70 °C 158 °F	9.58	4.0	18	22.0	41	Contains Cd, whose fumes are TOXIC.	
	66.3In–33.7Bi	72 °C 162 °F	7.99					Eutectic; very low melting temperature solder for thin Ag or Au films and contacting high-T_c superconductors; low strength	Mild $ZnCl_2$ solution
	55.5Bi–44.5Pb (Cerrobase)	124 °C 255 °F	10.44	4.0	4		44	Contracts slightly on solidification	

[a] Indium Corp. of America, http://www.indium.com/

[b] J. Ross (2002), Canfield Corp., personal communication

A3.8 Solder fluxes for soft-soldering common metals and alloys [a] (Sec. 3.3.4)

Material	Flux		
	Mild [b]	Corrosive [c]	Special Flux and/or Solder [d]
Aluminum			•
Aluminum–Bronze			•
Beryllium Copper		•	
Brass	•	•	
Copper	•	•	
Copper–Chromium		•	
Copper–Nickel		•	
Copper–Silicon		•	
Gold	•		
Inconel	•		
Lead	•	•	
Magnesium			•
Monel		•	
Nickel		•	
Nichrome			•
Platinum	•		
Silver	•	•	
Stainless Steel			•
Steel		•	
Tin	•	•	
Tin–Zinc	•	•	
Zinc		•	

[a] Information from J. F. Smith and D. M. Borcina, Lead Industries Assoc., Inc., New York, New York.

[b] Mild fluxes: rosin, rosin in alcohol, paste of petroleum jelly, zinc chloride, or ammonium chloride. After soldering, wash away flux with a solution of soap and water, or isopropanol. Be aware that fluxes other than pure rosin, or rosin dissolved in alcohol, will leave chloride residues trapped in the solder that eventually react with ambient moisture to form hydrochloric acid, which attacks electronic circuits and perforates thin (0.1 mm) stainless-steel tubing. For soldering copper electronic circuitry, use only pure rosin flux, not "activated" rosin flux or pastes. See Sec. 3.3.4 for more information.

[c] Corrosive flux: zinc-chloride solution (zinc dissolved in hydrochloric acid). After soldering, wash away flux with water or isopropanol; then neutralize the pH by blotting the area with a baking-soda/water solution or ammonia/detergent/water solution.

[d] Special Flux and/or Solder: Appendix A3.7 has information on highly-corrosive stainless-steel soldering fluxes as well as types of solders and fluxes that work with aluminum. After soldering, wash away corrosive acid fluxes with water or isopropanol; then neutralize the pH by blotting the area with a baking-soda/water solution or ammonia/detergent/water solution.

A3.9 Solder: Superconducting properties [a] *(Sec. 3.3.4)*

$T_c \equiv$ superconducting transition temperature of the solder
$H_c \equiv$ superconducting critical field of the solder

Solder [wt%]	T_c [K]	H_c (1.3K) [T]	Melting Temperature [^oC]
60Sn–40Pb	7.05	0.08	182–188
50Sn–50Pb	7.75	0.20	182–216
30Sn–70Pb	7.45	0.15	182–257
95Sn–5Sb	3.75	0.036	232–240
50In–50Sn	7.45	0.64	117–125
50In–50Pb	6.35	0.48	180–209
97.5Pb–1.0Sn–1.5Ag	7.25	0.11	309

[a] From W. H. Warren and W. G. Bader (1969), *Rev. Sci. Instrum.* **40**, 180–182.

A3.10 Sticky stuff for cryogenic applications (Sec. 3.3.5)

Material	Application and comments
Epoxies	
Araldite Type 1 ™ [a]	
Eccobond 2 ™ [b]	Low-viscosity, unfilled epoxy. Robust and good adhesion at cryogenic temperatures.
Scotch-Weld DP-460™ [c]	High performance urethane, two-part epoxy, Duo-Pak™ cartridge.
Silver-based epoxy [d]	Electrically and thermally conductive epoxy.
Stycast 1266™ [e]	Low-viscosity, unfilled epoxy. High thermal expansion, but thin films of this epoxy do not crack and provide good adhesion at cryogenic temperatures. Crack resistance can be improved by heating to 90 ^{o}C for 4 h after epoxy has hardened.
Stycast 2850 FT™ [e]	High-viscosity epoxy; filled with silica powder to provide a low thermal expansion matching that of copper.
Tapes	
Fiberglass Electrical Tape	Tough under cryogenic cycling and withstands cycling to higher-temperatures when soldering.
Kapton™ Tape	A robust tape, well suited for providing tough, durable electrical insulation between cryostat parts.
Masking Tape	All-purpose tape. The adhesion improves with thermal cycling. Tape becomes brittle with age and eventually becomes difficult to remove.
Mylar™ Electrical Tape (3M #56*f*, "yellow" tape)[f]	Maintains adhesion better than Kapton™ tape upon cryogenic cycling, but thinner (10^{-3} inch) and therefore better suited for applications where strength is not paramount. Commonly used for electrically isolating samples from Cu sample holders. Dielectric strength is 5500 V.

Material	Application and comments
Teflon™ Pipe-thread Tape	Excellent for wrapping wires to supports structure for mechanical support, or fastening samples to sample holders, especially where you do not want to deal with sticky tape that is hard to remove. For the same reason, this is also the best tape for corralling fine delicate wires. To protect small wires from mechanical damage, place a layer of tape *under* the wires as well as over them when wrapping them to a support structure.
Varnish and Glues	
Bostik™ Multibond Glue [g]	All-purpose glue that holds well at cryogenic temperatures. Easier to work with if thinned with acetone or methyl-ethyl-ketone.
Duco™ Household Cement (model-airplane glue)	All-purpose glue that survives thermal cycling well. Can be thinned or removed with acetone. Not good for wires because the acetone dissolves varnish insulation. Good for sticking samples to the sample rod in a vibrating sample magnetometer.
IMI 7031™ varnish (formerly GE 7031™) varnish [h]	Easier to work with if thinned to the consistency of water with ethanol (acetone also acts as a thinner, but it makes the varnish stringy and eats wire insulation). Baking the varnish under a heat lamp decreases drying time.
Loctite™ [i]	Low viscosity adhesive used in machine shops as a substitute for lock nuts, interference fits, or silver soldering. Good for securing tight-fitting metal parts. Cures at room temperature, but can be loosened by moderate heating with a torch. Works OK at cryogenic temperatures.
White Shellac	Useful for adhering sapphire to sapphire.
Miscellaneous	
Apiezon™ Black Wax [j]	Meltable adhesive.
Beeswax, and Alox 350™ (T_{melt}=38 °C to 43 °C), and Alox 2138F™ (T_{melt}=71 °C)[k]	Low-strength fillers. Although they yield at low stress, they are sometimes useful as magnet-coil filling agents to minimize the probability of thermal-runaway events that can otherwise result from microfracturing of epoxies used to impregnate superconducting coils.
BluTack™ [l]	A gummy clay-like adhesive for generally attaching leads to support structures or mechanically holding almost anything in place.
Dental Floss (waxed or no-wax)	Excellent for tying things together (like samples to samples holders) and overwrapping fragile instrumentation leads wound onto heat sinks. Waxed floss is a little easier to stick in place during wrapping and tying.

Material	Application and comments
Silver paste [d]	Electrically and thermally conductive weak adhesive.

Suppliers of specialty materials include:

[a] Ciba Specialty Chemicals Corp, 4917 Dawn Ave., East Lansing, MI 48823, Tel. 517-351-5900, Fax 517-351-9003, http://www.araldite.com/

[b] Emerson and Cuming Corp., http://www.emersoncuming.com/

[c] 3M, http://www.3M.com/; distributed by MSC Industrial Supply, PN: 65861684, (Duo-Pak cartridge PN: 65861569), Tel. 800-645-7270, http://www.mscdirect.com/; or McMaster–Carr Supply Co., PN: 7467A26, http://www.mcmaster.com/

[d] Ted Pella, Inc., P.O. Box 492477, Redding, CA 96049-2477, Tel. 800-237-3526; Fax. 530-243-3761, http://www.TedPella.com/

[e] Emerson & Cumming, http://www.emersoncumming.com/

[f] Essex Brownell Inc., 4670 Shelby Drive, Memphis, TN 38118, Tel. 800-805-4636, Fax. 219-461-4165; or from http://www.mpsupplies.com/3mtape56.html

[g] Bostik Pty. Ltd., 51–71 High Street, Thomastown, Vic., Australia 3074, Tel 3-465-5211

[h] Insulating Materials Inc., 1 W. Campbell Rd., Schenectady, NY 12306, Tel. 518-395-3200, Fax. 518-395-3300; small quantities available from Lake Shore Cryotronics, Westerville, OH 43081, Tel. 614-891-2244, Fax. 614-818-1600, http://www.lakeshore.com/

[i] Loctite, a Hendel Company, http://www.loctite.com/

[j] Apiezon Products, M&I Materials Ltd., P.O. Box 136, Manchester, M601AN, England. Tel. +44 161 875 4442, http://www.apiezon.com/

[k] Alox Corp., Niagara Falls, NY

[l] Bostik Findley, http://www/bostikfindley-us.com/

A3.11 Slippery stuff for cryogenic applications

Material	Application and comments
Lubricant coatings	
Graphite	Available as dry powder or spray-on coatings
Molybdenum disulfide	Spray coatings; good for higher forces
Teflon ™	Spray coatings, low coefficient of friction
Thicker lubricant coatings	
Emralon ® [a]	Flurocarbon lubricant in an epoxy mixture for thicker lubricating coatings or for making cast parts with a low coefficient of friction
Bearing materials	
Kel-F ™ [b]	Polychlorotrifluoroethylene. Stronger than Teflon ™
Nylon ™	Stronger than Teflon™, but higher coefficient of friction
Teflon ™	Polyamide, low coefficient of friction, but softer than other materials
Teflon™ materials reinforced with Nylon™, fiberglass and other materials	
Flurogold ® [c]	Reinforced Teflon™
Parmax ® [d]	High strength polymer, similar uses as Torlon ™
Rulon ® [b]	Teflon reinforced with Nylon, fiberglass, or other materials; available in various formulations. Type J has the lowest coefficient of friction of the Rulon® series. Applications include retainer rings for cryogenic ball-bearing raceways.
Teflon-coated Kapton ™ [e]	Useful, for example, as a cryogenic gasket material since the Teflon™ coating deforms for good sealing, but the stronger Kapton™ base keeps the gasket from extruding.

Material	Application and comments
Torlon ™ [e]	PolyAmide-Imide (Teflon™-Kapton™ combination) high strength polymer used for wear and friction parts. Capable of performing under continuous stress at temperatures to 260°C. Low coefficient of linear thermal expansion and high creep resistance provide good dimensional stability. Available as sheet, rod, or tube.

[a] Acheson Colloids Co., http://www.achesonindustries.com/
[b] San Diego Plastics, Inc., http://www.sdplastics.com/
[c] Granor Rubber and Engineering, http://www.granor.com.au/, Conroy & Knowlton Inc., http://conroyknowlton.com/materials.htm
[d] Mississippi Polymer Technologies, http://www.mptpolymers.com/
[e] Boedeker, http://www.boedeker.com/

A3.12 Degassing rates of synthetic materials [a] *(Sec. 3.8.3)*

Degassing rates of *metals* are given in Fig. 3.18.

Material	Degassing rate at room temperature before baking [$Pa \cdot m^3 \cdot s^{-1} \cdot m^{-2}$]	Baking temperature [^oC]	Degassing rate at room temp. after 24 h bake [$Pa \cdot m^3 \cdot s^{-1} \cdot m^{-2}$]
Araldite ATI™ epoxy [b]	3.4×10^{-4}	85	—
Mycalex™ [b]	2.7×10^{-6}	300	—
Nylon 31™ [b]	1.1×10^{-4}	120	8.0×10^{-7}
Perspex™ [b]	1.3×10^{-5}	85	7.8×10^{-6}
Polythene™ [b]	4.0×10^{-4}	80	6.6×10^{-6}
PTFE (Teflon™) [c]	2.0×10^{-4}	—	4.7×10^{-7} [a]
Viton A™ [b]	1.3×10^{-4}	200	2.7×10^{-6}
Polyimide (Kapton™) [d]	—	200*	6.6×10^{-8}
	—	300*	4.0×10^{-8}
Kalrez™ [e]	—	300	4.0×10^{-8}
Viton E60C™ [e]	—	150	$\sim 1 \times 10^{-6}$
	—	300	3.0×10^{-8}

* 12 h bake

[a] Compiled by G. F. Weston (1985), *Ultrahigh Vacuum Practice,* Butterworth, London.

[b] R. S. Barton and R. P. Govier (1965), *J. Vac. Sci. Tech.* **2**, 113.

[c] B. B. Dayton (1959), *Trans. 6th Nat. Symp. Vac. Technol., I*, p. 101.

[d] P. W. Hait (1967), *Vacuum* **17,** 547.

[e] L. DeChernatony (1977), *Vacuum* **27**, 605.

A3.13 Vapor pressures of metals [a] *(Sec. 3.8.3)*

Tabulated values in the three right-hand columns are expressed as the temperature required to produce the vapor pressures indicated at the head of each column.

These data are plotted in Figs. 3.19a and 3.19b.

Metal	Melting Temperature [K]	Temperature [K] giving a vapor pressure P		
		$P = 1.33\times10^{-9}$ Pa	$P = 1.33\times10^{-7}$ Pa	$P = 1.33\times10^{-5}$ Pa
Ag Silver	1234	721	800	899
Al Aluminum	932	815	906	1015
Au Gold	1336	915	1020	1150
Ba Barium	983	450	510	583
Be Beryllium	1556	832	925	1035
C Carbon	—	1695	1845	2030
Ca Calcium	1123	470	524	590
Cd Cadmium	594	293	328	368
Ce Cerium	1077	1050	1175	1325
Co Cobalt	1768	1020	1130	1265
Cr Chromium	2176	960	1055	1175
Cs Cesium	302	213	241	274
Cu Copper	1357	855	945	1060
Fe Iron	1809	1000	1105	1230
Ge Germanium	1210	940	1030	1150
Hg Mercury	234	170	190	214
In Indium	429	641	716	812
Ir Iridium	2727	1585	1755	1960
K Potassium	336	247	276	315
La Lanthanum	1193	1100	1220	1375
Mg Magnesium	923	388	432	487
Mn Manganese	1517	660	734	827
Mo Molybdenum	2890	1610	1770	1975
Na Sodium	371	294	328	370
Ni Nickel	1725	1040	1145	1270
Pb Lead	601	516	580	656

Metal	Melting	Temperature [K] giving a vapor pressure P		
	Temperature [K]	$P = 1.33\times10^{-9}$ Pa	$P = 1.33\times10^{-7}$ Pa	$P = 1.33\times10^{-5}$ Pa
Pd Palladium	1823	945	1050	1185
Pt Platinum	2043	1335	1480	1655
Re Rhenium	3463	1900	2100	2350
Rh Rhodium	2239	1330	1470	1640
Sb Antimony	903	447	526	582
Se Selenium	490	286	317	356
Sn Tin	505	805	900	1020
Sr Strontium	1043	433	483	546
Ta Tantalum	3270	1930	2120	2370
Th Thorium	1968	1450	1610	1815
Ti Titanium	1940	1140	1265	1410
W Tungsten	3650	2050	2270	2520
Zn Zinc	693	336	374	421
Zr Zirconium	2128	1500	1665	1855

[a] From G. F. Weston (1985), *Ultrahigh Vacuum Practice*, Butterworth, London, who extracted the data from compilations by R. E. Honig (1962), *RCA Rev.* **23**, 567; and R. E. Honig (1969), *RCA Rev.* **30**, 285.

A3.14 Gas permeation constant at room temperature for synthetic materials [a] [for use with Eq. (3.27) of Sec. 3.8.3]

Additional gas permeations rates are given for:

- helium through glass in Fig. 3.20
- helium through ceramics in Fig. 3.21
- hydrogen through metals in Fig. 3.22.

	Permeation constant K in [$m^2\ s^{-1}$] at 23 °C				
Material	Nitrogen	Oxygen	Hydrogen	Helium	Argon
Polythene™ [b]	9.9×10^{-13}	3.0×10^{-12}	8.2×10^{-12}	5.7×10^{-12}	2.7×10^{-12}
PTFE (Teflon™) [b]	2.5×10^{-12}	8.2×10^{-12}	2.0×10^{-11}	5.7×10^{-10}	4.8×10^{-12}
Perspex™ [b]	—	—	2.7×10^{-12}	5.7×10^{-12}	—
Nylon 31™ [b]	—	—	1.3×10^{-13}	3.0×10^{-13}	—
Polystyrene™ [b]	—	5.1×10^{-13}	1.3×10^{-11}	1.3×10^{-11}	—
Polystyrene™ [c]	6.4×10^{-12}	2.0×10^{-11}	7.4×10^{-11}	-	—
Polyethylene™ [c]	$6–11 \times 10^{-13}$	$2.5–3.4 \times 10^{-12}$	$6–12 \times 10^{-12}$	$4–5.7 \times 10^{-12}$	—
Mylar 25-V-200™ [c]	—	—	4.8×10^{-13}	8.0×10^{-13}	—
CS2368B (Neoprene™) [b]	2.1×10^{-13}	1.5×10^{-12}	8.2×10^{-12}	7.9×10^{-12}	1.3×10^{-12}
Viton A™ [b]	—	—	2.2×10^{-12}	8.2×10^{-12}	—
Polyimide (Kapton™) [d]	3.2×10^{-14}	1.1×10^{-13}	1.2×10^{-12}	2.1×10^{-12}	—

[a] Compiled by G. F. Weston (1985), *Ultrahigh Vacuum Practice,* Butterworth, London.
[b] J. R. Bailey (1964), *Handbook of Vacuum Physics,* Vol. 3, Part 4, Pergamon Press.
[c] D. W. Brubaker and K. Kammermeyer, *Ind. Eng., Chem.* **44**, 1465 (1952); **45**, 1148 (1953); **46**, 733 (1954).
[d] D. E. George, in an article by W. G. Perkins (1973), *J. Vac. Sci. Technol.* **10**, 543.

A4. Cryogenic apparatus wiring (ref. Chapter 4)

A4.1a Wire gauge size, area, resistivity, heat conduction, and optimum current (Secs. 4.1, 4.2, and 4.9.1)

To obtain the resistance-per-length for wire materials other than copper, multiply the room-temperature values for copper in the fourth column of the table by the ratio $\rho_{293K}/\rho_{Cu\ 293K}$, where ρ_{293K} and $\rho_{Cu\ 293K}$ are the resistivity values of the new material and copper, respectively. Ratio values for several common wire materials at room temperature follow the table.

At 77 K and 4.2 K, the resistance-per-length may be similarly calculated by using the low-temperature resistivity data given in Appendix A4.2.

In practice, resistivity values may vary from those tabulated below because of different impurity concentrations, alloy concentrations, and heat treatments.

American Wire Gauge (AWG) and *Brown & Sharpe* (B&S) are the same gauge.

The nearest common *metric* wire sizes are given in the next table, A4.1b.

American Wire Gauge (AWG) or Brown & Sharpe (B&S)	Diameter 20°C [a] [mm]	Cross-sectional area at 20°C [a] [mm^2]	Resistance of annealed copper wire at 20°C [a] [Ω/km]	Heat conducted along 1 m of copper wire between the indicated temperatures [b] [W]			Optimum current for 1 m of copper wire with one end at 4 K and the other at temperature T_{upper} [c] [A]	
				300K–4.2K	300K–76K	76K–4.2K	T_{upper} = 290K	T_{upper} = 77K
0000	11.68	107.2	0.161	17.4	10.0	7.35	536	1072
000	10.40	85.03	0.203	13.8	7.94	5.83	425	850
00	9.266	67.43	0.256	10.9	6.30	4.62	337	674
0	8.252	53.48	0.322	8.66	5.00	3.67	267	535
1	7.348	42.41	0.407	6.87	3.96	2.91	212	424
2	6.543	33.63	0.513	5.45	3.14	2.31	168	336
3	5.827	26 67	0.646	4.32	2.49	1.83	133	267

American Wire Gauge (AWG) or Brown & Sharpe (B&S)	Diameter 20°C [a] [mm]	Cross-sectional area at 20°C [a] [mm^2]	Resistance of annealed copper wire at 20°C [a] [Ω/km]	Heat conducted along 1 m of copper wire between the indicated temperatures [b] [W]			Optimum current for 1 m of copper wire with one end at 4 K and the other at temperature T_{upper} [c] [A]	
				300K–4.2K	300K–76K	76K–4.2K	T_{upper} = 290K	T_{upper} = 77K
4	5.189	21.15	0.815	3.43	1.98	1.45	106	212
5	4.621	16.77	1.03	2.72	1.57	1.15	84	168
6	4.115	13.30	1.30	2.15	1.24	0.912	66	133
7	3.665	10.55	1.63	1.71	0.985	0.724	53	106
8	3.264	8.366	2.06	1.36	0.781	0.574	42	84
9	2.906	6.634	2.60	1.08	0.620	0.455	33	66
10	2.588	5.261	3.28	0.852	0.491	0.361	26	53
11	2.305	4.172	4.13	0.676	0.390	0.286	21	42
12	2.053	3.309	5.21	0.536	0.309	0.227	16	33
13	1.828	2.624	6.57	0.425	0.245	0.180	13	26
14	1.628	2.081	8.28	0.337	0.194	0.143	10	21
15	1.450	1.650	10.4	0.267	0.154	0.113	8.2	16
16	1.291	1.309	13.2	0.212	0.122	0.0898	6.5	13
17	1.150	1.038	16.6	0.168	0.0969	0.0712	5.2	10
18	1.024	0.8231	21.0	0.133	0.0769	0.0565	4.1	8.2
19	0.9116	0.6527	26.4	0.106	0.0610	0.0446	3.3	6.5
20	0.8118	0.5176	33.3	0.0838	0.0483	0.0355	2.6	5.2
21	0.7230	0.4105	42.0	0.0665	0.0383	0.0282	2.0	4.1
22	0.6439	0.3255	53.0	0.0527	0.0304	0.0223	1.6	3.2
23	0.5733	0.2582	66.8	0.0418	0.0241	0.0177	1.3	2.6
24	0.5105	0.2047	84.2	0.0332	0.0191	0.0140	1.0	2.0
25	0.4547	0.1624	106	0.0263	0.0152	0.0111	0.81	1.6

American Wire Gauge (AWG) or Brown & Sharpe (B&S)	Diameter 20°C [a] [mm]	Cross-sectional area at 20°C [a] [mm^2]	Resistance of annealed copper wire at 20°C [a] [Ω/km]	Heat conducted along 1 m of copper wire between the indicated temperatures [b] [W]			Optimum current for 1 m of copper wire with one end at 4 K and the other at temperature T_{upper} [c] [A]	
				300K–4.2K	300K–76K	76K–4.2K	T_{upper} = 290K	T_{upper} = 77K
26	0.4049	0.1288	134	0.0209	0.0120	0.00884	0.64	1.3
27	0.3606	0.1021	169	0.0165	0.00954	0.00700	0.51	1.0
28	0.3211	0.08098	213	0.0131	0.00756	0.00556	0.40	0.81
29	0.2859	0.06422	268	0.0104	0.00600	0.00440	0.32	0.64
30	0.2548	0.05093	339	0.00825	0.00476	0.00349	0.25	0.51
31	0.2268	0.04039	427	0.00654	0.00377	0.00277	0.20	0.40
32	0.2019	0.03203	538	0.00519	0.00299	0.00220	0.16	0.32
33	0.1798	0.02540	679	0.00411	0.00237	0.00174	0.13	0.25
34	0.1601	0.02014	856	0.00326	0.00188	0.00138	0.10	0.20
35	0.1426	0.01597	1080	0.00259	0.00149	0.00110	0.080	0.16
36	0.1270	0.01267	1360	0.00205	0.00118	0.000869	0.063	0.13
37	0.1131	0.01005	1720	0.00163	0.000939	0.000689	0.050	0.10
38	0.1007	0.007967	2160	0.00129	0.000744	0.000546	0.040	0.080
39	0.08969	0.006318	2730	0.00102	0.000590	0.000433	0.032	0.063
40 [d]	0.07988	0.005010	3440	0.000812	0.000468	0.000344	0.025	0.050

[a] Data obtained partially from calculations (see following footnotes) and partially from tabulations in the *CRC Handbook of Chemistry and Physics* (1987; 2002), CRC Press, Inc., Boca Raton, Florida; and from the *Machinery's Handbook* (2000), 26th edition, Industrial Press, New York.

[b] Heat conduction for a length other than 1 m is obtained by dividing the values in the table by the desired wire length (in meters). In obtaining the values for heat conduction, it was assumed that there was no gas cooling of the wire. If helium gas boil-off were used to cool the wire with maximum efficiency, the resultant heat flow would be 1/12 of the values given for an upper temperature of 300 K, and 1/4 of the values shown for 77 K. Calculations were based on the thermal conductivity integrals of electrolytic-tough-pitch (ETP) copper, Appendix A2.1. From V. Johnson (1960), National Bureau of Standards; Wright Air Development Division (WADD) Technical Report 60-56, Part II; and D. H. J. Goodall (1970), A.P.T. Division, Culham Laboratory.

[c] Optimum current is for steady-state operation. For wires that carry current with only a low duty cycle, the optimum current should be adjusted to a higher value because in that case the Joule heating is intermittent, whereas the heat flow down the current lead is continuous. Optimum current for a length other than 1 m is obtained by dividing the values in the table by the desired wire length (in meters). Values were calculated from Eqs. (4.1) and (4.2) in Sec. 4.9.1, which were derived by R. McFee (1959), *Rev. Sci. Instrum.* **30**, 98–102.

[d] For wire sizes smaller than #40 AWG, the diameter can be calculated by using a ratio of 1 : 1.123 for consecutive AWG sizes.

Room-temperature resistivities for several common wire materials relative to copper.

These ratios can be used to obtain the resistance-per-length for wire materials other than copper by multiplying the room-temperature values given for copper in the fourth column of the above table by the ratio $\rho_{293K}/\rho_{Cu\ 293K}$. (Calculated from Appendix A4.2 and the *CRC Handbook of Chemistry and Physics* 2002.)

Material	$\rho_{293\ K}/\rho_{Cu\ 293\ K}$
Aluminum	1.579
Brass (70%Cu–30%Zn)	3.62
Constantan	29
Manganin	28
Nichrome	64
Phosphor Bronze	7.5
Platinum	6.26
Silver	0.946
Tungsten	3.15

A4.1b Wire gauge: Metric and American Wire Gauge (AWG) size comparison (Secs. 4.1 and 4.2)

American Wire Gauge (AWG) or Brown & Sharpe (B&S)	Nearest common metric gauge wire diameter at 20°C [mm]	Metric wire cross-sectional area at 20°C [mm^2]	Resistance of annealed copper wire at 20°C [Ω/km]
5	4.750	17.72	1.0
6	4.250	14.19	1.2
7	3.750	11.04	1.5
8	3.350	8.814	1.9
9	2.800	6.158	2.8
10	2.500	4.910	3.5
11	2.240	3.941	4.3
12	2.000	3.142	5.4
13	1.800	2.545	6.7
14	1.600	2.011	8.5
15	1.400	1.539	11.1
16	1.250	1.227	13.9
17	1.120	0.9852	17.4
18	1.000	0.7854	21.8
19	0.900	0.636	26.9
20	0.800	0.503	34.0
21	0.710	0.396	43.2
22	0.630	0.312	54.8
23	0.560	0.246	69.4
24	0.500	0.196	87.1
25	0.450	0.159	108
26	0.400	0.126	136
27	0.355	0.0990	173
28	0.315	0.0779	219
29	0.280	0.0616	278
30	0.250	0.0491	348
31	0.224	0.0394	434
32	0.200	0.0314	544

American Wire Gauge (AWG) or Brown & Sharpe (B&S)	Nearest common metric gauge wire diameter at 20°C [mm]	Metric wire cross-sectional area at 20°C [mm^2]	Resistance of annealed copper wire at 20°C [Ω/km]
33	0.180	0.0255	672
34	0.160	0.0201	850
35	0.140	0.0154	1110
36	0.125	0.0123	1390
37	0.112	0.00985	1740
38	0.100	0.00785	2180
39	0.090	0.0064	2700
40	0.080	0.0050	3400

A4.2 Physical properties of common wire materials: Composition, resistivity, melting temperature, thermal expansion, magnetoresistance, and magnetic susceptibility [a] *(Sec. 4.2)*

Wire Material	Chemical Composition	Resistivity at 293 K at 77 K at 4.2 K [μΩ·cm]	Melting Range	Coef. Thermal Expansion [$^oC^{-1}$]	Magnetores. $\Delta R/R_0$ @ 4.2 K and 10 T (perpendicular to wire) [d]	Volume Susceptibility [SI]
Copper (ETP)	100 wt% Cu	1.68 0.21 ~0.02	1056–1083°C	1.68×10^{-5} (20–100°C)	188 % [f]	3.2×10^{-5} @R.T. [b] 2.5×10^{-5} @4.2K [b]
Constantan	55 wt% Cu 45 wt% Ni	49.9	1300–1340°C [c]	1.5×10^{-5} (20–100°C)	–2.56 %	Ferromagnetic [d] Ferromagnetic [d]
Manganin	83 wt% Cu 13 wt% Mn 4 wt% Ni	48.2 45.4 42.9	1100–1160°C [c] (85wt%Cu–15wt%Mn)	1.9×10^{-5} (20–100°C)	–2.83 %	0.0027 @R.T. [d] 0.022 @76K [d] 0.0125 @4.2K [d]
Nichrome	80 wt% Ni 20 wt% Cr	109 107 106	1400°C	1.73×10^{-5} (20–1000°C)	0.69 %	5.2×10^{-4} @R.T. [d] 8.3×10^{-4} @76K [d] 5.6×10^{-3} @4.2K [d]
Phosphor Bronze A	94.8 wt% Cu 5 wt% Sn 0.2 wt% P	12.8 11.0 10.7	950–1050°C	1.78×10^{-5} (20–300°C)	4.5 % [e,g]	-5.2×10^{-5} @R.T. [d] -4.7×10^{-5} @76K [d] -3.3×10^{-5} @4.2K [d]

[a] Except where otherwise cited, data were compiled from *Metals Handbook,* (1961), Vol. 1, *Properties and Selection of Materials* (1995), 8th edition, American Society for Metals, Metals Park, Ohio; *Temperature Measurement and Control*, Lake Shore Cryotronics, Inc., Westerville, Ohio; and C. A. Thompson, W. M. Manganaro, and F. R. Fickett (1990), *Cryogenic Properties of Copper,* Wall Chart, NIST, and the references cited therein.

[b] F. R. Fickett (1992), *Adv. Cryog. Eng. (Mater.),* **38B**, 1191–1197.

[c] T. B. Massalski, ed. (1990), *Binary Alloy Phase Diagrams*, ASM International, Materials Park, Ohio

[d] M. Abrecht, A. Adare, and J. W. Ekin (2007), *Rev. Sci. Inst*. **78,** 046104. Susceptibilities at 4.2 K were determined from magnetization vs. magnetic field data;

room-temperature and 76 K susceptibilities were calculated from the magnetization measured at $H = 100$ Oe, except where noted.

[e] The magnetoresistance of phosphor bronze varies with (trace) impurities in the wire.

[f] The magnetoresistance of pure copper is strongly dependent on its purity; it can be determined from a normalized "Kohler" plot, such as that shown in Fig. 5.16 of F. R. Fickett, Chapter 5 in *Materials at Low Temperatures,* R. P. Reed and A. F. Clark, eds., ASM International, Metals Park, Ohio.

[g] At 76 K and 10 T, the magnetoresistance of phosphor bronze is much smaller than at 4 K, decreasing to about $\Delta R/R_0 = 0.08\%$ (Abrecht et al. 2006, footnote d).

A4.3 Residual Resistance Ratio (RRR) of selected wiring and conductor materials (Sec. 4.2)

RRR ≡ $R_{293\ K}/R_{4\ K} = \rho_{293\ K}/\rho_{4\ K}$

RRR values of additional materials are tabulated in Appendix A3.1.

Material	Resistivity at 293 K [μΩ·cm]	Resistivity at 4 K [μΩ·cm]	RRR ($\rho_{293\ K}/\rho_{4\ K}$)
Copper Electrolytic-Tough-Pitch, ETP (common wire, rod, and plate material)	1.68	~0.015	~110
Oxygen-free copper [a,b] 99.95% pure; annealed ~500°C for ~1 h in argon or vacuum ($\lesssim 10^{-4}$ torr)	1.68	~0.010	~160
Oxygen-free copper [a] 99.95% pure; unannealed	1.71	~0.038	~45
Copper ground strap [a] (1/4 inch wide flexible braid)	1.74	~0.070	~25
Silver foil [a] (rolled)	1.61	~0.019	~85
Aluminum 99.9995 % [c] (pure rolled foil annealed 350°C for 1 h)	2.65	~0.0005	~5000

[a] Measured by R. McDonough (1995), unpublished data, National Institute of Standards and Technology, Boulder, Colorado.

[b] See annealing information in footnote c of Appendix A3.1.

[c] Measured by P. Kirkpatrick (1997), unpublished data, National Institute of Standards and Technology, Boulder, Colorado.

A4.4 Wire insulation: Thermal ratings [a] *(Sec. 4.3)*

Wire Insulation	Thermal Rating	
Polyvinyl Formal (Formvar™)	105 °C	221 °F
Tetrafluoroethylene (Teflon™)	200 °C	392 °F
Polyimide (Kapton™)	220 °C	428 °F

[a] Data from *Temperature Measurement and Control* (2002), Sec. 3, Lake Shore Cryotronics, Inc., Westerville, Ohio.

A4.5 Thermal anchoring: Required wire lengths (Sec. 4.4)

Tabulated values give the tempering length required to bring the designated wire material to within 1 mK of the heat-sink temperature T_S.

T_1 is the temperature where the lead was last thermally anchored. [a]

Material	T_1 [K]	T_S [K]	Tempering Length for Various Wire Gauges [b] [cm]			
			0.005 mm^2 (#40 AWG)[c] (~0.080mm)[d] [cm]	0.013 mm^2 (#36 AWG) (~0.125mm) [cm]	0.032 mm^2 (#32 AWG) (~0.200mm) [cm]	0.21 mm^2 (#24 AWG) (~0.500mm) [cm]
Copper	300	80	1.9	3.3	5.7	16.0
	300	4	8.0	13.8	23.3	68.8
Phosphor-Bronze	300	80	0.4	0.6	1.1	3.2
	300	4	0.4	0.7	1.3	3.8
Manganin	300	80	0.2	0.4	0.4	2.1
	300	4	0.2	0.4	0.7	2.0
Stainless Steel 304	300	80	0.2	0.3	0.6	1.7
	300	4	0.2	0.3	0.5	1.4

[a] From D. S. Holmes and S. S. Courts (1998), Chapter 4 in *Handbook of Cryogenic Engineering,* ed. J. G. Weisend II, Taylor & Francis, Philadelphia, Pennsylvania; based on an earlier calculation by J. G. Hust (1970), *Rev. Sci. Instrum.* **41**, 622–624. (The difference in values between the earlier and later evaluations for copper stems from the use of mean thermal conductivity values by Hust and thermal-conductivity integrals by Holmes and Courts.)

[b] The calculated results pertain to wires with thin, well bonded insulation such as Formvar or polyimide (not Nylon™ or Teflon™ sleeve insulation) in a vacuum environment (i.e., not cooled by surrounding gas). The insulation-plus-adhesive layer attaching the wire to the heat sink is assumed to have a thickness about equal to the wire diameter and a thermal conductivity typical of varnish, namely 0.01, 0.02, and 0.05 W/(m•K) at 4 K, 20 K, and 78 K, respectively. The length of untempered conductor between T_1 and T_s is assumed to be 25 cm; however, increasing this length by a factor of 10 shortens the required tempering length by a factor of less than two.

[c] American Wire Gauge (Appendix A4.1a).

[d] Nearest metric wire size (Appendix A4.1b).

A4.6a Thermoelectric voltages of some elements *relative to copper* [a] *(Sec. 4.6)*

Tabulated thermoelectric voltages are *relative to copper* with the reference junction at 0 °C.

A positive sign means that, in a simple thermoelectric circuit, the resultant voltage direction produces a current from the material to the copper at the reference junction (0 °C).

Values have been *ordered by their absolute magnitude* at –100 °C or, when not available, at +100 °C. Thus, the higher a material's position in the table, the closer its thermoelectric voltage matches that of copper.

Element	–200 °C [mV]	–100 °C [mV]	0 °C [mV]	+100 °C [mV]	+200 °C [mV]
Gold	–0.02	–0.02	0	+0.02	+0.01
Silver	–0.02	–0.02	0	–0.02	–0.06
Iridium	–0.06	+0.02	0	–0.10	–0.34
Rhodium	–0.01	+0.03	0	–0.06	–0.22
Carbon	—	—	0	–0.06	–0.29
Indium	—	—	0	–0.07	—
Zinc	+0.12	+0.04	0	0.00	+0.06
Cadmium	+0.15	+0.06	0	+0.14	+0.52
Thallium	—	—	0	–0.18	–0.53
Tungsten	+0.62	+0.22	0	+0.36	+0.79
Lead	+0.43	+0.23	0	–0.32	–0.74
Cesium	+0.41	+0.24	0	—	—
Tin	+0.45	+0.25	0	–0.34	–0.76
Cerium	—	—	0	+0.38	+0.63
Tantalum	+0.40	+0.27	0	–0.43	–0.90
Magnesium	+0.56	+0.28	0	–0.32	–0.73
Platinum	+0.19	+0.37	0	–0.76	–1.83
Aluminum	+0.64	+0.43	0	–0.34	–0.77
Molybdenum	—	—	0	+0.69	+1.36
Thorium	—	—	0	–0.89	–2.09
Lithium	–0.93	+0.63	0	+0.06	—
Sodium	+1.19	+0.66	0	—	—
Rubidium	+1.28	+0.83	0	—	—

Element	–200 °C [mV]	–100 °C [mV]	0 °C [mV]	+100 °C [mV]	+200 °C [mV]
Calcium	—	—	0	–1.27	–2.96
Palladium	+1.00	+0.85	0	–1.33	–3.06
Mercury	—	—	0	–1.36	–3.16
Potassium	+1.80	+1.15	0	—	—
Cobalt	—	—	0	–2.09	–4.91
Nickel	+2.47	+1.59	0	–2.24	–4.93
Antimony	—	—	0	+4.13	+8.31
Bismuth	+12.58	+7.91	0	–8.10	–15.40
Germanium	–45.81	–26.25	0	+33.14	+70.57
Silicon	+63.32	+37.54	0	–42.32	–82.40

[a] Calculated from thermal emf data compiled in the *American Institute. of Physics Handbook* (1972), 3rd edition, Chapter 4, McGraw–Hill.

A4.6b Thermoelectric voltages of selected technical materials *relative to copper* [a] *(Sec. 4.6)*

Tabulated thermoelectric voltages are *relative to copper* with the reference junction at 0 °C.

A positive sign means that in a simple thermoelectric circuit the resultant voltage direction produces a current from the material to the copper at the reference junction (0 °C).

Values have been *ordered by their absolute magnitude* at +100 °C. The higher a material's position in the table, the closer its thermoelectric voltage matches that of copper.

Technical Material	–200 °C [mV]	–100 °C [mV]	0 °C [mV]	+100 °C [mV]	+200 °C [mV]
Silver Coin (90 Ag–10 Cu)	—	—	0	+0.04	+0.07
60 Ni–24 Fe–16 Cr	—	—	0	–0.09	+0.18
Copper–Beryllium	—	—	0	–0.09	–0.21
Manganin	—	—	0	–0.15	–0.28
Yellow Brass	—	—	0	–0.16	–0.34
Copper Coin (95 Cu–4 Sn–1 Zn)	—	—	0	–0.16	–0.35
Phosphor Bronze	—	—	0	–0.21	–0.49
Solder (50 Sn–50 Pb)	—	—	0	–0.30	—
Solder (96.5 Sn–3.5 Ag)	—	—	0	–0.31	—
18-8 Stainless Steel	—	—	0	–0.32	–0.79
80 Ni–20 Cr	—	—	0	+0.38	+0.79
Spring Steel	—	—	0	+0.56	+0.80
Gold–Chromium	—	—	0	–0.93	–2.15
Iron	–2.73	–1.47	0	+1.13	+1.71
Alumel	+2.58	+1.66	0	–2.05	–4.00
Chromel P	–3.17	–1.83	0	+2.05	+4.13
Nickel Coin (75 Cu–25 Ni)	—	—	0	–3.52	–7.84
Constantan	+5.54	+3.35	0	–4.27	–9.28

[a] Calculated from thermal emf data compiled in the *American Institute of Physics Handbook* (1972), 3rd edition, Chapter 4, McGraw–Hill.

A4.7 Thermal conductivity of YBCO coated conductors (Sec. 4.10)

Thermal conductivity values are tabulated separately for each of the major component materials of YBCO coated conductors. For any particular YBCO conductor, the total thermal conductivity λ_{total} of the composite conductor is the sum of the contribution of each component λ_i weighted by its fractional cross-sectional area. Thus, for tape conductors

$$\lambda_{total} = \Sigma\, (d_i/D)\, \lambda_i\ ,$$

where d_i is the layer thickness of the i^{th} component and D is the total thickness of the tape.

Thermal conductivity [W/(m·K)]

Material	20 K [W/(m·K)]	50 K [a] [W/(m·K)]	90 K [a] [W/(m·K)]	110 K [W/(m·K)]	295 K [W/(m·K)]
YBCO(*a*–*b*) 123 phase [b] (Calc. from melt-textured data)	14	27	22	21	~18
YBCO(*c*) 123 phase [b] (Calc. from melt-textured data) ($\lambda_{a-b}/\lambda_c \approx 6.3$)	3.5	4.4	3.2	3.0	~2.8
YBCO(*a*–*b*) 123 + 40% 211 phase [b] melt textured	10	19	16	15	~14
YBCO [c] sintered	5	8	5	5	5
Ag [d]	depends on Ag purity (Sec. 2.2)	1180	620	560	450
Cu (RRR = 100) [e]	2430	1220	497	452	397
Inconel 625 [f] $\lambda = 24.7992 \times 10^{-6}\, T^2 + 1.989348 \times 10^{-2}\, T + 7.899798$ (valid 116 K–1255 K)				7.4	9.8
Hastelloy C-276 [f] UNS N10276 $\lambda = 3.565928 \times 10^{-6}\, T^2 +$				7.0 (100 K)	10

$1.349819 \times 10^{-2}\ T + 5.726708$
(valid 105 K–811 K)

Nichrome [f] 13
UNS N06003 (77.3%Ni, 21%Cr)
$\lambda = 2.099567 \times 10^{-6}\ T^2 +$
$1.480732 \times 10^{-2}\ T + 8.265973$
(valid 273 K–1073 K)

---

[a] The abrupt rise in thermal conductivity below T_c is due to condensation of electrons into superconducting pairs, eliminating them as scatterers of phonons, and thus enhancing the dominant phonon contribution to the thermal conductivity.

[b] M. Ikebe, H. Fujishiro, T. Naito, K. Noto, S. Kohayashi, and S. Yoshizawa (1994), *Cryogenics* **34**, 57–61.

[c] A. Jezowski, J. Mucha, K. Rafalowicz, J. Stepien–Damm, C. Sulkowski, E. Trojnar, A. J. Zaleski, and J. Klamut (1987), *Phys. Lett. A* **122**, 431–433.

[d] Calculated from the resistivity of silver (Appendix A6.5a) by using the Wiedemann–Franz Law (Sec. 2.2) for electronic thermal conduction ($\lambda = L_N T/\rho$, where $L_N = 2.44 \times 10^{-8}\ V^2/K^2$).

[e] Cryogenic Materials Properties Program CD, Release B-01 (June 2001), Cryogenic Information Center, 5445 Conestoga Ct., Ste. 2C, Boulder, Colorado 80301-2724; Ph. (303) 442-0425, Fax (303) 443-1821.

[f] R. Radebaugh et al. (2003), *http://ww*w.cryogenics.nist.gov/ and the references listed therein.

A5. Temperature measurement tables and controller tuning (ref. Chapter 5)

A5.1 Vapor pressure vs. temperature (ITS-90) for cryogenic liquids [a] (Sections 5.1.6 and 5.4.1)

Values are tabulated from 200 kPa (~2 atmospheres) down to the triple point (i.e., the solidification temperature). A table of triple points follows the vapor-pressure table. Atmospheric pressure is 101.325 kPa, corresponding to 760 mm Hg at 0 ^{o}C and standard gravity.

Stratification: Because of temperature stratification within the cryogenic liquid, these vapor pressure data are useful when lowering the temperature of a cryogenic liquid (pumping on cryogenic bath), but not when raising the temperature (pressurizing the bath). In the latter case, the bottom of the bath is much colder than the surface unless a resistive heater is used to establish thermal equilibrium throughout the depth of the liquid. This can take a half hour or more depending on the heater power. Further information and methods to ensure accurate temperature measurements in cryogenic liquids are given in Secs. 1.2.1 and 5.4.1. The techniques to minimize temperature stratification in the cryogen liquid are particularly important.

Hydrostatic pressure head: Even when pumping on cryogenic fluids, be aware that after reaching a given pressure, the temperature at the sample depth in a static bath can increase slowly from the hydrostatic pressure of liquid above the sample. If there is a lot of turbulent mixing of the cryogenic liquid, such as from bubbles that occur during pumping or from a relatively large steady-state heat leak into the bath, the error is minimal. However, if the liquid is static for a while (tens of minutes or more), the temperature at the sample location beneath the liquid surface can rise.

This hydrostatic pressure-head correction can be significant, especially for the case of the more dense cryogens, such as liquid nitrogen. The correction is given by $\Delta P = \delta h$, where ΔP is the hydrostatic pressure increase, δ is the mass density of the cryogenic liquid, and h is the height of liquid above the sample. From the cryogen mass densities tabulated in Appendix A1.5 and the SI conversion factors in Appendix A1.3, we find that the pressure increase amounts to about 1.22 kPa at a depth of 1 m in liquid helium, and about 7.90 kPa at the same depth in liquid nitrogen. At atmospheric pressure, for example, this corresponds to a temperature correction of +13 mK in liquid helium, and a correction of +536 mK in liquid nitrogen. The temperature correction increases at lower bath pressures. Thus, for approximate temperature measurement, vapor-pressure data are fine, but for accuracies better than those just noted, it's safest to use a cryogenic thermometer in close thermal proximity to the sample (Sec. 5.3.1).

Note that neither of these errors (stratification or pressure head) occurs in *superfluid* helium (i.e., at temperatures below the dashed line in the ^{4}He column below). Superfluid helium has an extremely high thermal conductivity (see Sec. 1.2.2) and thus, in this case, vapor-pressure data serve to determine sample temperature very accurately.

An extensive tabulation of additional physical properties of cryogenic liquids is given in Appendix A1.5.

Vapor pressure vs. temperature for cryogenic liquids

Pressure [kPa]	^{3}He [b] [K]	^{4}He [c] [K]	Para* H_2 [d] [K]	Ne [e] [K]	N_2 [f] [K]	Ar [h] [K]	O_2 [i] [K]	CH_4 [j] [K]
200		5.036	22.805	29.558	83.626	94.290	97.245	120.622
190		4.970	22.596	29.357	83.115	93.722	96.672	119.894
180		4.901	22.379	29.148	82.584	93.130	96.077	119.137
170		4.829	22.153	28.931	82.030	92.514	95.454	118.347
160		4.754	21.918	28.703	81.451	91.869	94.805	117.521
150		4.676	21.672	28.466	80.845	91.194	94.123	116.655
140		4.594	21.413	28.216	80.207	90.483	93.406	115.744
130		4.507	21.142	27.952	79.533	89.732	92.649	114.782
120		4.416	20.855	27.672	78.819	88.936	91.845	113.762
110	3.269	4.319	20.550	27.376	78.059	88.087	90.989	112.674
105	3.224	4.269	20.389	27.219	77.659	87.641	90.538	112.102
101.325[†]	3.191	4.230	20.268	27.100	77.355	87.302	90.196	111.667
100	3.178	4.216	20.224	27.057	77.244	87.178	90.070	111.508
95	3.130	4.162	20.053	26.888	76.812	86.696	89.584	110.890
90	3.080	4.106	19.875	26.713	76.363	86.195	89.077	110.248
85	3.028	4.048	19.689	26.530	75.895	85.672	88.549	109.576
80	2.974	3.988	19.496	26.339	75.405	85.124	87.995	108.874
75	2.918	3.925	19.293	26.138	74.891	84.550	87.414	108.137
70	2.859	3.859	19.081	25.927	74.349	83.945	86.802	107.360
65	2.797	3.790	18.857	25.704	73.777		86.155	106.540
60	2.732	3.717	18.620	25.466	73.170		85.467	105.668
58	2.705	3.687	18.522	25.367	72.916		85.180	105.303
56	2.677	3.656	18.421	25.266	72.655		84.884	104.929
54	2.649	3.624	18.317	25.162	72.387		84.580	104.543
52	2.620	3.591	18.211	25.054	72.111		84.268	104.147
50	2.590	3.558	18.101	24.944	71.826		83.945	103.738
48	2.559	3.524	17.988	24.830	71.533		83.612	103.316
46	2.528	3.489	17.871	24.712	71.230		83.268	102.880
44	2.495	3.452	17.750	24.590	70.916		82.912	102.429

Pressure [kPa]	^{3}He [b] [K]	^{4}He [c] [K]	Para* H_2 [d] [K]	Ne [e] [K]	N_2 [f] [K]	Ar [h] [K]	O_2 [i] [K]	CH_4 [j] [K]
42	2.462	3.415	17.627		70.591		82.543	101.962
40	2.427	3.377	17.498		70.254		82.160	101.476
38	2.392	3.337	17.364		69.903		81.762	100.971
36	2.355	3.295	17.226		69.537		81.346	100.445
34	2.317	3.252	17.081		69.155		80.912	99.895
32	2.277	3.208	16.929		68.755		80.456	99.318
30	2.236	3.161	16.770		68.334		79.978	98.712
29	2.214	3.137	16.689		68.116		79.729	98.397
28	2.193	3.112	16.604		67.891		79.473	98.073
27	2.170	3.087	16.517		67.660		79.210	97.740
26	2.147	3.061	16.428		67.422		78.938	97.396
25	2.124	3.035	16.336		67.177		78.659	97.042
24	2.100	3.008	16.243		66.923		78.370	96.677
23	2.075	2.979	16.145		66.661		78.071	96.299
22	2.049	2.951	16.044		66.390		77.762	95.908
21	2.023	2.921	15.940		66.109		77.441	95.502
20	1.996	2.890	15.832		65.817		77.108	95.080
19	1.968	2.858	15.719		65.513		76.761	94.641
18	1.939	2.825	15.602		65.196		76.399	94.183
17	1.909	2.791	15.481		64.864		76.020	93.704
16	1.878	2.755	15.354		64.516		75.623	93.201
15	1.846	2.718	15.220		64.151		75.205	92.673
14	1.812	2.679	15.080		63.765		74.763	92.115
13	1.776	2.638	14.931		63.356		74.296	91.523
12	1.739	2.594	14.773				73.798	90.894
11	1.699	2.549	14.605				73.265	
10	1.658	2.500	14.424				72.690	
9	1.613	2.448	14.230				72.067	
8	1.565	2.392	14.018				71.383	
7	1.513	2.331					70.625	
6.5	1.485	2.298					70.213	
6	1.455	2.263					69.773	
5.5	1.424	2.227					69.301	
4	1.318	2.087					67.633	

Pressure [kPa]	^{3}He [b] [K]	^{4}He [c] [K]	Para* H_2 [d] [K]	Ne [e] [K]	N_2 [f] [K]	Ar [h] [K]	O_2 [i] [K]	CH_4 [j] [K]
3.5	1.277	2.039					66.960	
3.0	1.231	1.986					66.201	
2.5	1.181	1.926					65.327	
2.0	1.123	1.858					64.290	
1.8	1.097	1.827					63.814	
1.6	1.068	1.793					63.290	
1.4	1.038	1.757					62.707	
1.2	1.004	1.716					62.049	
1.0	0.966	1.670					61.289	
0.9	0.946	1.644					60.859	
0.8	0.923	1.616					60.387	
0.7	0.898	1.585					59.860	
0.6	0.871	1.551					59.266	
0.5	0.841	1.512					58.578	
0.45	0.824	1.490					58.188	
0.4	0.806	1.467					57.760	
0.35	0.786	1.441					57.281	
0.3	0.763	1.411					56.741	
0.25	0.739	1.378					56.115	
0.2	0.710	1.339					55.368	
0.15	0.675	1.292					54.439	
0.1	0.631	1.230						
0.09	0.620	1.214						
0.08	0.609	1.197						
0.07	0.596	1.179						
0.06	0.582	1.158						
0.05	0.566	1.134						
0.04	0.547	1.106						
0.03	0.524	1.072						
0.02		1.026						
0.01		0.956						
0.008		0.935						
0.006		0.910						
0.004		0.875						

Pressure [kPa]	^{3}He [b] [K]	^{4}He [c] [K]	Para* H_2 [d] [K]	Ne [e] [K]	N_2 [f] [K]	Ar [h] [K]	O_2 [i] [K]	CH_4 [j] [K]
0.002		0.822						

† Atmospheric pressure

Reference are listed after next table.

Boiling temperature and triple points for cryogenic liquids [a]

Cryogenic Liquid	Boiling Temperature (ITS-90) 1 atm (101.325 kPa, 760 mm Hg) [K]	Triple Point Temperature (ITS-90) [K]	Triple Point Pressure [kPa]
^{3}He [b]	3.1905	—	
^{4}He [c]	4.230	2.1768†	4.856
H_2 (para) [d, *]	20.268	13.80	7.04
Neon [e]	27.100	24.557	43.46
Nitrogen [f]	77.355	63.151	12.52
Liquid Air [g]	78.903	59.75‡	5.26
Argon [h]	87.302	83.806	68.89
Oxygen [i]	90.196	54.359	0.146
Methane [j]	111.67	90.694	11.70

Footnotes and references for both of the above tables:

* Hydrogen can exist in two molecular forms: higher-energy orthohydrogen (nuclear spins aligned) and lower-energy parahydrogen (nuclear spins opposed). The equilibrium ratio is determined by temperature: at room temperature and above, hydrogen consists of about 25 % para and 75 % ortho (so-called "normal" hydrogen), but at the atmospheric boiling temperature of liquid hydrogen (20.27 K) and below, the equilibrium shifts almost completely to parahydrogen (99.79 % para and 0.21 % ortho at 20.27 K). The boiling temperatures of parahydrogen and normal hydrogen are nearly equal.

† Superfluid λ point

‡ Solidification point

[a] Data were evaluated by E. W. Lemmon, (2003) from equations of state given in references c through j; National Institute of Standards and Technology, Boulder, Colorado, personal communication.

[b] E. W. Lemmon (2002), National Institute of Standards and Technology, Boulder, Colorado, personal communication.

[c] R. D. McCarty and V. D. Arp (1990), *Adv. Cryog. Eng.* **35**, 1465–1475.

[d] B. A. Younglove (1982), *J. Phys. Chem. Ref. Data* **11**, Suppl. 1, 1–11.

[e] R. S. Katti, R. T. Jacobsen, R. B. Stewart, and M. Jahangiri (1986), *Adv. Cryog. Eng. (Mater.)* **31**, 1189–1197.

[f] R. Span, E. W. Lemmon, R. T. Jacobsen, W. Wagner, and A. Yokozeki (2000), *J. Phys. Chem. Ref. Data* **29**(6), 1361–1433.

[g] E. W. Lemmon, R. T. Jacobsen, S. G. Penoncello, and D. G. Friend (2000), *J. Phys. Chem. Ref. Data* **29**(3), 1–54.

[h] C. Tegeler, R. Span, and W. Wagner (1999), *J. Phys. Chem. Ref. Data* **28**(3), 779–850.

[i] R. Schmidt and W. Wagner (1985), *Fluid Phase Equilibria* **19**,175–200.

[j] U. Setzmann and W. Wagner (1991), *J. Phys. Chem. Ref. Data* **20**(6), 1061–1151.

A5.2 Properties of cryogenic thermometers (~1 K to ~300 K) [a] *(Sections 5.1.2, 5.1.3, and 5.5)*

This table is designed for use in conjunction with the reference compendium, Sec. 5.5, where comments on the properties and practical use of each type of thermometer are given (in corresponding order).

Sensor Type	Temp. Range	Accuracy* (± value)	Reproducibility† (± value)	Long-term Calibration Drift	Inter-change-ability‡	Magnetic Field Use	Best Use	Cost
Metallic Resistance Sensors (positive temperature coefficient):								
Platinum	77 K to 800 K With impurity correction: 20 K to 77 K (Appendix A5.3b)	Without indiv. calib: 0.6 K at 70 K 0.2 K at 300 K With indiv. calibration: 20 mK at 77 K 35 mK at 300 K 55 mK > 330 K 200 mK > 480 K	10 mK from 77 K to 305 K	±10 mK/yr from 77 K to 273 K	Yes	Recommended above 70 K; error < 0.1 % with standard correction factors given in Appendix A5.5	Measurements above 77 K Excellent reproducibility interchange-ability, low mag. field error Many shapes & sizes	Low without calibration High with individual. calibration
Rh–Fe	0.5 K to 900 K	With indiv. calibration: 10 mK 4.2 K 25 mK 100 K 35 mK 300K	10 mK from 1.4 K to 325 K High purity, strain-free: 0.1 mK at 4.2 K	±20 mK/yr from 1.4 K to 325 K	No	Not recommended below ~77 K	Secondary standard thermometer Measurements over a wide temp. range down to 0.5 K	High with indiv. calib.
Semiconductor-like Resistance Sensors (negative temperature coefficient):								
Germanium	0.05 K to 100 K	Must be indiv. calibrated. With indiv. calib: 5 mK at < 10 K 15 mK at < 20 K 35 mK at < 50 K	0.5 mK at 4.2 K	±1 mK/yr at 4.2 K ±10 mK/yr at 77 K	No	Not recommended	Secondary standard thermometer Excellent reproducibility	High with indiv. calib.

Sensor Type	Temp. Range	Accuracy* (± value)	Reproducibility† (± value)	Long-term Calibration Drift	Inter-change-ability‡	Magnetic Field Use	Best Use	Cost
Zirconium oxynitride (Cernox™)	0.3 K to 420 K	Must be indiv. calibrated. With indiv. calib: 5 mK at 4.2 K 20 mK at 20 K 50 mK at 100 K 140 mK at 300 K 230 mK at 400 K	3 mK at 4.2 K	±25 mK/yr over the range 1 K to 100 K 0.05% of reading 100 K to 300 K	No	Recommended Lowest error Correction factors given in Appendix A5.6	One of the best sensors for use in mag. fields Good sensitivity over wide temp. range Fast response time as chip	High with indiv. calib.
Carbon glass	1 K to ~325 K	Must be indiv. calibrated. With indiv. calib: 5 mK at < 10 K 20 mK at 20 K 55 mK at 50 K	0.75 mK at 4.2 K	–5 mK/yr at 4.2 K –30 mK/yr at 15 K –100 mK/yr at 77 K –600 mK/yr at 300 K	No	Recommended Correction factors given by Sample et al. (1982)	One of the best sensors for use in mag. fields High sensitivity at 4.2 K, low sens. >100K Fragile; calib. easily invalidated	High with indiv. calib.
Bi ruthenate/ ruthenium oxide	0.05 K to 40 K	With indiv. calib: 5 mK at 0.05 K 7 mK at 1.4 K 11 mK at 4.2 K 77 mK at 20 K 470 mK at 77 K 1.7 K at 200 K 7 K at 300 K	10 mK at 4.2 K	±15 mK/yr at 4.2 K	Yes, but only within each lot	Recommended	Most useful below 20 K Calibration interchangeability (20-40 mK) for sensors of the same lot	High with indiv. calib.

Diode Voltage Sensors:

Silicon diode	1.4 K to 475 K	Without calib: 1 K < 100 K 1% at 100 K–475 K With indiv. calib: 20 mK 1.4-10 K 55 mK 10-475 K	5 mK at 4.2 K 20 mK at 77 K 15 mK at 300 K	±10 mK/yr at 4.2 K ±40 mK/yr at 77 K ±25 mK/yr at 300 K	Yes	Not recommended below ~60 K	Relatively inexpensive, easily measured, interchangeable thermometer Small size	Medium without calib. High with indiv. calib.
GaAlAs diode	1.4 K to 325 K	Must be indiv. calibrated. With indiv. calib: 15 mK < 20 K 50 mK at 50 K 110 mK at 300 K	5 mK at 4.2 K	±15 mK/yr at 4.2 K ±50 mK/yr over the range 77 K to 330 K	No	Acceptable error (~10 times less than Si diode, but >10 times greater error than Cernox™	When diode sensor is required in mag. field	High with indiv. calib.

Special Purpose Sensors:

Thermocouples Chromel–AuFe(0.07%) Type E (Chromel–CuNi)	1.4 K to 325 K 3 K to 1274 K	1.7 K from 73 K to 273 K	20 mK at 77 K	—	Yes	Not recommended Difficult to use in magnetic field	Low mass sensor - Chromel-AuFe for lower temp. range - Type E for higher temp. range	Requires low dc voltage measurement
Capacitance Sensor	1 K to 290 K	Used as transfer control element only, not absolute measurement	> 500 mK 10 mK after cooling and stabilizing	±1 K/yr	No	Recommended for temperature *control*	Excellent magnetic field stability for temp. control	Sensor: medium Requires capacitance measurement

Definitions:

[*] Accuracy: The difference between the measured and true temperature value.

[†] Reproducibility: The change in apparent temperature when the sensor is subjected to repeated thermal cycling from room temperature.

[‡] Interchangeability: The ability to substitute one sensor for another with little change in calibration.

[a] Information compiled from *Temperature Measurement and Control* (2000, 2002), Lake Shore Cryotronics, Westerville, Ohio; L. M. Besley (1993), National

Measurements Laboratory, Sydney, Australia; and L. G. Rubin (2002), Francis Bitter National Magnet Laboratory, Cambridge, Massachusetts.

References:

Carbon resistors: H. H. Sample, L. J. Neuringer, and L. G. Rubin (1974), *Rev. Sci. Instrum*., **45**, 64–73.

Carbon-glass thermometers: H. H. Sample, B. L. Brandt, and L. G. Rubin (1982), *Rev. Sci. Instrum*. **53**, 1129–1136.

Cernox™: B. L. Brandt, D. W. Liu, and L. G. Rubin (1999), *Rev. Sci. Instrum.* **70**, 104–110.

Platinum thermometers: B. L. Brandt, L. G. Rubin, and H. H. Sample (1988), *Rev. Sci. Instrum.* **59**, 642–645.

Thermocouples: H. H. Sample and L. G. Rubin (1977), *Cryogenics* **17**, 597–606.

A5.3a Platinum-resistance-thermometer resistivity vs. temperature) above *70 K DIN EN 60751 (Sections 5.1.3, 5.1.6, and 5.5.1)*

This table gives a standard calibration of the temperature dependence of platinum resistance thermometers (PRTs) for use above liquid-nitrogen temperature. This calibration is not recommended at lower temperatures, however, because the role of impurity resistivity increases in the low-temperature range. A standard calibration below 70 K that compensates for varying impurity resistivities is given in the next table, Appendix A5.3b.

For platinum thermometers having an ice-point resistance R_{273K} other than 100 Ω, multiply the resistance values in this table by the ratio of the ice-point resistance to 100 Ω. For example, for a 500 Ω *PRT*, multiply all the values in the table by 5 to obtain the calibration for such a thermometer.

Calculation of temperature values (ITS-90): Temperatures other than those listed in the table can be calculated according to DIN EN 60751 for Class A and Class B platinum resistance thermometers {alpha ≡ $[R_{100°C} - R_{0°C}]/[100\ R_{0°C}] = 0.00385$}, where the temperature T is in kelvins:

For $T < 273.15$ K (0 °C):

$$R(T) = R_0\,[1 + A\,(T - 273.15) + B\,(T - 273.15)^2 + C\,(T - 373.15)\,(T - 273.15)^3]$$

For $T \geq 273.15$ K (0 °C):

$$R(T) = R_0\,[1 + A\,(T - 273.15) + B\,(T - 273.15)^2]$$

where the constants in these two equations have the values

$A = 3.9083 \times 10^{-3}\ °C^{-1}$

$B = -5.775 \times 10^{-7}\ °C^{-2}$

$C = -4.183 \times 10^{-12}\ °C^{-4}$

$R_0 = 100\ \Omega$

Interchangeability tolerance:

Class A: $\Delta T\,(K) = \pm\,(0.15 + 0.002\,|\,T - 273.15\,|\,)$

Class B: $\Delta T\,(K) = \pm\,(0.3 + 0.005\,|\,T - 273.15\,|\,)$

DIN EN 60751 resistance vs. temperature (ITS-90) for platinum-resistance thermometers. (Thermometer resistance at 273.15 K is 100 Ω, alpha [a] = 0.00385.)

T [K]	*R* [Ω]	Interchange-ability Tolerance [K] Class A, B	*T* [K]	*R* [Ω]	Interchange-ability Tolerance [K] Class A, B	*T* [K]	*R* [Ω]	Interchange-ability Tolerance [K] Class A, B
60	12.80		140	46.71		225	81.04	
65	14.98		145	48.77		230	83.02	
70	17.16	±0.6, ±1.3	150	50.82	±0.4, ±0.9	235	85.00	
75	19.32		155	52.87		240	86.98	
80	21.47		160	54.91		245	88.95	
85	23.62		165	56.95		250	90.92	±0.2, ±0.4
90	25.75		170	58.98		255	92.89	
95	27.88		175	61.01		260	94.85	
100	30.00	±0.5, ±1.2	180	63.03		265	96.81	
105	32.12		185	65.05		270	98.77	
110	34.22		190	67.06		273.15	100.00	
115	36.32		195	69.07		275	100.72	
120	38.41		200	71.07	±0.3, ±0.7	280	102.67	
125	40.49		205	73.07		285	104.62	
130	42.57		210	75.07		290	106.57	
135	44.64		215	77.06		295	108.51	
			220	79.05		300	110.45	±0.2, ±0.4

[a] Alpha ≡ $[R_{100°C} - R_{0°C}]/100\ R_{0°C}]$

A5.3b Platinum-resistance-thermometer resistivity vs. temperature below *70 K (Sections 5.1.3, 5.1.6, and 5.5.1)*

This table provides a calibration for platinum resistance thermometers (PRTs) if they must be used for thermometry below ~70 K (such as a when a platinum film-type sensor is used for a rapid time response). In this low-temperature range, differences in impurity levels in the thermometers lead to significant errors in the standard calibration table (Appendix A5.3a). Consequently, the temperature should be determined by calculating the Z ratio (defined below).

With this scheme, the impurity resistivity of an individual PRT can be compensated. The PRT's resistance is first measured at or near liquid-helium temperature in order to determine its impurity resistivity $R_{4.2K}$. This is then used with the measured resistance of the sensor R_T to determine the ratio:

$$Z \equiv (R_T - R_{4.2K})/(R_{273K} - R_{4.2K}),$$

where R_{273K} is the sensor's ice-point resistivity. The value of this Z-ratio can then be used to determine temperature from the following table.

Values of $\Delta Z/\Delta T$ are also provided to facilitate interpolation between tabulated temperature values.

This Z-ratio procedure has a typical error of about ± 25 mK down to 30 K, below which temperature the error increases to about ± 120 mK at 14 K (Besley and Kemp 1978). Use below 14 K is not recommended.

Z-ratio for platinum resistance thermometers [a]

T [K]	$10^6\ Z$	$10^6\ \Delta Z/\Delta T$ [K^{-1}]
14.0	908.7	256
14.5	1043.5	284
15.0	1192.9	314
15.5	1358.2	347
16.0	1540.4	382
16.5	1740.3	418
17.0	1958.9	457
17.5	2197.2	497
18.0	2456.2	539
18.5	2736.7	583
19.0	3039.7	629
19.5	3366.1	677
20.0	3716.7	726
21.0	4493.6	829
22.0	5376.0	937
23.0	6368.3	1049
24.0	7474.2	1164
25.0	8696.8	1282
26.0	10038	1401
27.0	11500	1522
28.0	13083	1644
29.0	14788	1766
30.0	16615	1887
31.0	18562	2007
32.0	20628	2126
33.0	22812	2242
34.0	25111	2356
35.0	27523	2468
36.0	30045	2576
37	32674	2681
38	35406	2783
39	38238	2880

T [K]	$10^6\ Z$	$10^6\ \Delta Z/\Delta T$ [K^{-1}]
40	41166	2974
42	47293	3151
44	53758	3311
46	60528	3456
48	67572	3586
50	74862	3701
52	82368	3803
54	90065	3892
56	97929	3970
58	105937	4037
60	114071	4095
65	134839	4205
70	156050	4274
75	177535	4316
80	199174	4337
85	220881	4344
90	242600	4342
95	264293	4334
100	285935	4322

[a] Table values were calculated by L. M. Besley and R. C. Kemp (1978), *Cryogenics* **18**, 497–500, from data on 50 high-quality platinum thermometers. Data were compiled by C. G. Kirby and R. E. Bedford, and J. Kathnelson (1975), *Metrologia* **11**, 117–124, and J. P. Compton and S. D. Ward (1975), *Temperature Measurement*, p. 91, Institute of Physics London Conference Series No. 26. See also the discussion and summary given in G. K. White (1989), *Experimental Techniques in Low-Temperature Physics*, pp. 100–104, Oxford University Press.

A5.4 Diode and thermocouple voltage-vs.-temperature tables [a] (Sections 5.1.3, 5.1.6, 5.5.7, and 5.5.9)

Silicon Diode [b] DT-470 Curve 10		Thermocouple [c] Chromel vs. Au–0.07at%Fe		Type E [d] Thermocouple Chromel vs. Constantan		Type K [e] Thermocouple Chromel vs. Alumel		Type T [f] Thermocouple Copper vs. Constantan	
[K]	[V]	[K]	[mV]	[K]	[mV]	[K]	[mV]	[K]	[mV]
1.4	1.6981	1.4	–5.298	3.0	–9.836	3.0	–6.458	3.0	–6.258
2.0	1.6879	3.0	–5.281	5.6	–9.830	6.0	–6.455	6.5	–6.252
3.8	1.6390	4.8	–5.259	9.0	–9.818	10.0	–6.449	11.0	–6.240
9.0	1.4505	7.0	–5.223	13.5	–9.796	14.5	–6.438	16.5	–6.218
12.0	1.3681	10.5	–5.174	19.0	–9.757	19.5	–6.421	22.0	–6.189
15.5	1.2946	19.0	–5.032	25.0	–9.701	25.0	–6.395	29.0	–6.140
20.0	1.2144	26.0	–4.193	32.0	–9.620	32.0	–6.353	38.0	–6.062
24.0	1.1360	48.0	–4.549	40.0	–9.507	40.0	–6.291	48.0	–5.954
25.0	1.1246	58.0	–4.381	50.0	–9.337	48.0	–6.215	60.0	–5.800
26.0	1.1190	70.0	–4.173	60.0	–9.135	58.0	–6.102	75.0	–5.575
27.0	1.1152	80.0	–3.995	70.0	–8.903	65.0	–6.010	90.0	–5.320
28.0	1.1121	90.0	–3.813	80.0	–8.648	75.0	–5.863	105	–5.034
32.0	1.1026	100	–3.627	90.0	–9.367	85.0	–5.699	120	–4.719
36.0	1.0949	110	–3.437	105	–7.906	95.0	–5.516	135	–4.377
44.0	1.0809	120	–3.244	120	–7.394	105	–5.317	155	–3.878
60.0	1.0527	135	–2.948	135	–6.839	120	–4.988	175	–3.328
77.35	1.0203	150	–2.645	150	–6.240	135	–4.624	195	–2.734
100	0.9755	165	–2.337	170	–5.383	150	–4.227	220	–1.930
120	0.9338	180	–2.042	190	–4.456	165	–3.799	245	–1.059
140	0.8907	200	–1.600	210	–3.470	185	–3.187	270	–0.125
170	0.8240	220	–1.169	235	–2.161	205	–2.526	300	+1.062
200	0.7555	245	–0.623	260	–0.767	230	–1.646	330	+2.325
230	0.6856	270	–0.071	290	+0.995	260	–0.519	360	+3.664
273.15	0.5833	300	+0.599	320	+2.843	295	+0.869	395	+5.310
320	0.4707	305	+0.716	350	+4.770	350	+3.130	430	+7.042
360	0.3734	310	+0.843	385	+7.115	395	+5.000	470	+9.111
400	0.2746	315	+0.994	420	+9.557	460	+7.616	510	+11.276
440	0.1746	320	+1.194	460	+12.443	510	+9.613	555	+13.805
475	0.0906	325	+1.484	475	+13.557	575	+12.279	575	+14.968

[a] Data from Lake Shore Cryotronics, Inc. (2002), *Temperature Measurement and Control* , Westerville, Ohio.

[b] Accuracy: 1 K at < 100 K, 1% at 100 K–475 K. Reproducibility: ±5 mK at 4.2 K, ±20 mK at 77 K, ±15 mK at 300 K. See Appendix A5.2 for more information.

[c] For accuracy information, refer to L. L. Sparks and R. L. Powell (1973), *J. Res. Nat. Bur. Std.* **76A**, 263–283. Thermocouple voltages are referenced to zero at 273 K.

[d] Accuracy: 1.7 K from 73 K to 273 K. See Appendix A5.2 for more information. Thermocouple voltages are referenced to zero at 273 K.

[e] Accuracy: 2.2 K from 73 K to 273 K. Thermocouple voltages are referenced to zero at 273 K.

[f] Accuracy: 1.0 K from 73 K to 273 K. Thermocouple voltages are referenced to zero at 273 K.

A5.5 Magnetic-field correction factors for platinum resistance thermometers (Sections 5.1.6, 5.2 and 5.5.1)

These magnetic-field correction factors were calculated from magnetoresistance data obtained by Brandt et al. (1988) and are tabulated here as relative temperature errors $(T_{\text{apparent}} - T_{\text{actual}})/T_{\text{actual}}$ [%]. The corrections were nearly the same for measurements on thirteen platinum resistance thermometers (PRTs) of varying purity (alpha = 3.85 to 3.925 × 10^{-3} $^{\circ}C^{-1}$), as well as varying construction types (wire-wound and thick-film types), manufacturers, and ice-point resistances (100 Ω to 500 Ω). For all the sensors, the *standard deviation* of the correction is simply about ± 10 % of the correction value itself, irrespective of temperature or magnetic field.

> *Example*: Suppose we wish to correct the reading a platinum resistance thermometer that indicates an apparent temperature of 100 K in a magnetic field of 10 T.
>
> From the table below we see that, at 100 K and 10 T, this temperature reading would actually be too high by 0.40 %. Thus, the actual temperature would be 100 K / (1 + 0.004) = 99.6 K. The standard deviation for this correction would be about 10 % of the correction (0.1 × 0.40 %), or only 0.04 % (i.e., 0.04 K).

The *orientation* of the magnetic field has a negligible effect on these correction factors for film-type PRTs, but the effect is significant for wire-wound PRTs. The data below correspond to wire-wound PRTs oriented with the applied magnetic field parallel to the long axis of their package (see Fig. 5.17). Thus, to use the table, it is recommended that wire-wound PRTs be installed with this orientation. Alternatively, when the sensor must be used in varying field orientations, a thin-film PRT is preferred.

Magnetic-Field Correction Factors for Platinum Resistance Thermometers [a]

Tabulated values are $(T_{apparent} - T_{actual})/T_{actual}$ (in percent) at magnetic field B.
The standard deviation of these corrections is about ±10 % of the tabulated values.

T [K]	B = 5 T [%]	B = 10 T [%]	B = 15 T [%]	B = 19 T [%]
40	1.5	4.1	6.7	8.9
50	1.05	2.9	5.0	6.7
60	0.59	1.8	3.2	4.5
70	0.27	0.97	1.9	2.8
80	0.18	0.67	1.4	2.1
90	0.13	0.50	1.0	1.6
100	0.11	0.40	0.85	1.4
120	0.068	0.26	0.57	0.91
150	0.038	0.16	0.35	0.56
200	0.019	0.085	0.19	0.31
220	0.017	0.074	0.17	0.28
250	0.015	0.058	0.14	0.22
300	0.010	0.030	0.080	0.13

[a] Correction factors calculated from magnetoresistance data from B. L. Brandt, L. G. Rubin, and H. H. Sample (1988), *Rev. Sci. Instrum.* **59**, 642–645.

A5.6 Magnetic-field correction factors for zirconium-oxynitride resistance thermometers (Sections 5.1.6, 5.2 and 5.5.4)

These magnetoresistance correction factors were interpolated to even temperature values by using a cubic-spline fit to magnetoresistance data measured by Brandt et al. (1999). The corrections are applicable to a wide range of zirconium-oxynitride (Cernox™) resistance thermometers having 4.2 K resistances from about 300 Ω to 8000 Ω, and 4.2 K dimensionless sensitivities $(dR/R)/(dT/T)$ in the range –0.74 to –1.9 (with –1.2 to –1.9 recommended).

The data are presented as the percentage change in *resistance* rather than *temperature* (unlike platinum in Appendix A5.5), because Brandt et al. found that, for zirconium-oxynitride sensors, the standard deviations in resistance were much smaller than the standard deviations in temperature. [This results from the wide range of dimensionless sensitivities $S \equiv (dR/R)/(dT/T)$ of the individual sensors and the differing temperature dependences of S.] The standard deviation of the magnetoresistance correction is given as a ± quantity below each magnetoresistance correction. The standard deviations show that this correction procedure is most beneficial at temperatures below about 3 K and from about 6 K to 15 K.

> *Example*: Let us assume that a particular zirconium-oxynitride thermometer indicates an apparent temperature of about 10 K in a magnetic field of 16 T. We wish to correct for the magnetoresistance error of this particular sensor.
>
> From the table below, we see that, at 10 K and 16 T, the sensor's resistance would exceed its zero-field resistance by 1.40 %. We use the dimensionless sensitivity $S \equiv (dR/R)/(dT/T)$ supplied with the calibration data for our particular sensor to calculate the equivalent shift in its apparent temperature. For our sensor, suppose that $S = –1.16$ at 10 K. Then, we would calculate $(T_{apparent} – T_{actual})/T_{actual} = (1.40\ \%)/(–1.16) = –1.21\ \%$ and accordingly adjust the apparent temperature reading by this percentage to obtain the actual temperature. Since $T_{apparent} – T_{actual}$ is negative at 10 K and 16 T, the apparent temperature is lower than the actual temperature, and it would need to be *increased* by 1.21 % to give the actual temperature. From the standard deviation of ±0.30 for the resistivity correction at 10 K and 16 T, we find the standard deviation of the temperature correction is ±0.26 %.

At liquid-nitrogen temperatures, the effect of magnetic-field *orientation* on these correction factors was observed to be insignificant. However, at 4.2 K the situation was more complex, giving rise to a positive orientation effect in some sensors, negative in others (for example, apparent temperature shifts of –0.2 % to +0.4 % were observed at 16 T; Brandt et al. 1999). Since the tabulated corrections were determined for field *perpendicular* to the film surface (canister aligned parallel to the field), it is best to orient these sensors accordingly so they can be used with the correction data.

Magnetic Field Correction for Zirconium-Oxynitride (Cernox™) Resistance Thermometers [a]

Tabulated values are $[R(B) - R(0)]/R(0)$ (in *percent*) at magnetic field B.

The standard deviation of the correction is shown as a ± factor (also in percent) below each correction.

T [K]	B=2 T [%]	B=4 T [%]	B=6 T [%]	B=8 T [%]	B=10 T [%]	B=12 T [%]	B=14 T [%]	B=16 T [%]	B=18 T [%]	B=20 T [%]	B=23 T [%]	B=26 T [%]	B=29 T [%]	B=32 T [%]
2	–2.20 ±0.39	–4.47 ±1.08	–5.52 ±1.58	–6.10 ±1.83	–6.61 ±1.90	–7.19 ±1.79	–7.85 ±1.59	–8.59 ±1.35	–10.12 ±1.09	–10.39 ±0.85	–10.96 ±1.00	–12.87 ±1.28	–14.87 ±1.80	–16.92 ±2.35
2.5	–1.21 ±0.25	–2.55 ±0.77	–3.09 ±1.20	–3.25 ±1.46	–3.35 ±1.55	–3.55 ±1.51	–3.88 ±1.35	–4.14 ±1.13	–5.07 ±0.86	–5.65 ±0.59	–6.31 ±1.40	–8.06 ±1.80	–9.87 ±2.25	–11.74 ±2.76
3	–0.65 ±0.16	–1.42 ±0.52	–1.65 ±0.88	–1.57 ±1.12	–1.43 ±1.24	–1.37 ±1.24	–1.47 ±1.15	–1.69 ±0.98	–2.17 ±0.76	–2.73 ±0.57	–3.42 ±1.73	–5.00 ±2.16	–6.73 ±2.62	–8.55 ±3.12
3.5	–0.38 ±0.11	–0.76 ±0.35	–0.80 ±0.64	–0.57 ±0.87	–0.28 ±1.00	–0.06 ±1.04	0.02 ±1.00	–0.11 ±0.92	–0.34 ±0.79	–0.75 ±0.71	–1.57 ±1.92	–3.02 ±2.37	–4.63 ±2.84	–6.34 ±3.30
4.2	–0.17 ±0.03	–0.30 ±0.20	–0.20 ±0.42	0.11 ±0.61	0.50 ±0.73	0.82 ±0.81	1.07 ±0.81	1.06 ±0.85	1.02 ±0.74	0.79 ±0.72	0.03 ±2.03	–1.20 ±2.50	–2.63 ±2.97	–4.22 ±3.43
5	–0.09 ±0.02	–0.07 ±0.15	0.10 ±0.31	0.42 ±0.44	0.82 ±0.55	1.20 ±0.59	1.47 ±0.64	1.62 ±0.67	1.22 ±0.65	1.55 ±0.68	1.00 ±1.89	0.06 ±2.37	–1.23 ±2.84	–2.65 ±3.30
6	–0.08 ±0.02	0.02 ±0.07	0.21 ±0.19	0.51 ±0.31	0.90 ±0.40	1.29 ±0.45	1.61 ±0.51	1.85 ±0.55	2.01 ±0.58	1.96 ±0.68	1.69 ±1.87	0.91 ±2.31	–0.12 ±2.78	–1.26 ±3.25
7	–0.06 ±0.01	0.03 ±0.03	0.23 ±0.11	0.52 ±0.21	0.89 ±0.27	1.26 ±0.34	1.60 ±0.39	1.88 ±0.45	2.26 ±0.53	2.08 ±0.66	1.88 ±1.75	1.29 ±2.17	0.48 ±2.62	–0.48 ±3.08
8	–0.05 ±0.02	0.03 ±0.03	0.24 ±0.07	0.52 ±0.13	0.85 ±0.18	1.19 ±0.24	1.52 ±0.30	1.80 ±0.37	1.97 ±0.48	2.03 ±0.62	1.78 ±1.53	1.38 ±1.95	0.73 ±2.38	–0.11 ±2.81
9	–0.04 ±0.03	0.02 ±0.03	0.21 ±0.06	0.46 ±0.10	0.76 ±0.14	1.07 ±0.18	1.37 ±0.24	1.63 ±0.32	1.71 ±0.44	1.86 ±0.57	1.62 ±1.36	1.32 ±1.76	0.78 ±2.16	0.08 ±2.56
10	–0.05 ±0.03	0.01 ±0.04	0.16 ±0.06	0.38 ±0.09	0.64 ±0.12	0.92 ±0.15	1.18 ±0.21	1.40 ±0.30	1.54 ±0.40	1.65 ±0.52	1.43 ±1.23	1.17 ±1.59	0.72 ±1.96	0.16 ±2.34
12	–0.05	–0.01	0.08	0.23	0.43	0.66	0.85	1.01	1.21	1.24	1.04	0.81	0.48	0.09

T [K]	*B*=2 T [%]	*B*=4 T [%]	*B*=6 T [%]	*B*=8 T [%]	*B*=10 T [%]	*B*=12 T [%]	*B*=14 T [%]	*B*=16 T [%]	*B*=18 T [%]	*B*=20 T [%]	*B*=23 T [%]	*B*=26 T [%]	*B*=29 T [%]	*B*=32 T [%]
	±0.02	±0.04	±0.05	±0.08	±0.11	±0.13	±0.18	±0.26	±0.34	±0.43	±1.02	±1.31	±1.62	±1.95
15	–0.03 ±0.02	–0.03 ±0.03	0.02 ±0.05	0.12 ±0.06	0.24 ±0.08	0.37 ±0.11	0.50 ±0.15	0.61 ±0.20	0.70 ±0.26	0.76 ±0.33	0.48 ±0.77	0.32 ±0.99	0.07 ±1.23	–0.27 ±1.48
20	–0.03 ±0.01	–0.04 ±0.02	–0.04 ±0.03	–0.01 ±0.05	0.03 ±0.06	0.09 ±0.08	0.13 ±0.11	0.17 ±0.14	0.20 ±0.18	0.22 ±0.23	–0.03 ±0.51	–0.17 ±0.67	–0.37 ±0.83	–0.65 ±1.00
30	–0.01 ±0.00	–0.02 ±0.01	–0.03 ±0.01	–0.04 ±0.02	–0.04 ±0.03	–0.05 ±0.05	–0.05 ±0.07	–0.07 ±0.09	–0.09 ±0.11	–0.12 ±0.13	–0.35 ±0.27	–0.49 ±0.34	–0.64 ±0.42	–0.83 ±0.51
40	0.00 ±0.00	–0.01 ±0.00	–0.01 ±0.01	–0.02 ±0.01	–0.04 ±0.02	–0.06 ±0.03	–0.08 ±0.04	–0.10 ±0.05	–0.14 ±0.07	–0.17 ±0.08	–0.38 ±0.16	–0.50 ±0.19	–0.61 ±0.24	–0.76 ±0.29
50	0.00 ±0.00	–0.01 ±0.00	–0.02 ±0.01	–0.03 ±0.01	–0.05 ±0.02	–0.06 ±0.02	–0.08 ±0.03	–0.11 ±0.04	–0.14 ±0.05	–0.17 ±0.06	–0.32 ±0.10	–0.41 ±0.13	–0.51 ±0.16	–0.63 ±0.19
60	–0.01 ±0.00	–0.02 ±0.01	–0.03 ±0.01	–0.04 ±0.02	–0.05 ±0.02	–0.07 ±0.03	–0.09 ±0.04	–0.11 ±0.05	–0.13 ±0.07	–0.16 ±0.08	–0.27 ±0.07	–0.34 ±0.10	–0.43 ±0.12	–0.53 ±0.14
70	–0.01 ±0.01	–0.01 ±0.01	–0.02 ±0.01	–0.03 ±0.02	–0.04 ±0.02	–0.06 ±0.03	–0.08 ±0.05	–0.10 ±0.06	–0.12 ±0.08	–0.15 ±0.09	–0.23 ±0.06	–0.30 ±0.07	–0.37 ±0.09	–0.45 ±0.11
77	0.00 ±0.01	–0.01 ±0.01	–0.02 ±0.01	–0.02 ±0.01	–0.04 ±0.02	–0.05 ±0.03	–0.07 ±0.04	–0.09 ±0.06	–0.11 ±0.07	–0.13 ±0.08	–0.21 ±0.05	–0.27 ±0.06	–0.34 ±0.07	–0.41 ±0.09
80	0.00 ±0.01	–0.01 ±0.01	–0.01 ±0.01	–0.02 ±0.01	–0.03 ±0.02	–0.04 ±0.02	–0.06 ±0.03	–0.08 ±0.04	–0.10 ±0.06	–0.12 ±0.07	–0.20 ±0.05	–0.26 ±0.06	–0.33 ±0.07	–0.40 ±0.09
90	0.00 ±0.00	0.00 ±0.00	–0.01 ±0.01	–0.02 ±0.01	–0.02 ±0.01	–0.03 ±0.01	–0.04 ±0.00	–0.05 ±0.00	–0.06 ±0.00	–0.07 ±0.00	–0.18 ±0.04	–0.23 ±0.04	–0.29 ±0.04	–0.34 ±0.06
100	0.00 ±0.00	0.00 ±0.00	–0.01 ±0.01	–0.01 ±0.01	–0.02 ±0.01	–0.03 ±0.01	–0.02 ±0.02	–0.03 ±0.03	–0.03 ±0.04	–0.04 ±0.04	–0.15 ±0.04	–0.20 ±0.02	–0.25 ±0.02	–0.29 ±0.04
120	0.00 ±0.00	0.00 ±0.00	–0.01 ±0.01	–0.01 ±0.01	–0.02 ±0.01	–0.02 ±0.01	–0.01 ±0.03	–0.01 ±0.04	–0.01 ±0.06	–0.02 ±0.06	–0.09 ±0.02	–0.13 ±0.02	–0.17 ±0.02	–0.18 ±0.00
150	0.00 ±0.00	0.00 ±0.00	0.00 ±0.01	0.00 ±0.01	–0.01 ±0.01	–0.01 ±0.01	–0.02 ±0.01	–0.02 ±0.01	–0.03 ±0.01	–0.03 ±0.01	0.08 ±0.08	0.09 ±0.12	0.10 ±0.16	0.16 ±0.17
200	0.00 ±0.01	0.00 ±0.01	0.00 ±0.01	0.00 ±0.01	–0.01 ±0.01	–0.01 ±0.01	–0.01 ±0.01	–0.01 ±0.01	–0.02 ±0.01	–0.02 ±0.02	0.27 ±0.17	0.35 ±0.25	0.41 ±0.33	0.56 ±0.35
250	0.00	0.00	0.00	0.00	0.00	–0.01	–0.01	–0.01	–0.01	–0.01	0.47	0.60	0.72	0.96

T [K]	*B*=2 T [%]	*B*=4 T [%]	*B*=6 T [%]	*B*=8 T [%]	*B*=10 T [%]	*B*=12 T [%]	*B*=14 T [%]	*B*=16 T [%]	*B*=18 T [%]	*B*=20 T [%]	*B*=23 T [%]	*B*=26 T [%]	*B*=29 T [%]	*B*=32 T [%]
	±0.01	±0.01	±0.01	±0.01	±0.01	±0.01	±0.01	±0.01	±0.01	±0.02	±0.26	±0.37	±0.49	±0.53
300	0.00 ±0.01	0.00 ±0.01	0.00 ±0.01	0.00 ±0.01	0.00 ±0.01	0.00 ±0.01	0.00 ±0.01	0.00 ±0.01	0.00 ±0.01	0.00 ±0.02	0.67 ±0.35	0.85 ±0.50	1.02 ±0.65	1.35 ±0.71

[a] These temperature corrections were interpolated to even temperature values by using a cubic-spline fit to magnetoresistance data measured by B. L. Brandt, D. W. Liu, and L. G. Rubin (1999), *Rev. Sci. Instrum*. **70**, 104–110.

A5.7 Temperature-controller tuning with the Ziegler–Nichols method (Sec. 5.4.3)

Temperature controllers do not always have an auto-tuning feature, and, even if they do, it does not work well for some applications. Here we describe a time-proven, relatively simple, step-by-step procedure for manually optimizing a proportional-integral-differential (PID) controller's settings of gain G, integral time t_i, and the derivative time t_d for a specific system. The settings for a proportional-integral (PI) controller and a simple proportional (P) controller are also given. The optimum settings enable a controller to react quickly to a change in heat demand without much overshoot, oscillation, or droop below the set point (Sec. 5.4.3).

Before describing the tuning procedure, we first define a few terms.

Definitions

Cycle time (sometimes referred to as *duty cycle*): This denotes the time it takes an on–off or time-proportional controller to complete an on–off cycle, illustrated in Fig. 5.15. This applies only to time-proportional controllers and not to analog voltage or current controllers.

Proportional band, and gain: Let P_b be the proportional band around the set point (see Fig. 5.16), usually expressed as a percent of full scale. This is also be referred to as the *gain*, G, which is the reciprocal of the proportional band; that is, $G \equiv 1/P_b$

Integration-time constant (sometimes called *reset*): Let t_i be the characteristic time constant for integration to eliminate the offset error. (The offset error is the steady-state difference between the system temperature and the set point, illustrated in Fig. 5.16).

Derivative-time constant (sometimes called *rate*): Let t_d be the characteristic time constant to correct transient disturbances in the system with a minimum of overshoot or undershoot.

(The terms *proportional band, reset,* and *rate* are those generally used in the field of industrial controls, whereas *gain, integration-time constant*, and *derivative-time constant* are the terms employed by physicists and the companies that sell controllers to them.

Procedure

1. The tuning procedure is easier to observe with a recorder or scrolling data-acquisition display to monitor the process temperature, since the time constants for cycling may be as long as 30 min or more.
2. For time-proportional controllers only, adjust the cycle time to a short time so that the system will not be limited in its time response because of the duty cycle of the heater power.
3. Set the gain to a small value (proportional band to a large value) so the system is overdamped to start with.
4. Turn the integral (reset) and derivative (rate) controls *off*.

5. Enter the set point where control is desired and wait until the temperature is close to that point, or use the manual heater control (manual reset) to reach a temperature near the set point. When the sample temperature is close to the desired temperature, increase the gain (decrease the proportional band) until the system just becomes unstable and starts to oscillate. This is easiest to observe by looking directly at the output power to the heater. Let us denote this critical value of the gain as G'.
6. Measure the time period of the oscillations and let us denote this as t'.
7. Initial optimum values, G and t_i, for optimum stable control are calculated from the following table by using the measured values of G' and t'. These values are given for three types of controllers: proportional control (P), proportional-integral control (PI), and for proportional-integral-differential control (PID).
8. After entering these initial values into the controller and turning on the integral and derivative control, the parameters can be fine tuning. If overshoot occurs in response to step changes in the set-point temperature, it can be eliminated by decreasing the derivative (rate) time constant t_d. When changes are made in the derivative time constant, a corresponding change should also be made in the integral time constant to keep their *ratio* about the same as that given in the table.
9. For time proportional controllers only, increase the cycle time after satisfactory tuning has been achieved to extend the contactor life of the power-supply. Increase the cycle time as much as possible without causing the system to breaking into oscillation when the heater power cycles on and off.

Calculation of control parameters for critical damping with the Ziegler–Nichols tuning formula.[a,b]

Control Type [c]	PID	PI	P
Proportional gain	$G = 0.6\ G'$	$G = 0.45\ G'$	$G = 0.5\ G'$
Integral time (reset time constant)	$t_i = 0.5\ t'$	$t_i = 0.85 t'$	
Derivative time (rate time constant)	$t_d = 0.125\ t'$		

[a] J. G. Ziegler and N. B. Nichols (1942), *Trans. ASME* **64**, 759–768.
[b] P. B. Deshpande and R. H. Ash (1981), "Computer process control," ISA pub., USA.
[c] P ≡ proportional control, PI ≡ proportional-integral control, and PID ≡ proportional-integral-differential control.

For large time constants, where the Ziegler–Nichols method becomes time-consuming, a refinement that improves performance based on set-point weighting has been suggested by C. C. Hang, K. J. Astrom, and W. K. Ho (1991), *IEEE Proc.-D* **138**, 111–118.

If a computer is available to monitor the temperature, it is easy to implement an improved form of PID control with software described by C. K. Chan (1988), *Rev. Sci. Instr.* **59**, 1001–1003.

A good reference for understanding PID control at cryogenic temperatures is E. M. Forgan (1974), *Cryogenics* **14**, 207–214.

A6. Properties of solids at low temperature (ref. Chapter 6)

Additional sources of materials data in the literature and on the Internet are given in the suggested reading and web sites listed in Secs. 6.7.1 and 6.7.2, respectively.

A6.1 Elements: Physical properties at room temperature [a]

For anisotropic elements, polycrystalline values are listed unless otherwise noted.

Element	Atomic Weight	Crystal Structure	Density (298 K) [g/cm^3]	Debye Temp. θ_D [b] (295K) [K]	Specific Heat (at const. press.) (298 K) [J/(g·K)]	Coef. of Thermal Linear Expansion (298 K) [10^{-6} K^{-1}]	Electrical Resistivity (295 K) [μΩ·cm]	Thermal Cond-uctivity (300 K) [W/(m·K)]	Magnetic Susceptibility [e] [10^{-6} SI]	Supercon-ducting Transition Temperature [f] [K]
Aluminum	26.98	f.c.c.	2.70	380	0.904	23.1	2.67	237	20.8	1.175
Antimony	121.76	rhombohedral	6.68	210	0.207	11.0	41.3 [c]	24.3		
									–68.3	
Arsenic	74.91 [d]	rhombohedral	5.73 [c]	290	0.329	5.6 [c] (293 K)	29 [c]	37 [d]	–5.4	
Barium	137.33	b.c.c.	3.62	110	0.205	20.6	33.5	18.4		
									0.1	
Beryllium	9.013	h.c.p.	1.85	920	1.82	11.3	3.62	200	–23.1	0.026

Element	Atomic Weight	Crystal Structure	Density (298 K) [g/cm^3]	Debye Temp. θ_D [b] (295K) [K]	Specific Heat (at const. press.) (298 K) [J/(g·K)]	Coef. of Thermal Linear Expansion (298 K) [10^{-6} K^{-1}]	Electrical Resistivity (295 K) [μΩ·cm]	Thermal Cond-uctivity (300 K) [W/(m·K)]	Magnetic Susceptibility [e] [10^{-6} SI]	Supercon-ducting Transition Temperature [f] [K]
Bismuth	208.98	rhombohedral	9.79	120	0.122	13.4	116 [c]	7.87	–165.0	
Boron	10.81	hexagonal	2.535	1300	1.277	8.3	1012 [d]	30 [d]	–19.7	
Cadmium	112.41	h.c.p.	8.69	175	0.231	30.8	7.27 [c]	96.8	–19.0	0.517
Calcium	40.08	f.c.c.	1.54	210	0.646	22.3	3.38	98 [d]	19.4	
Carbon:										
graphite	12.01	hexagonal	2.22	400	0.709	3	10^2–10^6 [d]	200	–13.9	
diamond	12.01	diamond	3.51	2000	0.4715	1.18	10^{12} [d]	990		
Cesium	132.91	b.c.c.	1.93	45	0.242	97	20.6	35.9	5.1	
Chromium	52.00	b.c.c.	7.15	480	0.450	4.9	12.5	93.7	290.5	
Cobalt	58.93	h.c.p.	8.86	380	0.421	13.0	5.80 [c]	100	ferro	

Element	Atomic Weight	Crystal Structure	Density (298 K) [g/cm^3]	Debye Temp. θ_D [b] (295K) [K]	Specific Heat (at const. press.) (298 K) [J/(g·K)]	Coef. of Thermal Linear Expansion (298 K) [10^{-6} K^{-1}]	Electrical Resistivity (295 K) [μΩ·cm]	Thermal Cond-uctivity (300 K) [W/(m·K)]	Magnetic Susceptibility [e] [10^{-6} SI]	Supercon-ducting Transition Temperature [f] [K]
Copper	63.55	f.c.c.	8.96	310	0.385	16.5	1.69	401	–9.7	
Gallium	69.72	orthorhombic	5.91	240	0.374	18	14.85 [c]	40.6	–23.2	1.083
Germanium	72.59	diamond	5.32	400	0.3219	6.1	5×10^7 [d]	64	–10.7	
Gold	196.97	f.c.c.	19.3	185	0.129	14.2	2.23	317	–34.5	
Hafnium	178.49	h.c.p.	13.3	210	0.144	65.9	33.3	23	66.4	0.128
Indium	114.82	tetragonal	7.31	110	0.233	32.1	8.75 [c]	81.6	–8.2	3.408
Iridium	192.22	f.c.c.	22.5	290	0.131	6.4	5.07 [c]	147	36.8	0.112
Iron	55.85	b.c.c.	7.87	400	0.449	11.8	9.71	80.2	ferro	
Lead	207.20	f.c.c.	11.3	88	0.127	28.9	20.9	35.3	–15.8	7.196
Lithium	6.94	b.c.c.	0.534	360	3.57	46	9.36	84.7	13.6	
Magnesium	24.30	h.c.p.	1.74	330	1.024	24.8	4.43	156	11.8	

Element	Atomic Weight	Crystal Structure	Density (298 K) [g/cm^3]	Debye Temp. θ_D [b] (295K) [K]	Specific Heat (at const. press.) (298 K) [J/(g·K)]	Coef. of Thermal Linear Expansion (298 K) [10^{-6} K^{-1}]	Electrical Resistivity (295 K) [μΩ·cm]	Thermal Cond-uctivity (300 K) [W/(m·K)]	Magnetic Susceptibility [e] [10^{-6} SI]	Supercon-ducting Transition Temperature [f] [K]
Manganese	54.94	cubic (complex)	7.43	410	0.479	21.7	144	7.82	869.7	
Mercury	200.59	rhombohedral	13.534	110 (220 K)	0.139	60.4	95.9 [c]	83.4	–21.4	4.154 [b]
Molybdenum	95.94	b.c.c.	10.2	380	0.251	4.8	5.39	138	96.2	0.915
Nickel	58.69	f.c.c.	8.90	390	0.445	13.4	7.01	90.7	ferro	
Niobium	92.91	b.c.c.	8.57	250	0.265	7.3	14.5 [c]	53.7	241.1	9.25
Osmium	190.23	h.c.p.	22.59	400	0.130	5.1	9.13 [c]	87.6	16.3	0.66
Palladium	106.42	f.c.c.	12.0	290	0.244	11.8	10.6	71.8	766.6	1.4
Platinum	195.08	f.c.c.	21.5	225	0.133	8.8	10.6	71.6	266.7	
Potassium	39.10	b.c.c.	0.89	98	0.757	83.3	7.28	102.4	5.7	
Rhenium	186.21	h.c.p.	20.8	275	0.137	6.2	18.6 [c]	47.9	94.9	1.697
Rhodium	102.91	f.c.c.	12.4	350	0.243	8.2	4.78 [c]	150	154.9	

Element	Atomic Weight	Crystal Structure	Density (298 K) [g/cm^3]	Debye Temp. θ_D [b] (295K) [K]	Specific Heat (at const. press.) (298 K) [J/(g·K)]	Coef. of Thermal Linear Expansion (298 K) [10^{-6} K^{-1}]	Electrical Resistivity (295 K) [μΩ·cm]	Thermal Cond-uctivity (300 K) [W/(m·K)]	Magnetic Susceptibility [e] [10^{-6} SI]	Supercon-ducting Transition Temperature [f] [K]
Rubidium	85.47	b.c.c.	1.53	61	0.364	90	12.9	58.2	3.8	
Ruthenium	101.07	h.c.p.	12.1	450	0.238	6.4	7.37 [c]	117	59.4	0.49
Selenium (gray)	78.96	hexagonal	4.81	250	0.293	17.89 (‖ c) 74.09 (⊥ c)	$>10^{12}$ [d] $\sim10^{7}$ [d]	0.45 (‖ c) 0.13 (⊥ c)	–17.1	
Silicon	28.09	diamond	2.328	700	0.702	2.49	$>10^{10}$ [d]	124	–3.2	
Silver	107.87	f.c.c.	10.5	220	0.235	18.9	1.60	429	–23.8	
Sodium	22.99	b.c.c.	0.97	160	1.225	71	4.81	141	8.5	
Strontium	87.62	f.c.c.	2.64	140	0.306	22.15	13.3	35.3	34.3	
Tantalum	180.95	b.c.c.	16.4	230	0.140	6.3	13.2	57.5	177.5	4.47
Tellurium	127.61	hexagonal	6.23	180	0.197	18.0 [d]	0.4×10^{6} [d]	3.38	–23.4	

Element	Atomic Weight	Crystal Structure	Density (298 K) [g/cm^3]	Debye Temp. θ_D [b] (295K) [K]	Specific Heat (at const. press.) (298 K) [J/(g·K)]	Coef. of Thermal Linear Expansion (298 K) [10^{-6} K^{-1}]	Electrical Resistivity (295 K) [μΩ·cm]	Thermal Cond-uctivity (300 K) [W/(m·K)]	Magnetic Susceptibility [e] [10^{-6} SI]	Supercon-ducting Transition Temperature [f] [K]
Thallium	204.38	h.c.p.	11.8	94	0.129	29.9	16.4 [c]	46.1	–36.4	2.38
Thorium	232.04	f.c.c.	11.7	140	0.118	11.0	15 [c]	54.0	61.4	1.38
Tin	118.71	tetragonal	7.26	160	0.227	22.0	11.0 [c]	66.6	–28.9	3.722
Titanium	47.88	h.c.p.	4.51	360	0.522	8.6	43.1 [c]	21.9	178	0.40
Tungsten	183.84	b.c.c.	19.3	315	0.132	4.5	5.33 [c]	174	69.9	0.0154
Uranium	238.03	orthorhombic	19.1	160	0.116	13.9	25.7 [c]	27.6	411.3	0.2
Vanadium	50.94	b.c.c.	6.0	380	0.489	8.4	19.9	30.7	429.5	5.40
Zinc	65.39	h.c.p.	7.14	240	0.388	30.2	5.94	116	–12.6	0.85
Zirconium	91.22	h.c.p.	6.52	250	0.278	5.7	42.4	22.7	107.5	0.61

[a] Unless otherwise noted, data are from the *CRC Handbook of Chemistry and Physics* (2002), 83st edition, CRC Press, Boca Raton, Florida.

[b] Values of the Debye temperature θ_D are from G. K. White (1987), *Experimental Techniques in Low-Temperature Physics,* Oxford University Press, determined from specific heat data in the range $\theta_D/2$–θ_D. These data were compiled from the *American Institute of Physics Handbook* (1972), 3rd edition. McGraw-Hill; Touloukian et al., ed. (1970–1977), *Thermophysical Properties of Matter,* Plenum Press; *Landolt–Börnstein*, Springer-Verlag, Berlin, 1968, 1971, etc.; and K. A. Gschneidner (1964), *Solid State Phys.* **16**, 275–476.

[c] American Inst. of Physics Handbook (1972), 3rd edition, coordinating ed. D. E. Gray, Table 9d, p. 9-39, McGraw Hill, NY.

[d] G. K. White. and P. J. Meeson. (2002), *Experimental Techniques in Low-Temperature Physics,* 4th edition, Oxford University Press.

[e] Magnetic susceptibility data were recalculated from molar susceptibilities given in the *CRC Handbook of Chemistry and Physics* (2000), 81st edition, CRC Press, Boca Raton, Florida; and from compilations given in *Landolt–Börnstein*, *Numerical Data and Functional Relationships in Science and Technology,* New Series, II/16 (1986); III/19, subvolumes a to i2 (1986–1992); and II/2, II/8, II10, II11, and II12a, (1966-1984), Springer-Verlag, Heidelberg; *Tables de Constantes et Donnees Numerique* (1957), Vol. 7, *Relaxation paramagnetique*, Masson, Paris.

[f] Superconducting critical temperatures are from B. W. Roberts (1978), "Properties of selected superconductive materials," 1978 Supplement, *NBS Technical Note* **983**, U.S. Government Printing Office, Washington, D.C.; tabulated in the *CRC Handbook of Chemistry and Physics* (2000), 81st edition, CRC Press, Boca Raton, Florida. Note that thin films of these elements generally have higher critical temperatures than those listed here for bulk materials (see the CRC handbook).

A6.2 Specific heat vs. temperature of technical materials (Sec. 6.1)

To convert these values of specific heat at constant pressure to *volumetric* heat capacity, multiply each value by the density of the material (densities of elements are given in Appendix A6.1).

Specific Heat C_P $[J/(g\cdot K)] \equiv [10^{-3}\ J/(kg\cdot K)]$

Material	4 K	10 K	20 K	30K	50K	77 K	100 K	150 K	200 K	300 K
Metals										
Al [a]	0.00026	0.00140	0.0089	0.032	0.142	0.336	0.481	0.684	0.797	0.902
Cu [a, b]	0.00009	0.00088	0.0070	0.027	0.097	0.192	0.252	0.323	0.356	0.386
Fe [a]	0.00038	0.00124	0.0045	0.012	0.055	0.144	0.216	0.323	0.384	0.447
In [a]	0.00095	0.0155	0.061	0.108	0.162	0.191	0.203	0.219	0.225	0.233
Nb [a]	0.00040	0.00220	0.0113	0.035	0.099	0.167	0.202	0.239	0.254	0.268
Ni [a]	0.00050	0.00162	0.0058	0.017	0.068	0.163	0.232	0.328	0.383	0.445
Si [a]	0.000017	0.00028	0.0034	0.017	0.079	0.177	0.259	0.425	0.556	0.714
Ti [a]	0.00032	0.00126	0.0070	0.025	0.099	0.218	0.300	0.407	0.465	0.522
W [a]	0.00004	0.00023	0.0019	0.008	0.033	0.068	0.089	0.114	0.125	0.136
Alloys										
Al 2024 [e]	—	—	—	—	—	0.478	0.534	0.639	0.736	0.855
Al-6061-T6 [f]	0.00029	0.00157	0.0089	0.033	0.149	0.348	0.492	0.713	0.835	0.954
Brass (65wt%Cu–35wt%Zn [g] (yellow brass)	0.00015 [e]	—	0.011	0.041	0.118	0.216	0.270	0.330	0.360	0.377
Constantan (60wt%Cu–40wt%Ni) [a]	0.00049	0.00169	0.0068	0.022	0.083	0.175	0.238	0.322	0.362	0.410
Inconel (77wt%Ni–15wt%Cr–7wt%Fe) [e]	—	—	—	—	—	0.275	0.291	0.334	0.369	0.427
Stainless Steel 304L [f]	0.0017	0.0047	0.016	—	—	—	—	—	—	—
Stainless Steel 310 [d]	0.0020	0.0052	0.017	0.01	0.10	0.20	0.25	0.35	0.40	0.48
Ti–6wt%Al–4wt%V [e]	—	—	—	0.007	0.098	0.217	0.300	0.410	0.477	0.529
Polymers & Composites										
Epoxy (Stycast 2850FT™) [h]	0.0005	0.0063	0.0226	0.042	0.083	0.154	0.240	—	—	—
Epoxy (CY221) [c]	—	0.022	0.085	0.170	0.270	0.400	0.480	—	1.000	1.300

Material	4 K	10 K	20 K	30K	50K	77 K	100 K	150 K	200 K	300 K
G-10CR [f] glass/resin	0.0020	0.0154	0.047	0.081	0.149	0.239	0.317	0.489	0.664	0.999
Glass/resin (S 901Glass/ NASA Resin 2) [i]	0.00064	0.0067	0.028	0.050	0.094	0.169	0.262	0.56	0.96	1.94
Plexiglas™ (PMMA) [c]	—	0.017	0.080	0.147	0.280	0.420	0.550	—	0.920	—
Polyamide (Nylon™) [f]	0.0016	0.020	0.100	0.200	0.380	0.574	0.717	0.984	1.21	1.62
Polyimide (Kapton™) [f]	0.00079	0.0117	0.0579	0.116	0.224	0.338	0.414	0.537	0.627	0.755
Teflon™ (PTFE) [c]	—	0.026	0.079	0.126	0.210	0.310	0.392	0.550	0.677	0.870
Ceramics and Nonmetals										
AlN [e]	—	—	—	—	—	0.074	0.139	0.305	0.471	0.739
Apiezon N™ [f]	0.00203	0.0243	0.0925	0.172	0.332	0.522	0.657	0.913	1.201	—
Carbon (diamond) [a]	—	0.00002	0.0001	0.000	0.002	0.008	0.020	0.084	0.195	0.518
Ice [a]	0.00098	0.0152	0.114	0.229	0.440	0.689	0.882	1.230	1.570	—
MgO [a]	—	—	0.0022	0.006	0.024	0.101	0.208	0.465	0.680	0.940
Pyrex™ [a]	0.00020	0.0042	—	—	—	—	—	—	—	—
Sapphire (Al_2O_3) [e]	—	0.00009	0.0007	0.003	0.015	0.060	0.126	0.314	0.502	0.779
SiC [e]	—	—	—	—	—	0.052	0.107	0.253	0.405	0.676
Silica glass (SiO_2), Quartz Crystal (SiO_2)[a]	—	0.00070	0.0113	0.035	0.097	0.185	0.261	0.413	0.543	0.745
$SrTiO_3$ [e]	—	—	—	—	—	0.181	0.246	0.358	0.439	0.536
ZrO_2 [e]	—	—	—	—	—	0.100	0.153	0.261	0.347	0.456

[a] R. J. Corruccini and J. J. Gniewek (1960), National Bureau of Standards Monograph 21, U.S. Government Printing Office, Washington,. D.C.

[b] C. Y. Ho and A. Cezairliyan (1988), *Specific Heat of Solids*, Hemisphere Publishing Corp., New York.

[c] G. Hartwig (1994), *Polymer Properties at Room and Cryogenic Temperatures,* Plenum Press, New York,

[d] L. L. Sparks (1983), Chapter 2 in *Materials at Low Temperatures,* R. P. Reed and A. F. Clark, eds., ASM International, Metals Park, Ohio.

[e] Y. S. Touloukian and E. H. Buyco (1970), *Specific Heat,* Vols. 4 and 5, Plenum Press, New York.

[f] R. Radebaugh et al. (2003), *http://ww*w.cryogenics.nist.gov/ and the references listed therein.

[g] G. K. White and P. J. Meeson (2002), *Experimental Techniques in Low-Temperature Physics,* 4th edition, Oxford University Press.

[h] C. A. Swenson (1997), *Rev. Sci. Instrum.* **68**, 1312–1315.

[i] E. W. Collings and R. D. Smith (1978), *Adv. in Cryog. Eng.* **24**, 290–296.

A6.3 Debye model values of the molar heat capacity and molar internal energy as a function of temperature (Sections 6.1.2 and 6.1.3)

Tabulated values of the molar heat capacity are at constant volume, designated as C_V .

Molar internal energy U is obtained by integrating the heat capacity, tabulated here as $(U–U_o)/T \equiv T^{-1} \int_0^T C_V \, dT$ and plotted in Fig. 6.2.

Values of the Debye temperature θ_D are tabulated for common elements in Appendix A6.1.

T/θ_D	θ_D/T	C_V [J/(mol·K)]	$(U–U_o)/T \equiv T^{-1} \int_0^T C_V \, dT$ [J/(mol·K)]
∝	0.0	24.94	24.94
10	0.1	24.93	24.02
5	0.2	24.89	23.12
2.5	0.4	24.74	21.40
2.0	0.5	24.63	20.58
1.667	0.6	24.50	19.78
1.25	0.8	24.16	18.25
1.0	1.0	23.74	16.82
0.833	1.2	23.24	15.48
0.714	1.4	22.66	14.24
0.625	1.6	22.02	13.08
0.556	1.8	21.33	12.00
0.500	2.0	20.59	11.00
0.400	2.5	18.60	8.83
0.333	3.0	16.53	7.07
0.286	3.5	14.48	5.66
0.250	4.0	12.55	4.53
0.222	4.5	10.78	3.64
0.200	5.0	9.195	2.93
0.1667	6.0	6.625	1.94
0.143	7.0	4.760	1.31
0.125	8.0	3.447	0.912
0.111	9.0	2.531	0.654
0.100	10.0	1.891	0.481

T/θ_D	θ_D/T	C_V [J/(mol·K)]	$(U-U_o)/T \equiv T^{-1}\int_0^T C_V\,dT$ [J/(mol·K)]
0.0909	11.0	1.440	0.363
0.0833	12.0	1.117	0.281
0.0769	13.0	0.882	0.221
0.0714	14.0	0.707	0.177
0..0625	16.0	0.474	0.119
0.0556	18.0	0.333	0.083
0.0500	20.0	0.243	0.061
0.0400	25.0	0.124	0.031
0.0333	30.0	0.072	0.018

[a] From G. T. Furukawa, T. B. Douglas, and N. Pearlman (1972), Chapter 4e in *American Institute of Physics Handbook,* McGraw–Hill.

A6.4 Thermal expansion/contraction of technical materials (Sec. 6.2)

The total linear contraction from room temperature to the indicated temperature T is defined as

$$\Delta L/L \equiv (L_{293\mathrm{K}} - L_T)/L_{293\mathrm{K}}.$$

The coefficient of linear expansion at room temperature is defined as

$$\alpha \equiv (1/L)\, \mathrm{d}L/\mathrm{d}T.$$

Since the thermal expansion/contraction is approximately linear above room temperature, the total contraction from an upper reference temperature T_u above room temperature (such as soldering temperature) to a low temperature T can be determined approximately from

$$\Delta L/L_{T_u - T} = \Delta L/L_{293\mathrm{K}-T} + (\alpha_{293\mathrm{K}})\,(T_\mathrm{u} - 293\ \mathrm{K}).$$

Data on Invar, glasses, ceramics, and other materials having a very low thermal contraction are given in Figs. 6.8 and 6.9. Thermal contraction data at 4 K and 77 K for a few additional materials are tabulated in Appendixes A7.4 and A7.5.

Thermal Expansion/Contraction of Technical Materials

Definitions: $\Delta L/L \equiv (L_{293K} - L_T)/L_{293K}$; $\alpha \equiv (1/L)\, dL/dT$

Material	$\Delta L/L$ at 4 K [%]	$\Delta L/L$ at 40 K [%]	$\Delta L/L$ at 77 K [%]	$\Delta L/L$ at 100 K [%]	$\Delta L/L$ at 150 K [%]	$\Delta L/L$ at 200 K [%]	$\Delta L/L$ at 250 K [%]	α at 293 K [10^{-6} K^{-1}]
Metals								
Ag [b]	0.413	0.405	0.370	0.339	0.259	0.173	0.082	18.5 [h]
Al [a]	0.415	0.413	0.393	0.370	0.295	0.201	0.097	23.1 [b]
Au [b]	0.324	0.313	0.281	0.256	0.195	0.129	0.061	14.1
Be [b]	0.131	0.131	0.130	0.128	0.115	0.087	0.045	11.3 [d]
Cu [a]	0.324	0.322	0.302	0.282	0.221	0.148	0.070	16.7 [i]
Fe [a]	0.198	0.197	0.190	0.181	0.148	0.102	0.049	11.6 [b]
Hg [b,*]	0.843	0.788	0.788	0.592	0.396	0.176	*	57.2 [*]
In [b]	0.706	0.676	0.602	0.549	0.421	0.282	0.135	32.0
Mo [b]	0.095	0.094	0.090	0.084	0.067	0.046	0.022	4.8 [d]
Nb [a]	0.143	0.141	0.130	0.121	0.094	0.063	0.030	7.3 [d]
Ni [a]	0.224	0.223	0.212	0.201	0.162	0.111	0.053	13.4 [d]
Pb [b]	0.708	0.667	0.578	0.528	0.398	0.263	0.124	29
Ta [b]	0.143	0.141	0.128	0.117	0.089	0.059	0.028	6.6
Sn [b] (white) [r]	0.447	0.433	0.389	0.356	0.272	0.183	0.086	20.5
Ti [a]	0.151	0.150	0.143	0.134	0.107	0.073	0.035	8.3 [b]
W [b]	0.086	0.085	0.080	0.075	0.059	0.040	0.019	4.5
Alloys								
Al-6061-T6 [c]	0.414	0.412	0.389	0.365	0.295	0.203	0.097	22.5
Brass (65%Cu–35%Zn) [b] (yellow brass)	0.384	0.380	0.353	0.326	0.253	0.169	0.080	19.1 [b]
Constantan (50Cu–50Ni) [b]	—	0.264	0.249	0.232	0.183	0.124	0.043	13.8 [b]
Cu–2%Be-0.3%Co (Beryllium copper, Berylco 25) [b]	0.316	0.315	0.298	0.277	0.219	0.151	0.074	18.1 [b]
Fe–9%Ni [a]	0.195	0.193	0.188	0.180	0.146	0.100	0.049	11.5
Hastelloy C [q]	0.218	0.216	0.204	0.193	0.150	0.105	0.047	10.9 [c]
Inconel 718 [a]	0.238	0.236	0.224	0.211	0.167	0.114	0.055	13.0 [k]
Invar (Fe–36%Ni) [a]	—	0.040	0.038	0.036	0.025	0.016	0.009	3.0 [k]
50%Pb–50%Sn solder [a]	0.514	0.510	0.480	0.447	0.343	0.229	0.108	23.4 [d]

Material	$\Delta L/L$ at 4 K [%]	$\Delta L/L$ at 40 K [%]	$\Delta L/L$ at 77 K [%]	$\Delta L/L$ at 100 K [%]	$\Delta L/L$ at 150 K [%]	$\Delta L/L$ at 200 K [%]	$\Delta L/L$ at 250 K [%]	α at 293 K [10^{-6} K^{-1}]
Stainless Steel (AISI 304) [b]	0.296	0.296	0.281	0.261	0.206	0.139	0.066	15.1 [l]
Stainless Steel (AISI 310) [b]	—	—	—	0.237	0.187	0.127	0.061	14.5
Stainless Steel (AISI 316) [b]	0.297	0.296	0.279	0.259	0.201	0.136	0.065	15.2 [l]
Ti–6Al–4V [a]	0.173	0.171	0.163	0.154	0.118	0.078	0.036	8.0 [m]
Superconductors								
Bi-2212 *a,b*-axes [u,y]	0.152	0.150	0.139	0.132	0.106	0.074	0.036	8.3
Bi-2212 *c*-axis [u,y]	0.295	0.289	0.266	0.250	0.199	0.136	0.064	15.1
Bi (2223)/Ag tape [g]								
($\geq 2^{nd}$ cool-down)	—	0.31	0.30	0.28	0.22	0.15	0.07	13
Bi-2223 *a,b*-axes [z,u,y]	0.15	0.15	0.14	0.13	0.11	0.07	0.04	8.3
Bi-2223 *c*-axis [z,u,y]	0.30	0.29	0.27	0.25	0.20	0.14	0.06	15
Bi-2223/61%Ag-alloy tape [w,x]			0.24					
Nb_3Sn [a]	0.16	0.16	0.14	0.13	0.095	0.065	0.03	7.6 [t]
Nb_3Sn(10vol%)/Cu wire [s]	0.30		0.28					
Nb–45 Ti [a]	0.188	0.184	0.169	0.156	0.117	0.078	0.038	8.2
Nb–Ti/Cu wire [a]	0.265	0.262	0.247	0.231	0.179	0.117	0.054	12.5
YBCO *a*-axis [f]	—	—	0.12	0.12	0.10	0.070	0.04	7.4
YBCO *b*-axis [f]	—	—	0.16	0.15	0.13	0.10	0.05	9.6
YBCO *c*-axis [f]	—	—	0.34	0.33	0.25	0.17	0.09	17.7
Polymers								
Epoxy [a]	1.16	1.11	1.028	0.959	0.778	0.550	0.277	66
Epoxy (Stycast 2850FT™) [e]	0.44	0.43	0.40	0.38	0.32	0.225	0.12	28
CTFE (Teflon™) [a]	1.135	1.070	0.971	0.900	0.725	0.517	0.269	67 [b]
TFE (Teflon™) [a]	2.14	2.06	1.941	1.85	1.600	1.24	0.750	250 [n]
PMMA (Plexiglas™) [a]	1.22	1.16	1.059	0.99	0.820	0.59	0.305	75 [o]
Polyamide (Nylon™) [a]	1.389	1.352	1.256	1.172	0.946	0.673	0.339	80
Polyimide (Kapton™) [c]	0.44	0.44	0.43	0.41	0.36	0.29	0.16	46
Composites [a]								
G-10CR epoxy/glass (‖ glass fibers)	0.241	0.234	0.213	0.197	0.157	0.108	0.052	12.5
G-10CR epoxy/glass (normal)	0.706	0.690	0.642	0.603	0.491	0.346	0.171	41 [p]

Material	$\Delta L/L$ at 4 K [%]	$\Delta L/L$ at 40 K [%]	$\Delta L/L$ at 77 K [%]	$\Delta L/L$ at 100 K [%]	$\Delta L/L$ at 150 K [%]	$\Delta L/L$ at 200 K [%]	$\Delta L/L$ at 250 K [%]	α at 293 K [10^{-6} K^{-1}]
Ceramics & Nonmetals								
Al N (‖ *a*-axis) [q]	—	—	0.032	0.031	0.028	0.020	0.011	3.7
Al N (‖ *c*-axis) [q]	—	—	0.025	0.025	0.022	0.017	0.009	3.0
C (diamond) [b]	0.024	0.024	0.024	0.024	0.023	0.019	0.011	1.0
Glass (Pyrex™)	0.055	0.057	0.054	0.050	0.040	0.027	0.013	3.0 [o]
MgO [b]	0.139	0.139	0.137	0.133	0.114	0.083	0.042	10.2
Quartz (‖ optic axis) [b]	—	—	—	0.104	0.085	0.061	0.030	7.5
Sapphire (Al_2O_3) [m] (‖*c*-axis)	—	0.079	0.078	0.075	0.066	0.048	0.025	5.4 [q]
Si [b]	0.022	0.022	0.023	0.024	0.024	0.019	0.010	2.32
α-SiC (polycrystalline) [q]	—	—	0.030	0.030	0.029	0.024	0.013	3.7
Silica glass [b]	-0.008	-0.005	-0.002	-0.0001	0.002	0.002	0.002	0.4

***** For mercury, all data are referenced to its solidification temperature, 234 K.

[a] A. F. Clark (1983), Chapter 3 in *Materials at Low Temperatures*, ASM International, Materials Park, Ohio.

[b] R. J. Corruccini, and J. J. Gniewek. (1961), *Thermal Expansion of Technical Solids at Low Temperatures*, National Bureau of Standards Monograph 29, U.S. Government Printing Office, Washington, D.C.

[c] R. Radebaugh. et al. (2001), http://www.cryogenics.nist.gov/ and the references listed therein.

[d] *CRC Handbook of Chemistry and Physics* (2001), 82nd edition, CRC Press, Boca Raton, Florida.

[e] C. A. Swenson (1997), *Rev. Sci. Instrum.* **68**, 1312–1315.

[f] Calculated from data by H. You, J. D. Axe, X. B. Kan, S. Hashimoto, S. C. Moss, J. Z. Liu, G. W. Crabtree, and D. J. Lam (1988), *Phys. Rev.* **B38**, 9213–9216.

[g] N. Yamada, K. Nara, M. Okaji, T. Hikata, T. Kanedo, and N. Sadakata (1998). *Cryogenics* **38**, 397–399.

[h] V. J. Johnson, ed. (1961). *Properties of Materials at Low Temperature, Phase 1*, U.S. Government Printing Office.

[i] T. A. Hahn (1970). *J. Appl. Phys.* **41**, 5096–5101.

[j] N. J. Simon, E. S. Drexler, and R. P. Reed (1992), *Properties of Copper and Copper Alloys at Cryogenic Temperatures,* NIST Monograph 177, U.S. Government Printing Office, Washington, D.C.; N. Cheggour and D. P. Hampshire, *Rev. Sci. Instr.* **71**, 4521–4529 (2000).

[k] A. F. Clark (1968), *Cryogenics* **8**, 282–289.

[l] *Handbook on Materials for Superconducting Machinery* (1974, 1976), National Bureau of Standards, U. S. Government Printing Office, Washington, D. C.

[m] V. Arp, J. H. Wilson, L. Winrich, and P. Sikora (1962), *Cryogenics* **2**, 230–235.

[n] R. K. Kirby (1956), *J. Res. Natl. Bur. Stand.* **57**, 91–94.

[o] H. L. Laquer and E. L. Head (1952). *Low Temperature Thermal Expansion of Plastics*. AECU-2161, Technical Information Service A.E.C., Oak Ridge, Tennessee.

[p] A. F. Clark, G. Fujii, and M. A. Ranney (1981), *IEEE Trans. Magn.* **MAG-17**, 2316–2319.

[q] Y. S. Touloukian, *Thermal Expansion* **12**, 1248.

[r] Tin is anisotropic. Mean values were calculated as 1/3(‖) + 2/3(⊥), where (‖) and (⊥) signify the contraction parallel and perpendicular to the tetragonal axis. White tin is the ordinary ductile variety; it may transform

to brittle grey tin (with a diamond-type lattice) at low temperatures, but usually it does not because of impurity stabilization. (See ref. b for more information.)

[s] L. F. Goodrich, S. L. Bray, and T. C. Stauffer (1990), *Adv. Cryog. Eng. (Mater.)* **36A**, 117–124.

[t] D. S. Easton, D. M. Kroeger, W. Specking, and C. C. Koch (1980), *J. Appl. Phys*. **51**, 2748.

[u] M. Okaji, K. Nara, H. Kato, K. Michishita, and Y. Kubo (1994), *Cryogenics* **34**, 163.

[v] S. Ochiai, K. Hayashi, and K. Osamura (1991), *Cryogenics* **31**, 959.

[w] E. Harley (2004), American Superconductor Corp., personal communication.

[x] J. P. Voccio, O. O. Ige, S. J. Young, and C. C. Duchaine (2001). *IEEE Trans. Appl. Supercon.* **11**, 3070–3073.

[y] M. Mouallem-Bahout, J. Gaudé, G. Calvarin, J.–R. Gavarri, and C. Carel, (1994), *Mater. Lett.* **18**, 181–185.

[z] Data are for Bi-2212 oriented crystals, but the atomic structures of the Bi-2223 and Bi-2212 phases are close enough that the Bi-2212 crystal data should approximately apply to both.

A6.5a Ideal electrical resistivity vs. temperature for pure metals (Sec 6.3)

The *ideal* resistivity $\rho_i(T)$ is tabulated below for *ideally* pure metals. The *total* resistivity $\rho(T)$ of *nearly* pure metals is approximated by summing the temperature-dependent ideal resistivity $\rho_i(T)$ and the temperature-*in*dependent residual resistivity ρ_{res} (that arises from defects). This is expressed as Matthiessen's rule:

$$\rho(T) \equiv \rho_{res} + \rho_i(T).$$

(Deviations from Matthiessen's rule are briefly described in Sec. 6.3.4.)

In nearly pure metals, ρ_{res} is highly variable from specimen to specimen, because ρ_{res} depends on trace impurity levels and cold-work conditions. Therefore, it must be measured on an individual material basis (typically with a dip test in liquid helium) or estimated from such a measurement on a similar material. The total resistivity is then calculated from the above equation.

The *Residual Resistance Ratio* (RRR $\equiv R_{RT}/R_{4K} = \rho_{295K}/\rho_{4K}$) is often used as an indicator of sample purity for pure metals [that is, the residual resistivity $\rho_{res} \approx \rho_{4K} = \rho_{i\,295K}/(\text{RRR} - 1)$]. The higher the value of RRR, the lower ρ_{res}, and the more defect-free the metal. (Appendix A3.1 lists RRR values for common conductor materials, which can be used to estimate ρ_{res}; an example is given in Sec. 6.3.4.)

Values of the ideal resistivity $\rho_i(T)$ tabulated below were determined experimentally by assuming the validity of Matthiessen's rule and subtracting the measured value of ρ_{res} from precise measurements of the total $\rho(T)$ measured for very pure metals.

For convenience, the *total* resistivities of two oxygen-free copper (OFHC) samples are also listed, one with RRR ≅ 100, and the other 60% cold-drawn. Unlike the rest of the data, entries for these two material listings are not *ideal* resistivities and apply only to copper samples of comparable RRR or cold work.

Resistivity data at room temperature for additional elements are given in Appendix A6.1.

Ideal Resistivity ρ_i [$\Omega\cdot m \times 10^{-8} \equiv \mu\Omega\cdot cm$]

Pure Metal	10 K	20 K	50 K	77 K	100K	150 K	200 K	250 K	295 K
[RRR ≡ ρ_{RT}/ρ_{4K}]									
Ag (RRR=1800) [a]	0.0001	0.003	0.103	0.27	0.42	0.72	1.03	1.39	1.60
Al (RRR=3500) [a]	—	0.0007	0.047	0.22	0.44	1.01	1.59	2.28	2.68
Au (RRR=300) [b]	0.0006	0.012	0.20	0.42	0.62	1.03	1.44	1.92	2.20
Cu (RRR=3400) [k]	—	0.0010	0.049	0.19	0.34	0.70	1.05	1.38	1.69
Cu(OFHC) (RRR≅100)[i]									
(*total* ρ)	0.015	0.017	0.084	0.21	0.34	0.70	1.07	1.41	1.70
Cu (OFHC) (60 % cold									
drawn) [i] (*total* ρ)	0.030	0.032	0.10	0.23	0.37	0.72	1.09	1.43	1.73
Fe (RRR=100) [c]	0.0015	0.007	0.135	0.57	1.24	3.14	5.3	7.55	9.8
In (RRR=5000) [d]	0.018	0.16	0.92	1.67	2.33	3.80	5.40	7.13	8.83
Nb (RRR=213) [e]	—	0.062	0.89	2.37	3.82	6.82	9.55	12.12	14.33
Ni (RRR=310) [c]	—	0.009	0.15	0.50	1.00	2.25	3.72	5.40	7.04
Pb (RRR=14000, [f]									
RRR=10^5) [g]	—	0.53 [f]	2.85 [f]	4.78 [f]	6.35 [g]	9.95 [g]	13.64 [g]	17.43 [g]	20.95 [g]
Pt (RRR=600) [c]	0.0029	0.036	0.72	1.78	2.742	4.78	6.76	8.70	10.42
Ta (RRR=77) [c]	0.0032	0.051	0.95	2.34	3.55	6.13	8.6	11.0	13.1
Ti (RRR=20) [h]	—	0.020	1.4	4.45	7.9	16.7	25.7	34.8	43.1
W (RRR=100) [j]	0.0002	0.0041	0.150	0.56	1.03	2.11	3.20	4.33	5.36

[a] R. S. Seth and S. B. Woods (1970), *Phys. Rev.* **B2**, 2961; J. Bass, ed. (1982), *Landolt–Börnstein*, Vol. III/15a, *Metals: Electronic Transport Phenomena,* Springer-Verlag, Berlin.

[b] D. Damon, M. P. Mathur, and P. G. Klemens (1968), *Phys. Rev.* **176**, 876; J. Bass, ed. (1982), *Landolt–Börnstein*, Vol. III/15a *Metals: Electronic Transport Phenomena,* Springer-Verlag, Berlin.

[c] G. K. White and S. B. Woods (1959), *Philos. Trans. Roy. Soc.* **A251,** 273; J. Bass, ed. (1982), *Landolt–Börnstein,* Vol. III/15a, *Metals: Electronic Transport Phenomena,* Springer-Verlag, Berlin.

[d] G. K. White and S. B. Woods (1957), *Rev. Sci. Instrum.* **28**, 638; J. Bass, ed. (1982), *Landolt–Börnstein,* Vol. III/15a, *Metals: Electronic Transport Phenomena,* Springer-Verlag, Berlin.

[e] J. M. Abraham, C. Tete, and B. Deviot (1974), *J. Less-comm. Met.* **37**, 181; J. Bass, ed. (1982), *Landolt–Börnstein,* Vol. III/15a, *Metals: Electronic Transport Phenomena,* Springer-Verlag, Berlin.

[f] B. N. Aleksandrov and I. G. D'Yakov (1963), *Sov. Phys. JETP* (English Transl.) **16**, 603–608; *Zh. Eksp. Teor. Fiz.* (1962) **43**, 399; J. Bass, ed. (1982), *Landolt–Börnstein,* Vol. III/15a, *Metals: Electronic Transport Phenomena,* Springer-Verlag, Berlin.

[g] J. P. Moore and R. S. Graves (1973), *J. Appl. Phys*. **44**, 1174; J. Bass, ed. (1982), *Landolt–Börnstein,* Vol. III/15a, *Metals: Electronic Transport Phenomena,* Springer-Verlag, Berlin.

[h] R. J. Wasilewski (1962), *Trans. Met. Soc. AIME* **224**, 13; J. Bass, ed. (1982), *Landolt–Börnstein,* Vol. III/15a, *Metals: Electronic Transport Phenomena,* Springer-Verlag, Berlin.

[j] J. G. Hust (1976), *High Temp.- High Press.* **8**, 377–390.
[k] J. S. Dugdale (1965), unpublished data, Univ. of Leeds, Leeds, UK.

A6.5b Total electrical resistivity vs. temperature for technical alloys and common solders [a] *(Sec 6.3)*

For *alloys,* values of the *total* resistivity $\rho(T)$ are tabulated [i.e., $\rho(T) \equiv \rho_{res} + \rho_i(T)$], since there is little specimen-to-specimen variation in the residual resistivity contribution from defects.

Resistivities of solid alloys at room temperature are tabulated in Appendix A3.7.

Alloy total resistivity ρ [Ω·m $\times 10^{-8} \equiv \mu\Omega$·cm]

Alloy	10 K	20 K	50 K	77 K	100K	150 K	200 K	250 K	295 K
Al 1100–0	0.08	0.08	0.16	0.32	0.51	1.07	1.72	2.37	2.96
Al 5083–0	3.03	3.03	3.13	3.33	3.55	4.15	4.79	5.39	5.92
Al 6061–T6	1.38	1.39	1.48	1.67	1.88	2.46	3.09	3.68	4.19
Hastelloy C	123	123	123	124	—	—	126	—	127
Inconel 625	124	124	125	125	—	—	127	—	128
Inconel 718	108	108	108	109	—	—	114	134	156
Berylco 25 (Cu-2%Be-0.3%Co)	6.92	6.92	7.04	7.25	7.46	7.96	8.48	8.98	9.43
Phosphor Bronze A	8.58	8.58	8.69	8.89	9.07	9.48	9.89	10.3	10.7
Cartridge Brass (70%Cu–30%Zn)	4.22	4.22	4.39	4.66	4.90	5.42	5.93	6.42	6.87
CuNi 30 (67Ni–30Cu) (Monel)	36.4	36.5	36.6	36.7	36.9	37.4	37.9	38.3	38.5
Ti–6%Al–4%V	—	147	148	150	152	157	162	166	169
Stainless Steel (304L)	49.5	49.4	50.0	51.5	53.3	58.4	63.8	68.4	72.3
Stainless Steel (310)	68.6	68.8	70.4	72.5	74.4	78.4	82.3	85.7	88.8
Stainless Steel (316)	53.9	53.9	54.9	56.8	58.8	63.8	68.9	73.3	77.1
Invar (Fe–36%Ni)	50.3	50.5	52.1	54.5	57.0	63.3	70.0	76.5	82.3

[a] Values were interpolated with a cubic spline fit to data obtained by A. F. Clark, G. E. Childs, and G. H. Wallace (1970), *Cryogenics* **10**, 295–305.

A6.6 Superconductor properties (Sec. 6.3.6)

Property values of these high-field superconductors are representative because there is some variation with sample composition, inhomogeneities, and impurity levels.

Additional data on critical-temperature values of superconducting *elements* are included in the general table of Appendix A6.1

Superconductor	Crystal Structure [*]	Lattice Constants [Å] [†]			T_c	$\mu_0 H_{c2}$ (0 K)	λ_{GL}(0 K) [‡]	ξ_{GL}(0 K) [ζ]
		a	*b*	*c*	[K]	[T]	[nm]	[nm]
<u>*Low* T_c</u>								
Nb–Ti [e]	A2				9.3 [j]	13	300	4
V_3Ga [e]	A15	4.816 [n]	—	—	15	23	90	2–3
V_3Si [e]	A15	4.722 [n]	—	—	16	20	60	3
Nb_3Sn [e]	A15	5.289 [n]	—	—	18	23	65	3
Nb_3Al [o]	A15	5.187 [n]	—	—	18.9	32		
Nb_3Ga [o]	A15	5.171 [n]	—	—	20.3	34		
$Nb_3(Al_{75}Ge_{25})$ [b]	A15				20.5	41		
Nb_3Ge [e]	A15	5.166 [n]	—	—	23	38	90	3
NbN [e]	B1				16	15	200	5
V_2(Hf,Zr) [o]	C15				10.1	24		
$PbMo_6S_8$ [e]	Chevrel				15	60	200	2
MgB_2	hexagonal	3.086 [m]	—	3.521 [m]	39	~16 (*a*,*b*) [l] ~2.5 (*c*)	140 [k]	5.2 [k]

Superconductor	Crystal Structure [*]	Lattice Constants [Å] [†]			T_c	$\mu_0 H_{c2}$ (0 K)	λ_{GL}(0 K) [‡]	ξ_{GL}(0 K) [ζ]
		a	*b*	*c*	[K]	[T]	[nm]	[nm]
High T_c [a]								
$La_{1.85}Sr_{0.15}CuO_{4-\delta}$ [e]	I4/mmm	3.779	3.779	1.323	40	50	80 (*a,b*)	~4 (*a,b*)
							400 (*c*)	0.7 (*c*)
$YBa_2Cu_3O_{7-\delta}$ [d]	Pmmm	3.818	3.884	11.683	90	670 (*a,b*)	150 (*a,b*)	~2 (*a,b*)
(YBCO)						120 (*c*)	900 (*c*)	0.4 (*c*)
$Bi_2Sr_2CaCu_2O_{8-\delta}$ [d]	A2aa	5.410	5.420	30.930	90	280 (*a,b*)	300 (*a,b*)	~3 (*a,b*)
(Bi-2212)						32 (*c*)		0.4 (*c*)
$(Bi,Pb)_2Sr_2Ca_2Cu_3O_{10+\delta}$	Perovskite	5.39	5.40	37	110			
(Bi-2223)	(orthorhombic)							
$Tl_2Ba_2CaCu_2O_{8+\delta}$ [d,p]	I4/mmm	3.856	3.856	29.260	110		215 (*a,b*)	2.2 (*a,b*)
(Tl-2212)								0.5 (*c*)
$Tl_2Ba_2Ca_2Cu_3O_{10-\delta}$ [d,p]	I4/mmm	3.850	3.850	35.88	125	120	205 (*a,b*)	1.3 (*a,b*)
(Tl-2223)							480 (*c*)	
$HgBa_2Ca_2Cu_3O_{8+\delta}$ [a]	Pmmm	3.85	—	15.85	133	160 [q]		1.42 (*a,b*) [q]

Notation:

[*] Crystal structures for the low-T_c superconductors are listed here mostly by the Strukturbericht designation, whereas for the high-T_c materials they are mostly listed by the Space group designation. Tables of cross lists to different nomenclatures are given in the appendixes to the *ASM Handbook* (1992), Vol. **3,** *Alloy Phase Diagrams*, ASM International, Materials Park, Ohio.

[†] (*a*, *b*) refers to magnetic field, penetration depth, or coherence length being coplanar with the *a,b* crystallographic direction or Cu–O planes (usually parallel to the flat faces of practical conductors); (*c*) refers to an orientation along the *c*-axis; that is, perpendicular to the Cu–O planes (usually perpendicular to the flat faces of most practical conductors).

[‡] The penetration depth $\lambda_{GL}(0\ K)$ is the constant prefactor in the Ginzburg–Landau expression $\lambda_{GL}(T) = \lambda_{GL}(0\ K)\,(1 - T/T_c)^{-0.5}$.

[ζ] The coherence length $\xi_{GL}(0\ \mathrm{K})$ is the constant prefactor in the Ginzburg–Landau expression $\xi_{GL}(T) = \xi_{GL}(0\ \mathrm{K})\,(1-T/T_c)^{-0.5}$.

References:

[a] *CRC Handbook of Chemistry and Physics* (2002), 83rd edition., CRC Press, Boca Raton, Florida.

[b] G. Bogner (1977), "Large scale applications of superconductivity," in *Superconductor Applications: SQUIDS and Machines,* eds. B. B. Schwartz and S. Foner, Plenum, New York.

[c] B. W. Roberts (1978), *Properties of Selected Superconducting Materials*, NBS Technical Note 983, U.S. Government Printing Office, Washington, D.C..

[d] T. Datta (1992), "Oxide superconductors: physical properties," pp. 414–423 in *Concise Encyclopedia of Magnetic & Superconducting Materials,* J. Evetts, ed., Pergamon Press.

[e] R. J. Donnelly (1981), in *Physics Vade Mecum,* ed. H. L. Anderson, Am. Inst. of Physics; T. P. Orlando and K. A. Delin, (1991), *Foundations of Applied Superconductivity,* Addison-Wesley.

[j] L. F. Goodrich and T. C. Stauffer (2003), unpublished data, National Institute of Standards and Technology, Boulder, Colorado.

[k] D. K. Finnemore, J. E. Ostenson, S. L. Bud'ko, G. Lapertot, and P. C. Canfield (2001), *Phys. Rev. Lett.* **86**, 2420–2422.

[l] P. C. Canfield and G. W. Crabtree (2003), *Physics Today* **56**, 34–40.

[m] T. Vogt, G. Schmneider, J. A. Hriljac, G. Yang, and J. S. Abell (2001), *Phys. Rev*. B **63**, 220505/1–3.

[n] M. Weger and I. B. Goldberg (1973), p. 3 in *Solid State Physics,* Vol. 28, eds. H. Ehrenreich, F. Seitz, and D. Turnbull, Academic Press, p. 3.

[o] J. W. Ekin (1983), Chapter 13 in *Materials at Low Temperatures*, eds. R. P. Reed and A. F. Clark, ASM International, Materials Park, Ohio.

[p] E. Bellingeri and R. Flükiger (2003), in *Handbook of Superconducting Materials*, Vol. 1, D. A. Cardwell and D. S. Ginley, eds., Inst. of Phys. Publishing, pp. 993–1027.

[q] J. Schwartz and P.V.P.S.S. Sastry (2003), in *Handbook of Superconducting Materials*, Vol. 1, D. A. Cardwell and D. S. Ginley, eds., Inst. of Phys. Publishing, pp. 1029–1048.

A6.7 Thermal conductivity vs. temperature for selected metals, alloys, glasses, and polymers (Sec. 6.4).

Additional thermal-conductivity data for various amorphous solids (vitreous silica, germania, selenium) and amorphous materials (polystyrene and PMMA) are shown in Fig. 6.14. Thermal conductivity integrals are tabulated for selected cryostat construction materials in Appendix A2.1. Properties of metals with very high thermal conductivities are given in Appendix A3.1.

Thermal conductivity [W/(m·K)]

Material	4 K	10 K	20 K	40 K	77 K	100 K	150 K	200 K	295 K
Metals & Alloys									
Al 5083 [a]	3.3	8.4	17	33	55	66	85	99	118
Al 6061-T6 [a]	5.3	14	28	52	84	98	120	136	155
Beryllium–Copper [g]	1.9	5.0	11	21	36	43	57	72	95
Brass (UNS C36000) (61.5wt%Cu–35.4wt%Zn–3.1st%Pb) [b]	2.0	5.7	12	19	29	40	47	64	86
Brass (68wt%Cu–32wt%Zn) [d]	3.0	10	22	38	53	—	—	—	—
Copper OFHC (RRR≈100) [a]	630	1540	2430	1470	544	461	418	407	397
Inconel 718 [a]	0.46	1.5	3.0	4.7	6.4	7.1	8.1	8.7	9.7
Invar [b]	0.24	0.73	1.7	2.6	4.2	6.2	7.6	10	12
Manganin (Cu–12wt%Mn–3wt%Ni) [d]	0.44	1.4	3.2	6.8	11	—	—	—	—
Soft-Solder (Sn–40wt%Pb) [d]	16	43	56	53	53	—	—	—	—
Stainless Steel 304,316 [a]	0.27	0.90	2.2	4.7	7.9	9.2	11	13	15
Ti (6%Al–4%V) [a]	—	—	0.84	1.9	3.5	3.8	4.6	5.8	7.4
Polymers									
G-10CR (Normal) [a]	0.072	0.11	0.16	0.22	0.28	0.31	0.37	0.45	0.60
G-10CR (Warp) [a]	0.073	0.14	0.20	0.27	0.39	0.45	0.57	0.67	0.86
HDPE [c]	0.029	0.090	—	—	0.41	0.45	—	—	0.40
Kevlar 49 [a]	0.030	0.12	0.29	0.59	1.0	1.2	1.5	1.7	2.0

Material	4 K	10 K	20 K	40 K	77 K	100 K	150 K	200 K	295 K
PMMA (Plexiglas™) [c]	0.033	0.060	—	—	—	0.16	0.17	0.18	0.20
Polyamide (Nylon™) [a]	0.012	0.039	0.10	0.20	0.29	0.32	0.34	0.34	0.34
Polyimide (Kapton™) [a]	0.011	0.024	0.048	0.083	0.13	0.14	0.16	0.18	0.19
Polyethylene terepthalate (Mylar™) [b]	0.038	0.048	0.073	0.096	0.12	—	—	—	—
PVC [c]	0.027	0.040	—	—	—	0.13	0.13	0.13	0.14
PTFE (Teflon™) [a]	0.046	0.10	0.14	0.20	0.23	0.24	0.26	0.27	0.27
Ceramics and Nonmetals									
Alumina (Al_2O_3, sintered) [d]	0.49	5.6	24	80	157	136	93	50	—
Macor™ [e]	0.075	0.25	0.60	—	—	—	—	—	—
MgO (crystal) [d]	82	1130	2770	2160	507	294	135	91	61
Pyrex™ glass [d]	0.10	0.12	0.15	0.25	0.45	0.58	0.78	0.92	1.1
Sapphire (Al_2O_3, synthetic crystal) [d, f]	230	2900	15700	12000	1100	450	150	82	47
α-SiC (single crystal, $\perp$ to *c*-axis) [d]	27	420	2000	4700	4000	3000	1500	950	510
SiO_2 crystal (avg. of $\parallel$ and $\perp$ to *c*-axis) [d]	185	1345	545	134	43	30	18	13	9

[a] Cryogenic Materials Properties Program CD, Release B-01 (June 2001), Cryogenic Information Center, 5445 Conestoga Ct., Ste. 2C, Boulder, CO 80301-2724, Ph. (303) 442-0425, Fax (303) 443-1821.

[b] R. Radebaugh. et al. (2003), *http://ww*w.cryogenics.nist.gov/ and the references listed therein.

[c] G. Hartwig (1994), *Polymer Properties at Room and Cryogenic Temperatures*, Plenum Press, New York.

[d] Y. S. Touloukian and E. H. Buyco (1970), *Thermal Conductivity*, Vols. 1 and 2, Plenum Press, New York.

[e] W. N. Lawless (1975), *Cryogenics,* **15**, 273–277.

[f] For sapphire, the direction of heat flow is 60 degrees to the hexagonal axis; values are thought to be accurate to within 10 % to 15 % at temperatures above 60 K, but highly sensitive to small physical and chemical variations below 60 K.

[g] D. E. Gray, ed. (1972), *Thermal Conductivity of Alloys*, Am. Inst. of Physics Handbook, McGraw Hill, Table 4g–9.

A6.8a Magnetic mass *susceptibility from 1.6 K to 4.2 K of materials commonly used in cryostat construction (Sec. 6.5)*

Mass susceptibility is useful for small samples or irregularly shaped parts where the mass of the sample is more easily determined than its volume. It is not difficult, however, to convert between the two with the relation

$$(\text{mass susceptibility } \chi/\rho) \equiv (\text{volume susceptibility } \chi) / (\text{density in kg/m}^3)$$

Mass susceptibility is defined as $\chi/\rho \equiv \sigma/H$, where σ is the magnetic moment per unit mass and H is the magnetic intensity.

The coefficients B and C tabulated below (fourth and fifth columns) are used to calculate mass susceptibility in the temperature range 1.6 K to 4.2 K through the Curie law

$$\chi/\rho \equiv B + (C/T).$$

Mass susceptibility χ/ρ has been evaluated at 4.2 K in the third column.

Values are tabulated in SI units (mks). To convert to cgs units, divide the values in this table by $4\pi \times 10^{-3}$ to get χ/ρ in cm^3/g; see Appendix A1.4.

Magnetic mass susceptibility χ/ρ

Material	Supplier	χ/ρ at 4.2 K [10^{-8} m^3/kg]	B at 1.6K to 4.2 K [10^{-8} m^3/kg]	C at 1.6K to 4.2K [10^{-8} m^3K/kg]
Dielectric Structural Materials				
Alumina [a]	Alcoa	2.8	1.0 ± 0.8	7.5 ± 2
Alscobond Y-725™ and catalyst [c]	Alloy Supply Co.	–9.4	–3.3 ± 0.1	–25.5
Bakelite™, type 950 [c]	Thiokil Chemical Co.	0.3	0.7 ± 0.16	–1.8
Epibond 100A™ [b]	Furane Plastics, Inc.	–0.5	–0.5 ± 0.1	0.1 ± 0.2
Epibond 104™ [a]	"	60	30 ± 3	160 ± 10
Epibond 121™ [a]	"	0.4	0.1 ± 1	1 ± 3.1
Glass				
Plate 7740 [a]	Corning Glass Co.	14	3.8 ± 1	44 ± 5
Test tubes, Pyrex™ [a]	"	7.3	2.5 ± 1	20 ± 4
Tubing 7740 [a]	"	5.6	2.0 ± 1	15 ± 4
Lava, grade A [c]	American Lava Corp.	–21.1	–4.2 ± 0.7	–71
Nylon™ 101, type 66 [b]	Polypenco Ltd.	–0.81	–0.79 ± 0.01	–0.08 ± 0.03
PTFE (Teflon™) [b]	"	–0.40	–0.41 ± 0.01	0.06 ± 0.01
Resin 3135 w/catalyst 7111 [c]	Crest Products Co.	1.24	1.44 ± 0.2	–0.86
Resin 3170 w/catalyst 7133 [c]	"	0.53	0.59 ± 0.017	–0.25
Resin 7343 w/catalyst 7139 [c]	"	1.70	2.24 ± 0.18	–2.24
Quartz [a]		3	4 ± 1.9	–4.4 ± 4.4
Silica				
No washing [a]	Fisher Scientific Co.	1.2	1.8 ± 0.5	–2.3 ± 2.3
Acid washing [a]		–0.1	–0.3 ± 0.9	0.6 ± 1.9
Stycast 2850GT™ w/catalyst No. 9 [a]		27	19 ± 5	33 ± 9
Tufnol™, Carp brand [b]	Tufnol Ltd.	0.5	–0.3 ± 0.3	3.0 ± 0.5
Fibrous Materials				
Absorbent cotton [a]	New Aseptic Labs, Inc.	570	380 ± 40	800 ± 100
Felt [a]	McMaster–Carr	60	42 ± 16	75 ± 50
Pyrex Wool™ [a]	Corning Glass Co.	240	150 ± 30	380 ± 50
Thread (white) [a]	Coates and Clark Co.	–15.3	–19 ± 16	15 ± 38
Fluids				
Apiezon "J"™ oil [a]	James G. Biddle Co.	–0.19	–0.04 ± 0.18	–0.6 ± 4

Material	Supplier	χ/ρ at 4.2 K [10^{-8} m^3/kg]	B at 1.6K to 4.2 K [10^{-8} m^3/kg]	C at 1.6K to 4.2K [10^{-8} m^3K/kg]
Apiezon "N"™ grease [a]	"	–0.5	0.1 ± 1.5	–2.5 ± 0.4
Aquadag™ [a]	Colloids Corp.	15	15 ± 2	0.1 ± 5
RTV-102™ adhesive [c]	General Electric	0.79	1.2 ± 0.5	–1.62
Silicone-oil 50 cs [a]	Dow–Corning	1.7	1.6 ± 1.6	0.1 ± 4
GE 7031™ Varnish-toluene (1:1 mixture) [a]	General Electric	0.4	3 ± 2	–9 ± 4
Metals				
Brass [a]	Central Steel & Wire Co.	–235	–226 ± 25	–38 ± 13
Copper magnet wire				
Formex insulated [a]	Anaconda Copper Co.	0.04	0.04 ± 1.3	0.01 ± 1.9
Sodereze insulated [a]	Phelps Dodge Inc.	0.1	0.6 ± 0.9	–2.0 ± 2.1
Evanohm				
Double silk covered [a]	Wilbur B. Driver Co.	86.0	–3.8 ± 7.5	377 ±38
Formex insulated [a]	"	155	11 ± 18	603 ± 75
Manganin, enamel insulated [a]	Driver–Harris Inc.	147	151 ± 13	–16 ± 4
Phosphor bronze [c]	Central Steel & Wire Co.	2.1	2.9 ± 1.1	–3.3
Beryllium copper Berylco 25 [c]	Meier Brass & Aluminum	254	254 ± 1.9	0.0
Stainless steels				
303 [a]	Central Steel & Wire Co.	148	144 ± 19	13 ± 13
304 [a]	"	134	136 ± 11	–7.2 ± 6
316 [a]	"	361	392 ± 31	–130 ± 25
321 [a]	"	133	126 ± 13	31 ± 13
347 [a]	"	215	250 ± 120	–150 ± 190
Sheets and Tapes				
Kapton™ H film [c]	Du Pont	0.8	1.3 ± 0.7	–2.1
Mylar™ [a]	Du Pont	63	63 ± 9	1.9 ± 8
Paper				
White [a]	W. M. Morgan Putnam Co.	4	–0.3 ± 3	18 ± 9
Black (photographic) [a]	"	3	1 ± 4	6 ± 8
Tapes				
Cellophane™ [a]	Minn. Mining & Mfg. Co.	0.7	0.1 ± 2	2 ± 6
Glass #27 [a]	"	30	9 ± 2	88 ± 10

Material	Supplier	χ/ρ at 4.2 K [10^{-8} m^3/kg]	B at 1.6K to 4.2 K [10^{-8} m^3/kg]	C at 1.6K to 4.2K [10^{-8} m^3K/kg]
Masking (Tuck Tape) [a]	Technical Tape Corp.	11	10 ± 2	3 ± 5
Special				
Cupro-Nickel (70–30) [a]	Superior Tube Co.	480	480 ± 100	
Eccosorb LS-22™ foam sheet [c]	Emerson and Cuming Inc.	–0.6	1.2 ± 0.9	–7.7
Germanium resistor [c]	Cryocal Inc.	6330	6380 ± 48	–215
Inconel™ [a]	Superior Tube Co.	2.6×10^5	$(3.3 \pm 0.25)\times10^5$	$(-2.9 \pm 0.25)\times10^5$
SC-13™ flexible silver micropaint [a]	Microcircuits Co.	1.5×10^4	$(1.3 \pm 0.9)\times10^4$	$(0.87 \pm 0.09)\times10^4$
Rubber (Neoprene™) [a]	Microdot Inc.	35	16 ± 24	78 ± 56

[a] G. L. Salinger and J. C. Wheatley (1961), *Rev. Sci. Instrum.* **32**, 872–874.
[b] R. J. Commander and C. B. P. Finn (1970), *J. Phys. E: Sci. Instrum.* **3**, 78–79.
[c] D. M. Ginsberg (1970), *Rev. Sci. Instrum.* **41**, 1661–1662.

A6.8b Magnetic volume *susceptibility at 295 K, 77 K, and 4.2 K of structural materials commonly used in cryostat construction (Sec. 6.5)*

Volume susceptibility is useful for structural parts with well defined shapes (such as tubes, rods, sheets, and blocks) where the volume of the part is readily determined. (In contrast, mass susceptibility is utilized in situations where the mass is easier to determine, such as with small or irregularly shaped parts.) The two quantities are simply related by

$$\text{(mass susceptibility } \chi/\rho) \equiv \text{(volume susceptibility } \chi) \,/\, \text{(density in kg/m}^3)$$

Volume susceptibility is defined by $\chi \equiv M/H$, where M is the magnetic moment per unit volume and H is the magnetic intensity.

Values in the table below are tabulated in SI units (mks). To convert to cgs units, divide these values by 4π (from Appendix A1.4).

Magnetic volume susceptibility χ

Material	Condition	Density [10^3 kg/m^3]	χ (293 K) [SI units]	χ (77 K) [SI units]	χ (4.2 K) [SI units]
Aluminum alloys					
pure [c]		2.70	2.07×10^{-5}		2.52×10^{-5}
2014 [c]		2.79	1.80×10^{-5}		1.72×10^{-5}
Copper alloys					
99.999% pure Cu [b]	cold drawn, etch, and annealed		-9.34×10^{-6}	-9.18×10^{-6}	-8.67×10^{-6}
99.96+% pure Cu [b]	as formed		-7.32×10^{-6}	-8.55×10^{-6}	-9.32×10^{-6}
Oxygen-free Cu [b]			-9.14×10^{-6}	-9.32×10^{-6}	-8.93×10^{-6}
ETP copper [c]		8.92	3.22×10^{-5}		2.53×10^{-5}
Beryllium copper [c] (Cu–2%Be)		8.33	1.56×10^{-3}		1.82×10^{-3}
Phosphor Bronze A [c] (94.8Cu–5Sn–0.2P)		8.95	-5.86×10^{-6}		-5.56×10^{-6}
90Cu–10Ni [b]			1.69×10^{-5}	1.57×10^{-5}	2.21×10^{-5}
Brass, plain (cartridge) [c]		8.52	-3.48×10^{-6}		-6.14×10^{-5}

(70%Cu–30%Zn)					
Brass, free-cutting [c] (61.5%Cu–35.4%Zn–3.1%Pb)		8.52	1.12×10^{-2}		-1.4×10^{-2}
Manganin [j] (83Cu–13Mn–4Ni)			2.7×10^{-3}		1.26×10^{-2}
Constantan [j] (Cu–45Ni)			0.45		4.3
Titanium alloys:					
Ti		4.51 [f]	1.78×10^{-4} [e]		
Ti–6%Al–4%V		4.41 [c]	1.80×10^{-4} [c]		-8.27×10^{-6} [c]
Stainless Steels:					
304		7.86 [g]	2.7×10^{-3} [h]	5.5×10^{-3} [h]	
304L	fully softened	7.86 [g]	2.6×10^{-3} [h]	4.9×10^{-3} [h]	
304N		7.86 [g]	2.6×10^{-3} [h]	5.2×10^{-3} [h]	4.8×10^{-3} [d]
309 [a]	fully softened		2.1×10^{-3}	6.2×10^{-3}	2.4×10^{-2}
	sensitized		2.6×10^{-3}	6.7×10^{-3}	2.1×10^{-2}
310 [a]	fully softened	7.85 [g]	2.2×10^{-3}	8.3×10^{-3}	F
	sensitized		2.3×10^{-3}	1.2×10^{-2}	F
310S		7.85 [g]	2.6×10^{-3} [h]	9.5×10^{-3} [h]	
316		7.97 [g]	3.0×10^{-3} [c, h]	7.7×10^{-3} [h]	1.6×10^{-2} [d]
316L		7.97 [g]	3.0×10^{-3} [h]	8.0×10^{-3} [h]	
316LN [a]	fully softened	7.97 [g]	2.6×10^{-3}	6.9×10^{-3}	1.1×10^{-2}
	sensitized		3.5×10^{-3}	7.2×10^{-3}	1.1×10^{-2}

Nickel alloys: [i]	*Maximum susceptibility*	
	at:	value:
Inconel 718-1153	19 K	13
Inconel 718-1094	16 K	3.2
Inconel 718-1	15 K	3.8
Inconel 625	< 5 K	0.0032

Nichrome (Ni–20Cr) [j]			5.2×10^{-4}		5.75×10^{-3}

Polymers:

Acrylic [c]	1.05	-6.98×10^{-6}	-2.65×10^{-6}
Nylon [c]	1.15	-9.04×10^{-6}	-7.46×10^{-6}
Composites: [c]			
G10CR	1.83	2.63×10^{-6}	5.34×10^{-4}
G11CR	1.90	2.59×10^{-6}	4.58×10^{-4}
Linen Phenolic	1.35	-4.26×10^{-6}	2.93×10^{-6}
Miscellaneous: [c]			
Hardwood	0.63	6.09×10^{-6}	1.22×10^{-5}
Quartz	2.21	-1.03×10^{-5}	-9.27×10^{-6}

F ≡ Ferromagnetic at this temperature.

[a] D. C. Larbalestier and H. W. King (1973), *Cryogenics* **13**, 160–168.

[b] *Handbook on Materials for Superconducting Machinery* (1977), MCIC-HB-04,. Battelle, Columbus, Ohio.

[c] F. R. Fickett (1992), *Adv. Cryog. Eng. (Mater.)* **38**, 1191–1197.

[d] E. W. Collings and R. L. Cappelletti (1985), *Cryogenics* **25**, 713–718.

[e] *Landolt–Börnstein* (1986), New Series, II/16, *Diamagnetic Susceptibility,* Springer-Verlag, Heidelberg; *Landolt–Börnstein* (1986–1992), New Series, III/19, Subvolumes a to i2, *Magnetic Properties of Metals,* Springer-Verlag, Heidelberg; *CRC Handbook of Chemistry and Physics* (2000), 81st edition, CRC Press, Boca Raton, Florida.

[f] *Metals Handbook* (1961), Vol. 1, *Properties and Selection of Materials,* 8th edition., ASM International, Materials Park, Ohio.

[g] H. I. McHenry (1983), Chapter 11 in *Materials at Low Temperatures*, eds. R. P. Reed and A. F. Clark, ASM International, Materials Park, Ohio

[h] E. W. Collings and S. C. Hart (1979), *Cryogenics* **19**, 521–530. (The coefficients given in Table 6 of this reference should be multiplied by 4π to correctly give mass susceptibility in units of m^3/kg^{-1}.)

[i] I. R. Goldberg, M. R. Mitchell, A. R. Murphy, R. B. Goldfarb, and R. J. Loughran (1990), *Adv. Cryog. Eng. (Mater.)* **36**, 755–762.

[j] M. Abrecht, A. Adare, and J. W. Ekin (2007), *Rev. Sci. Inst*. **78,** 046104.

A6.8c Ferromagnetic traces at 4.2 K induced by welding and cyclic cooling of austenitic stainless steels [a] *(Sec. 6.5)*

Austenitic stainless steels are paramagnetic, but most become unstable below room temperature and partially transform into a martensitic phase, which is ferromagnetic. The transformation depends critically on the exact chemical composition and heat treatment of the alloy, as evidenced by the difference in data below for various samples of the same type of steel, indicated by (a), (b), and (c). Welding can also induce ferromagnetic behavior. Only 316LN and X6CrNi 1811 show no ferromagnetic traces on cooling or welding.

Stainless Steel Alloy	Ferromagnetic Traces		
	on first cooling	on welding	on cyclic cooling
303	+	+	not tested
304 (a)	+	+	not tested
304 (b)	–	+	not tested
304 (c)	+	+	not tested
304N	+	–	+
310	+	+	+
310S	+	+	–
316 (a)	–	+	–
316 (b)	–	–	–
316 (c)	–	–	–
316L	+	+	–
316LN	–	–	–
316Ti	+	+	–
X6CrNi 1811	–	–	–
321 (a)	+	+	–
321 (b)	+	+	+

+ ≡ detected

– ≡ not detected

[a] Data from K. Pieterman, A. Ketting, and J. C. Geerse (1984), *J. Phys.,* **45**, C1-625–C1-631.

A6.9 Composition of austenitic stainless steels, nickel steels, and aluminum alloys (Sec. 6.6)

Compositions of austenitic stainless steels [a]

These are Fe–Cr alloys with sufficient Ni and Mn to stabilize the f.c.c. austenitic phase so they retain their strength, ductility, and toughness at cryogenic temperatures.

Temperature-dependent mechanical and physical properties of AISI [b] 304, 310, and 316 are tabulated in Appendix A6.10.

Composition [weight percent]

AISI [b] Type No.	Cr	Ni	Mn	C, max	N	Other
201	16–18	3.5–5.5	5.5–7.5	0.15	0.25, max	1.00 Si max 10.060 P max 0.030 S max
202	17–19	4–6	7.5–10	0.15	0.25, max	1.00 Si max 10.060 P max 0.030 S max
301	16–18	6–8		0.15		
302	17–19	8–10		0.15		
304	18–20	8–12		0.08		
304 L	18–20	8–12		0.03		
304 N	18–20	8–10.5	2.0 max	0.08	0.10–0.16	1.00 Si max 10.060 P max 0.030 S max
304 LN	18–20	8–12	2.0 max	0.03	0.10–0.16	1.00 Si max 10.060 P max 0.030 S max
305	17–19	10.5–13		0.12		
309	22–24	12–15		0.20		
310	24–26	19–22		0.25		1.5 Si max.
310 S	24–26	19–22		0.08		1.5 Si max.

AISI [b] Type No.	Cr	Ni	Mn	C, max	N	Other
316	16–18	10–14		0.08		2–3 Mo
316 L	16–18	10–14		0.03		2–3 Mo
316 N	16–18	10–14	2.0 max	0.08	0.10–0.16	1.00 Si max 10.060 P max 0.030 S max
316 LN	16–18	10–14	2.0 max	0.03	0.10–0.16	1.00 Si max 10.060 P max 0.030 S max
321	17–19	9–12		0.08		(5 × %C) Ti, min.
347	17–19	9–13		0.08		(10 × %C) Nb+Ta, min.
ASTM [c] XM-10	19–21.5	5.5–7.5	8–10	0.08	0.15–0.40	1.00 Si max 10.060 P max 0.030 S max
ASTM XM-11	19–21.5	5.5–7.5	8–10	0.04	0.15–0.40	1.00 Si max 10.060 P max 0.030 S max
ASTM XM-14	17–19	5–6	14–16	0.12	0.35–0.50	1.00 Si max 10.060 P max 0.030 S max
ASTM XM-19	20.5–23.5	11.5–13.5	4–6	0.06	0.20–0.40	0.10–0.30 Nb, 1.00 Si max 10.060 P max 0.030 S max
ASTM XM-29	17–19	2.25–3.75	11.5–14.5	0.08	0.20–0.40	0.10–0.30 V 1.5–3.0 Mo 1.00 Si max 10.060 P max 0.030 S max

[a] From H. I. McHenry (1983), Chapter 11 in *Materials at Low Temperatures*, eds. R. P. Reed and A. F. Clark, ASM International, Materials Park, Ohio.

[b] AISI: American Iron and Steel Institute, a designation system for steels.

[c] ASTM: Formerly known as the American Society for Testing and Materials, now ASTM International, an organization that provides a global forum for consensus standards for materials, products, systems, and services.

Composition of nickel steels [a]

These Fe–Ni alloys have a predominantly b.c.c. crystal structure that undergoes a ductile-to-brittle transition as temperature is reduced; the transition temperature decreases with increasing nickel content.

Temperature-dependent mechanical and physical properties of 3.5 Ni, 5 Ni, and 9 Ni alloys are tabulated in Appendix A6.10.

Composition [weight percent]

ASTM [b] Specifi-cation	Alloy	Minimum Service Temp.[K]	C max	Mn	P max	S max	Si	Ni	Mo	Cr
A203 Grade D	3.5 Ni	173	0.17	0.7 max	0.035	0.040	0.15–0.30	3.25–3.75		
A203 Grade E	3.5 Ni	173	0.20	0.7 max	0.035	0.040	0.15–0.30	3.25–3.75		
A645	5 Ni	102	0.13	0.30–0.60	0.025	0.025	0.20–0.35	4.75–5.25	0.20–0.35	
A645	5.5 Ni	77	0.13	0.90–1.50	0.030	0.030	0.15–0.30	5.0–6.0	0.10–0.30	0.10–1.00
A553 Type II	8 Ni	102	0.13	0.90 max	0.035	0.040	0.15–0.30	7.5–8.5		
A553 Type I	9 Ni	77	0.13	0.90 max	0.035	0.040	0.15–0.30	8.5–9.5		

[a] From H. I. McHenry (1983), Chapter 11 in *Materials at Low Temperatures*, eds. R. P. Reed and A. F. Clark, ASM International, Materials Park, Ohio.

[b] ASTM: Formerly known as the American Society for Testing and Materials, now ASTM International, an organization that provides a global forum for consensus standards for materials, products, systems, and services.

Composition of aluminum alloys [a]

Aluminum alloys have an f.c.c. crystal structure and thus retain their strength, ductility, and toughness at cryogenic temperatures. Temperature-dependent mechanical and physical properties of type 1100, 2219, 5083, and 6061 alloys are tabulated in Appendix A6.10.

Composition [weight percent]

Type	Si max	Fe max	Cu	Mn	Mg	Cr	Zn max	Ti	Other elements
1100	1.0 Si (+Fe)		0.05–0.20	0.05 max	—	—	0.10	—	99.00 Al min
2219	0.2	0.3	5.8–6.8	0.20–0.40	0.02 max	—	0.10	0.02–0.10	0.05–15 V
3003	0.6	0.7	0.05–0.20	1.0–1.5	—	—	0.10	—	0.10–0.25 Zr
5083	0.4	0.4	0.1 max	0.40–1.0	4.0–4.9	0.05–0.25	0.25	0.15 max	
6061	0.4–0.8	0.7	0.15–0.40	0.15 max	0.8–1.2	0.04–0.35	0.25	0.15 max	
7005	0.35	0.40	0.10	0.2–0.7	1.0–1.8	0.06–0.20	4.0–5.0	0.01–0.06	0.08–0.20 Zr

[a] From H. I. McHenry (1983), Chapter 11 in *Materials at Low Temperatures*, eds. R. P. Reed and A. F. Clark, ASM International, Materials Park, Ohio.

A6.10 Mechanical properties of structural materials used in cryogenic systems (Sec. 6.6)

The following four tables give the mechanical and physical properties of austenitic stainless steels, nickel steels, aluminum alloys, and other selected metal alloys and polymers.

Mechanical and Physical Properties of Austenitic Stainless Steels

Compositions of these and other stainless-steel alloys are tabulated in Appendix A6.9; a plot of the temperature dependence of the yield strength of AISI 304 with various cold-work conditions is given Fig. 6.17.

Alloy Temperature	Density [a] [g·cm^{-3}]	Young's Modulus [a] [GPa]	Shear Modulus [a] [GPa]	Poisson's Ratio [a]	Fracture Toughness [b] [MPa·m$^{0.5}$]	Thermal Conductivity [b] [W/(m·K)]	Thermal Expansion [b] (mean) (K^{-1}×10^{-6})	Specific Heat [b] [J/(kg·K)]	Electrical Resistivity [c] [μΩ·cm]	Magnetic Permeability [d] (initial)	0.2 % Yield Strength, annealed [e] [MPa]
AISI [f] 304											
295 K	7.86	200	77.3	0.290		14.7	15.8	480	70.4	1.02	240
77 K		214	83.8	0.278		7.9	13.0	—	51.4	—	—
4 K		210	82.0	0.279		0.28	10.2	1.9	49.6	1.09	—
AISI 310											
295 K	7.85	191	73.0	0.305	150	11.5	15.8	480	87.3	1.003	275
77 K		205	79.3	0.295	220	5.9	13.0	180	72.4	—	—
4 K		207	79.9	0.292	210	0.24	10.2	2.2	68.5	1.10	—
AISI 316											
295 K	7.97	195	75.2	0.294	350	14.7	15.8	480	75.0	1.003	240
77 K		209	81.6	0.283	510	7.9	13.0	190	56.6	—	—
4 K		208	81.0	0.282	430	0.28	10.2	1.9	53.9	1.02	—

Major data source: Compilation by H. I. McHenry (1983), Chapter 11 in *Materials at Low Temperatures*, eds. R. P. Reed and A. F. Clark, ASM International, Materials Park, Ohio.

[a] H. M. Ledbetter, W. F. Weston, and E. R. Naimon (1975), *J. Appl. Phys.* **46**, 3855–3860.

[b] D. B. Mann, ed. (1978), *LNG Materials and Fluids*, National Bureau of Standards, U.S. Government Printing Office, Washington, D. C.

[c] A. R. Clark, G. E. Childs, and G. H. Wallace (1970), *Cryogenics* **10**, 295–305.

[d] K. R. Efferson and W. J. Leonard (1976), *Magnetic Properties of Some Structural Materials Used in Cryogenic Applications,* ORNL-4150, p. 126, Oak Ridge National Laboratory, Oak Ridge, Tennessee.

[e] *Metals Handbook,* Vol. 1, *Properties and Selection of Materials* (1961), 8th edition, ASM International, Materials Park, Ohio.

[f] AISI: American Iron and Steel Institute; a designation system for steel alloys.

Mechanical and Physical Properties of Nickel Steels

Compositions of these and other nickel-steel alloys are tabulated in Appendix A6.9; a plot of the temperature dependence of the yield strength of quenched and tempered 9% Ni steel is given in Fig. 6.17.

Alloy / Temperature	Minimum Service Temp.[c] [K]	Density[a] [g·cm^{-3}]	Young's Modulus[a] [GPa]	Shear Modulus[a] [GPa]	Poisson's Ratio[a]	Fracture Toughness[b] [MPa·m$^{0.5}$]	Thermal Conductivity[b] [W/(m·K)]	Thermal Expansion[b] (mean) [K^{-1}×10^{-6}]	Specific Heat[b] [J/(kg·K)]
3.5 Ni	173								
295 K		7.86	204	79.1	0.282	190	35	11.9	450
172 K			210	81.9	0.281	210	29	10.2	350
5 Ni	102								
295 K		7.82	198	77.0	0.283	210	32	11.9	450
111 K			208	81.2	0.277	200	20	9.4	250
76 K			209	81.6	0.277	90	16	8.8	150
9 Ni	77								
295 K		7.84	195	73.8	0.286	155	28	11.9	450
111 K			204	77.5	0.281	175	18	9.4	250
76 K			205	77.9	0.280	170	13	8.8	150

Major data source: Compilation by H. I. McHenry (1983), Chapter 11 in *Materials at Low Temperatures*, eds. R. P. Reed and A. F. Clark, ASM International, Materials Park, Ohio.

[a] W. F. Weston, E. R. Naimon, and H. M. Ledbetter (1975), pages 397–420 in *Properties of Materials for Liquefied Natural Gas Tankage.* ASTM STP 579, American Society for Testing and Materials, Philadelphia.

[b] D. B. Mann, ed. (1978), *LNG Materials and Fluids,* National Bureau of Standards, U.S. Government Printing Office, Washington, D.C.

[c] The minimum service temperature arises because of the ductile-to-brittle-phase transition that occurs at low temperatures in the nickel steels.

Mechanical and Physical Properties of Aluminum Alloys

Compositions of these and other aluminum alloys are tabulated in Appendix A6.9; a plot of the temperature dependence of the yield strength of various aluminum alloys is given in Fig. 6.18.

Alloy Temperature	Density [g·cm^{-3}]	Young's Modulus [GPa]	Shear Modulus [GPa]	Poisson's Ratio	0.2% Yield Strength [g] [MPa]	Thermal Conductivity [W/(m·K)]	Thermal Expansion (mean) [K^{-1}×10^{-6}]	Specific Heat [J/(kg·K)]	Electrical Resistivity [μΩ·cm]
1100-0									
295 K	2.75	69			< 35				
Precipitation-hardened 2219-T6									
295 K	2.83	77.4 [d]	29.1[d]	0.330 [d]	393	120 [c]	23 [f]	900 [f]	5.7 [b]
77 K		85.1[d]	32.3 [d]	0.319 [d]		56 [c]	18.1[f]	340 [f]	
4 K		85.7 [d]	32.5 [d]	0.318 [d]		3 [c]	14.1[f]	0.28 [f]	2.9 [b]
Annealed 5083									
295 K	2.66	71.5 [a]	26.8 [a]	0.333 [a]	145 (half hard: 228)	120 [b]	23 [b]	900 [b]	5.66 [c]
77 K		80.2 [a]	30.4 [a]	0.320[a]		55 [b]	18.1[b]	340 [b]	3.32 [c]
4 K		80.9 [a]	30.7 [a]	0.318 [a]		3.3 [b]	14.1[b]	0.28 [b]	3.03 [c]
Precipitation-hardened 6061-T87									
295 K	2.700	70.1[b]	26.4 [b]	0.338 [b]	275		23 [b]	900 [c]	3.94 [c]
77 K		77.2 [b]	29.1[b]	0.328 [b]			18.1[b]	340 [c]	1.66 [c]
4 K		77.7 [b]	29.2 [b]	0.327 [b]			14.1[b]	0.28 [c]	1.38 [c]

Major data source: Compilation by H. I. McHenry (1983), Chapter 11 in *Materials at Low Temperatures*, eds. R. P. Reed and A. F. Clark, ASM International, Materials Park, Ohio.

[a] E. R. Naimon, H. M. Ledbetter, and W. F. Weston (1975), *J. Mater. Sci.* **10**, 1309–1316.

[b] D. B. Mann, ed. (1978), *LNG Materials and Fluids,* National Bureau of Standards, U.S. Government Printing Office, Washington, D.C.

[c] A. R. Clark, G. E. Childs, and G. H. Wallace (1970), *Cryogenics* **10**, 295–305.

[d] R. P. Read and H. M. Ledbetter (1977), *J. Engineering Materials and Technol*. **99**, 181–184.

[e] G. E. Childs, L. J. Ericks, and R. L. Powell (1973), *Thermal Conductivity of Solids at Room Temperature and Below,* NBS Monograph 131, U.S. Government Printing Office, Washington, D.C.

[f] Assumed to be the same as that of 5083 and 6061.

[g] Compiled by R. Radebaugh et al. (2001), http://www.cryogenics.nist.gov/ and the references listed therein.

Mechanical Properties of Metal Alloys and Polymers

All data are at room temperature, unless noted otherwise by three consecutive values corresponding to 295K/76K/4K.

Mechanical property data for additional materials are available in the literature (Sec. 6.7.1) and on the Internet (Sec. 6.7.2).

Material	Density [g·cm^{-3}]	Young's Modulus [GPa]	Yield Strength [MPa]
Metal Alloys			
Beryllium S-200F [a]	1.86	290	240
Copper, oxygen-free (annealed) [a]	8.95	117	70
Cu–2%Be (UNS C17200-TH 04) [b, c]	8.23	119	1030
Inconel 625 [d]	8.44 [f]	195/207/207	500/720/810
Inconel 718 [a]	8.20	200	1060
Hastelloy C-276 [d,e]	8.9	192/209/205	480/700/810
Ni (annealed) [d]	8.9	60/70/91	60/70/80
Ni–13at%Cr [d]	8.7	111/112/119	120/160/190
Ni–5at%W [d]	10.4	118/128/134	180/260/280
Titanium 3Al–2.5V [f] (various shapes)	4.5	100	830
Titanium 6Al–4V [a] (sheet form)	4.4	114	830
Polymers [a]			
G-10 Fiberglass epoxy	1.65	28	—
Kapton™ (film)	1.43	3.4	210
Mylar™	1.38	3.8	70
Nylon™	1.14	3.4	—
Teflon™	2.2	0.3	14

[a] R. Radebaugh et al. (2001), http://www.cryogenics.nist.gov/ and the references listed therein.

[b] *Metals Handbook* (1961), Vol. 1, *Properties and Selection of Materials,* 8th edition, ASM International, Materials Park, Ohio.

[c] N. J. Simon, E. S. Drexler, and R. P. Reed (1992), *Properties of Copper and Copper Alloys at Cryogenic Temperatures,* NIST Monograph 177. National Institute of Standards and Technology, U.S. Government Printing Office, Washington, D.C.

[d] C. C. Clickner, J. W. Ekin, N. Cheggour, C. L. H. Thieme, Y. Qiao, Y.-Y. Xie, and A. Goyal (2006), "Mechanical properties of pure Ni and Ni-alloy substrate materials for Y-Ba-Cu-O coated conductors," *Cryogenics*, to be published.

[e] Values averaged for three different batches of Hastelloy C-276

[f] www.matweb.com

A7. (i) Specialized resistivity measurement methods (ref. introduction to Part II)

A7.1 Sheet-resistance measurement of unpatterned films

When film properties are initially screened, it is convenient to measure the sheet resistance of the films without the need for patterning. This can be done by a four-probe contact method, wherein four equally spaced in-line probes (such as pogo pins) are pressed against the film near its middle, as illustrated by the insets in Fig. A7.1 for both circular- and rectangular-shaped samples. The usual four-terminal technique is used (described in detail in Sec. 7.2), wherein a small current I from a constant-current supply is passed through the outer two probes, and the voltage V is measured across the inner two probes. The *sheet resistance* R_s is given by

$$R_s = (V/I)\, C \qquad [\Omega/\text{sq}], \tag{A7.1}$$

in units of ohms per square, and C is a correction factor given by the curves in Fig. A7.1, valid for a thin film having a thickness d that is much less than the sides or diameter of the chip (A or D in the insets of Fig. A7.1). In the limit of small-probe spacing $s << D$, $C = \pi/\ln 2 = 4.53$. The *bulk resistivity* of the film is related to the sheet resistance by

$$\rho = R_s\, d \qquad [\Omega\cdot\text{cm}]. \tag{A7.2}$$

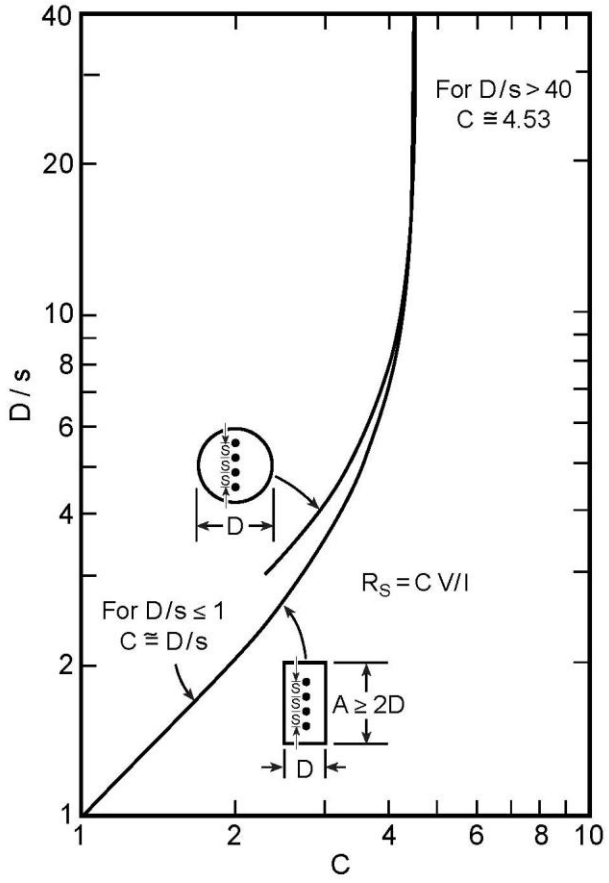

FIG. A7.1 Correction factor C used in Eq. (A7.1) for determining the sheet resistance of an unpatterned film using four, equally spaced, in-line probes. Adapted from Smits (1958) and Anner (1990).

This in-line probe technique is also insensitive to in-plane anisotropy between the *a*-axis and *b*-axis crystallographic directions, with

$$R_s = (R_{s\,a\text{-axis}} \cdot R_{s\,b\text{-axis}})^{0.5}.$$

Other probe/sample configurations are treated in Smits (1958) and also in Wasscher (1961).

References

Anner, G. E. (1990). *Planar Processing Primer*, p. 585, Van Nostrand Reinhold.

Smits, F. M. (1958), "Measurements of sheet resistivities with four-point probe," *Bell Syst. Tech. J.*, **37**, 711–718.

Wasscher, J. D. (1961). “Note on 4-point resistivity measurements on anisotropic conductors”, *Philips Res. Rep.* **16**, 301–306.

A7.2 van der Pauw method for measuring the resistivity and Hall mobility in flat isotropic samples of arbitrary shape

The van der Pauw method (van der Pauw 1958) is particularly useful for measurements on materials that are not easily fabricated into a long, uniform, bar shapes: the type of configuration that is usually required for common transport measurements. The method works for electrically isotropic samples of *arbitrary* shape, such as that shown in Fig. A7.2a. All that is required is that they have a uniform thickness and be *flat*. Thus, this method is well suited to transport measurements of isotropic crystals or brittle materials where it is difficult to cut out bridge-shaped samples without fracturing the narrow arms. (For electrically *an*isotropic materials, use the Montgomery method, described in the next section, Appendix A7.3.) The sample needs to be deposited or grown flat, or to be capable of being polished flat. Also, it cannot have any holes in it (sorry, a slice of Swiss cheese wouldn't work). For Hall-effect measurements, the van der Pauw method also has the advantage that clover-shaped samples (such as that shown in Fig. A7.2c) can be used, which give a larger Hall effect for the same amount of heat dissipation compared with the usual bridge-shape samples. This can be a significant advantage for materials with low electron mobility.

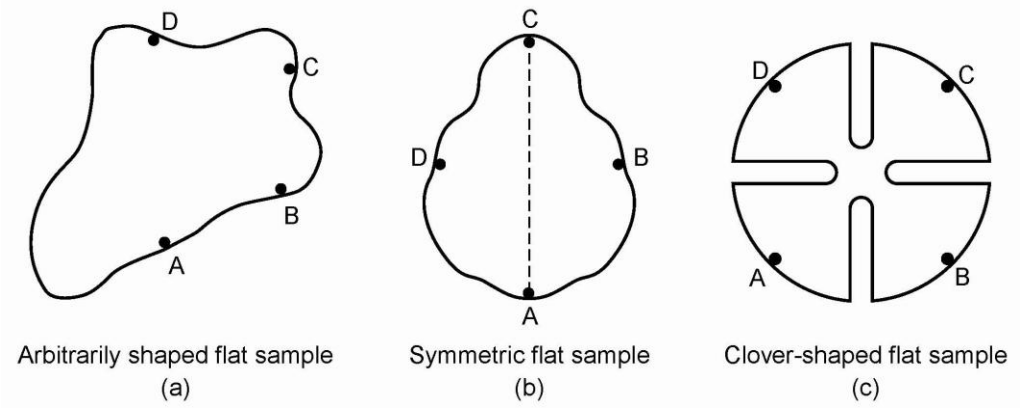

FIG. A7.2 (a) Arbitrarily shaped, flat sample with four small contacts at arbitrary places on the periphery, which can be used to measure the sample's resistivity and the Hall effect. (b) The resistivity measurement is simplified to one resistivity measurement if the sample has a line of symmetry; two of the contacts are situated along the symmetry line and the other two symmetrically with respect to this line. (c) Clover-shaped sample where the influence of the contact size and placement is significantly reduced. For Hall-effect measurements, the clover shape also gives a larger signal for the same amount of heat dissipation, which can improve the measurement sensitivity for materials with low electron mobility. (Adapted from van der Pauw 1958.)

Here, we present a practical description of how to *use* this method. For details of the derivation, please refer to van der Pauw (1958).

The method consists of attaching small contacts to the sample at its periphery, as illustrated in Figs. A7.2a, b, and c. The diameter of the contact δ should be small compared with the overall sample size or diameter D. Also, the contacts should be made right at the outer edge of the sample. For disk-shaped samples, the error in resistivity that results from using contacts of size δ or located a distance δ away from the sample's periphery is given approximately by (van der Pauw 1958)

$$\Delta\rho/\rho \approx (\delta/D)^2, \tag{A7.3}$$

whereas the error in the Hall coefficient R_H is given roughly by

$$\Delta R_H/R_H \approx \delta/D. \tag{A7.4}$$

The accuracy of the technique is improved if the contacts are spaced apart around the periphery of the sample, as illustrated in Fig. A7.2a. Use of a clover-shaped sample shown in Fig. A7.2c can help minimize the error due to the finite size and placement of the contacts.

After instrumenting the sample in this way, the resistivity of the sample is then determined by measuring two resistances $R_{AB,CD}$ and $R_{BC,DA}$. Here, $R_{AB,CD}$ is defined as the resistance calculated from the potential difference $V_D - V_C$ measured between contacts D and C in Fig. A7.2a, divided by the current entering contact A and leaving contact B. The other resistance $R_{BC,DA}$ is correspondingly defined. The sample's resistivity ρ is then given by (van der Pauw 1958)

$$\rho = \pi d (2 \ln 2)^{-1} (R_{AB,CD} + R_{BC,DA}) f(R_{AB,CD}/R_{BC,DA}), \tag{A7.5}$$

where f is a function only of the ratio $R_{AB,CD}/R_{BC,DA}$. Figure A7.3 gives f as a function of $R_{AB,CD}/R_{BC,DA}$. Notice from Eq. (A7.5) that there are no measurements of the sample's shape that enter into the determination of ρ, only the sample's thickness d.

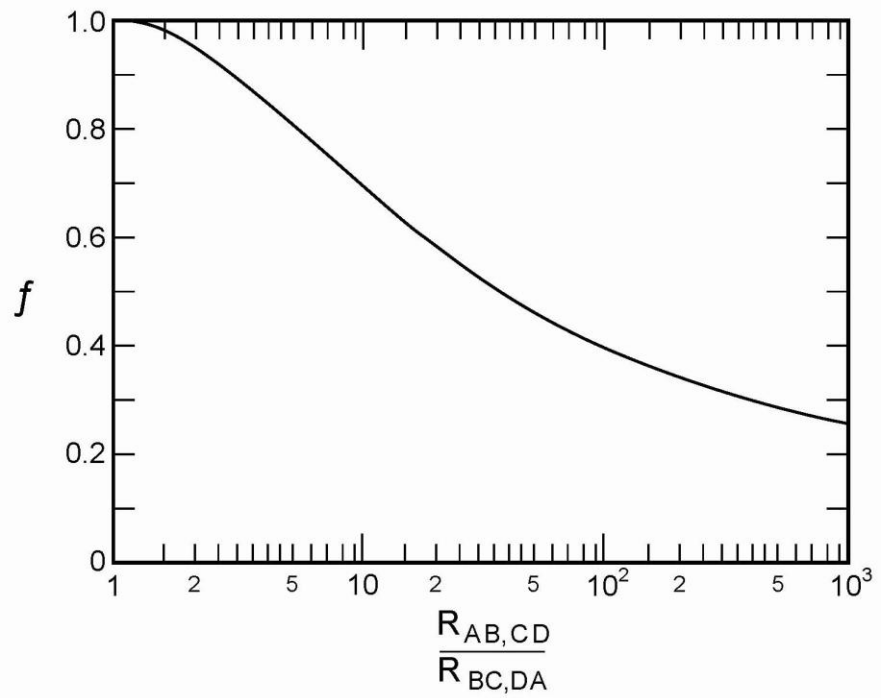

FIG. A7.3 The function $f(R_{AB,CD}/R_{BC,DA})$ in Eq. (A7.5) used to determine the resistivity of an arbitrarily shaped flat sample (from Van Der Pauw 1958).

The measurement is particularly straightforward if the sample has a line of symmetry. In this case, contacts A and C can be placed along this symmetry line, and B and D can be placed symmetrically with respect to this line (Fig. A7.2b). Then, from the reciprocity theorem for passive four poles (interchange of current and voltage contacts), we have, generally, that $R_{AB,CD} = R_{BC,DA}$. Thus, a single measurement of resistance is sufficient.

The van der Pauw method is also well suited for measurements of the Hall coefficient. The Hall coefficient is determined by measuring the *change* of the resistance $R_{AC,BD}$ before and after a uniform magnetic field B is applied perpendicular to the plane of the sample. In this case, current is applied to an arbitrary contact A and removed from contact C (not contact B as with the resistivity measurement described above). The sample's Hall coefficient R_H is then given by (van der Pauw 1958)

$$R_H = (d/B)\,\Delta R_{AC,BD}, \qquad \text{(A7.6)}$$

where $\Delta R_{AC,BD}$ is the change in the resistance $R_{AC,BD}$ produced by the magnetic field B.

Footnote on reverse-field reciprocity method: For Hall-coefficient or magnetoresistance measurements, the magnetic field is usually reversed and the resistance data averaged to correct

for sample inhomogeneities or voltage-terminal misalignment (in the case of a Hall-bar-geometry). The magnetic-field reversal can take a significant amount of time, especially in the case of high magnetic fields, and the extra time can present a problem for some measurements because of temperature drifts, for example.

For such cases, we call attention to the reverse-field reciprocity method by Sample et al. (1987). This method states that the equivalent of the reverse-field resistance measurement can be made by interchanging voltmeter and current sources, without the need to reverse the magnetic field. This is sometimes quite useful since, with computer-controlled data collection and switching, the second resistance measurement can be performed in hundredths of a second, whereas reversing the applied magnetic field can take several minutes.

References

Sample, H. H., Bruno, W. J., Sample, S. B., and Sichel, E. K. (1987). "Reverse-field reciprocity for conducting specimens in magnetic fields," *J. Appl. Phys.* **61**, 1079–1084.

Van der Pauw, L. J., (1958). "A method of measuring specific resistivity and Hall effect of discs of arbitrary shape," *Philips Res. Rep.* **13**, 1–9.

A7.3 Montgomery method for measuring the resistivity of anisotropic *materials*

The Montgomery method facilitates resistivity measurements of *anisotropic* crystals, providing an easier experimental technique of determining the various components of resistivity along their principal axes. (For isotropic materials, the van der Paaw method is better suited; see Appendix A7.2.) The Montgomery method is especially useful for anisotropic materials with two independent components of resistivity. In this two-component case, two samples are usually needed if the conventional four-terminal method is used, with each sample fabricated into long-bar shapes cut along the principal axes. However, with the Montgomery method, both components can be determined from *one* sample. The method is thus extremely useful for the common case where only one sample is available, or if both resistivity components must be measured simultaneously as, for example, when measuring changes in resistivity through a phase transition in a temperature-drift experiment.

Here, my aim is to present a clear, step-by-step description of the procedure for using this method, as well as some practical guidelines on its limitations. The derivation of the method based on the transformation of *anisotropic* sample coordinates into an equivalent *isotropic* space is given in detail in Montgomery (1971), Logan et al. (1971), and the background references cited therein.

Crystalline types appropriate for the application of this method are summarized in the Table A7.1 in order of increasing complexity. Here, we denote the various resistivity components of these crystal structures as ρ_1, ρ_2, and ρ_3.

Table A7.1 Application notes for Montgomery method.

Crystal structure	Number of independent resistivity components required to characterize the resistivity properties	Application comments
Trigonal Tetragonal Hexagonal	*Two*: ρ_2 along the *c*-axis; $\rho_1 = \rho_3$, mutually perpendicular to each other and to ρ_2.	ρ_1 and ρ_2 can be obtained from a *single sample face,* which is oriented with one edge along the *c*-axis and the other in any direction perpendicular to the *c*-axis.
Orthorhombic	*Three*: ρ_1, ρ_2, and ρ_3 orthogonal components along the principal crystal axes.	ρ_1, ρ_2, and ρ_3 can be obtained from *two sample faces* with edges along the three principal crystal axes.
Monoclinic Triclinic	*Four to six tensor components*: Three components are sufficient if specially oriented, but the required orientation cannot be determined from the crystal structure alone.	The Montgomery method is usually too cumbersome for these crystal systems.

The insets to Fig. A7.4 show the face of a sample with a typical contact arrangement for applying the Montgomery method. If the resistivities ρ_1 and ρ_2 along sides l_1' and l_2' are expected to be vastly different, it helps to cut the sample face so that $l_2'/l_1' \approx (\rho_1/\rho_2)^{1/2}$. This customized shaping avoids an extreme mismatch in the voltages measured along the two directions, which might otherwise make the smaller voltage difficult to measure.

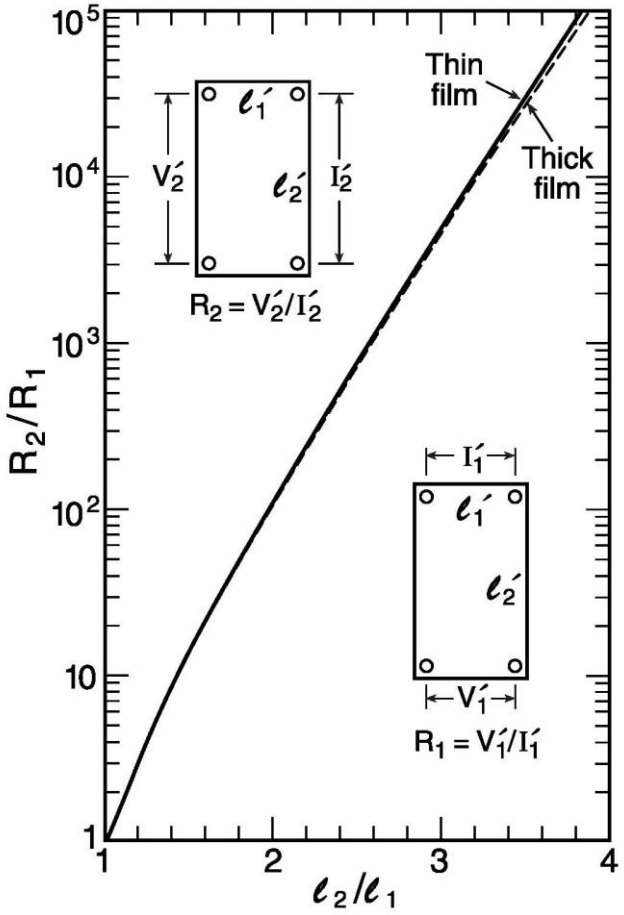

FIG. A7.4 Measured resistance ratio versus the sample-dimension ratio l_2/l_1. (Unprimed coordinates denote the equivalent isotropic coordinates; see text. The actual physical dimensions of the sample are indicated by primed coordinates l_1' and l_2' as shown in the insets.) (Adapted from Montgomery 1971.)

From a practical standpoint, the Montgomery method is easiest to implement if the sample is relatively *thin*. Thicker samples can be accommodated, but the method becomes more cumbersome, as described below under the heading "Thick samples." The simpler thin-sample formulas can be applied to thicker samples, however, if the voltage and current electrodes are extended along the edge of the sample perpendicular to the principal face.

Trigonal, tetragonal, and hexagonal crystal systems

Procedure for determining ρ_1 *and* ρ_2:

(1) After connecting instrumentation leads to the sample's principal face (as shown in the insets to Fig. A7.4), measure l_1', l_2', l_3', R_1, and R_2. The quantities R_1 and R_2 are defined in the

insets to Fig. A7.4. [Primes are used to indicate the actual physical dimensions l_i' of the *anisotropic* crystal; unprimed quantities denote the transformed sample dimensions in equivalent *isotropic* space. We have used this convention to keep the same notation as in Montgomery's original equations (Montgomery 1971). The figures shown in the first part of Montgomery's article are for the equivalent isotropic case, and then, later in the article, the real sample dimensions are transformed back to the isotropic case, which can be a bit confusing. The reason this works is that the quantities R_1 and R_2 are the same in either real or equivalent space; that is, $R_1 = V_1/I_1 = V_1'/I_1'$ and $R_2 = V_2/I_2 = V_2'/I_2'$. The figure insets shown here have been modified from Montgomery's article to help clarify the practical application of this method.]

(2) Determine the ratio l_2/l_1 in the equivalent isotropic space from the experimentally measured ratio R_2/R_1, by using the curves in Fig. A7.4.

(3) From the value determined for l_1/l_2 (equivalent space) and the value measured for l_1'/l_2' (the actual dimensions of the anisotropic crystal), calculate

$$(\rho_2/\rho_1)^{1/2} = (l_2/l_1) \times (l_1'/l_2'). \qquad \text{(A7.7)}$$

(4) From the ratio l_1/l_2 (equivalent space), determine the dimensionless quantity H from the curve in Fig. A7.5.

Thin samples:

(5) For thin samples [that is, $l_3/(l_1 l_2)^{1/2} \lesssim 0.5$, where l_3 is the thickness of the sample in equivalent space determined from Eq. (A7.9) below], calculate

$$(\rho_1\rho_2)^{1/2} = H\, l_3'\, R_1, \qquad \text{(A7.8)}$$

(where l_3' is the thickness of the sample in real space).

(6) Finally, from the quantitative values for $(\rho_2/\rho_1)^{1/2}$ and $(\rho_1\rho_2)^{1/2}$ [Eqs. (A7.7) and (A7.8)], calculate ρ_1 and ρ_2.

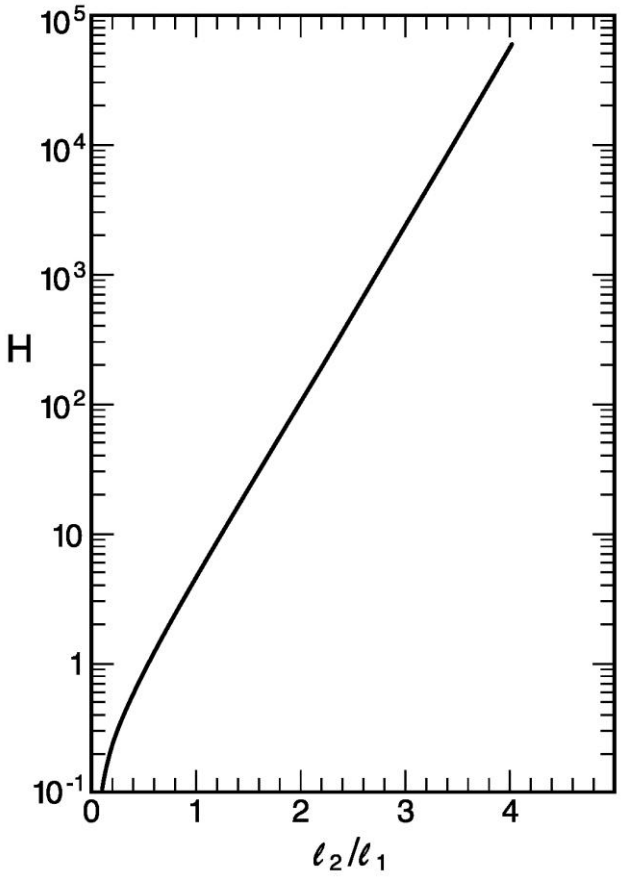

FIG. A7.5 The quantity H [used in Eq. (A7.8)] versus the sample-dimension ratio (in equivalent isotropic coordinates). (Adapted from Montgomery 1971.)

Thick samples:

Steps 1 through 4 are the same as above.

(5) For thick samples [$l_3/(l_1 l_2)^{1/2} \gtrsim 0.5$], instead of step 5 above, calculate

$$l_3/(l_1 l_2)^{1/2} = (\rho_1/\rho_2)^{1/4} \times l_3'/(l_1' l_2')^{1/2} , \qquad \text{(A7.9)}$$

where the numerical value of $(\rho_1/\rho_2)^{1/4}$ is calculated from the value of $(\rho_2/\rho_1)^{1/2}$ determined in step 3, and $l_3'/(l_1' l_2')^{1/2}$ is calculated from the sample dimensions measured in step 1. [In this step we have taken ρ_3 and ρ_1 to be the equivalent resistivity directions (with ρ_3 defined as the resistivity perpendicular to the sample face); if, on the other hand, $\rho_3 = \rho_2$, interchange subscripts 1 and 2 in Eq. (A7.9) above and in Eq. (A7.10) below.]

(6) Use the value of $l_3/(l_1 l_2)^{1/2}$ from Eq. (A7.9) to determine $E/(l_1 l_2)^{1/2}$ from Fig. A7.6 (where E is defined as the effective sample thickness in equivalent isotropic space).

(7) Calculate E' (the effective sample thickness in anisotropic real space) from

$$E'/(l_1'l_2')^{1/2} = (\rho_2/\rho_1)^{1/4} \times E/(l_1 l_2)^{1/2}, \qquad \text{(A7.10)}$$

where the value of ρ_2/ρ_1 was determined in step 3.

(8) Calculate

$$(\rho_1\rho_2)^{1/2} = H\,E'\,R_1, \qquad \text{(A7.11)}$$

(9) Finally, from the quantitative values for $(\rho_2/\rho_1)^{1/2}$ and $(\rho_1\rho_2)^{1/2}$ [Eqs. (A7.7) and (A7.11)], calculate ρ_1 and ρ_2.

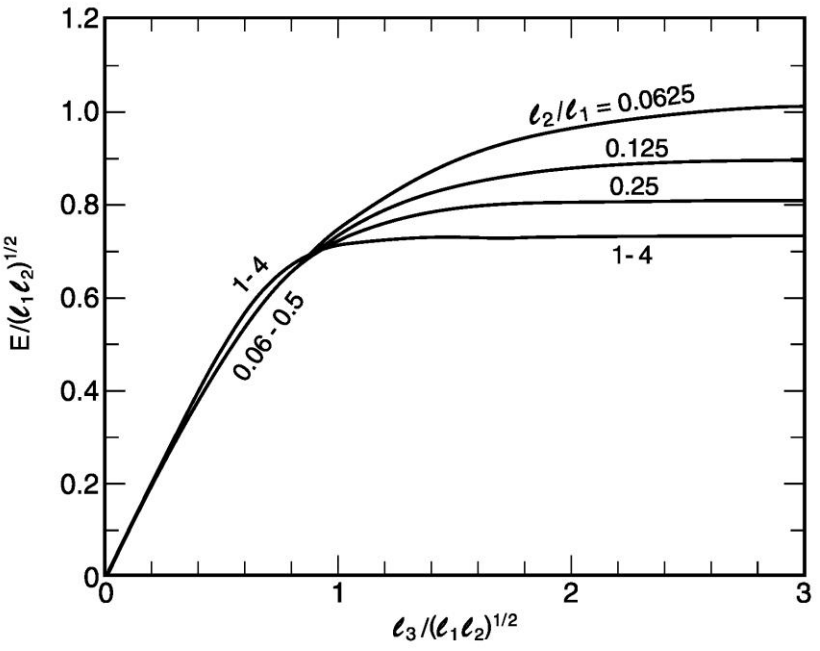

FIG. A7.6 Normalized effective thickness E vs. normalized sample thickness l_3 for various ratios of the sample dimensions l_2/l_1 (in equivalent isotropic coordinates). (The ratio l_2/l_1 was determined from Fig. A7.4 in Step 2 above.) (From Montgomery 1971.)

The numerical limit given in step (5) [i.e., $l_3/(l_1l_2)^{1/2} \gtrsim 0.5$] for the *thin* and *thicker* cases is my subjective estimate for the validity of these two approximations. That is, the thin-sample case requires that $E \approx l_3$, which from Fig. A7.6 would appear to be valid for $l_3/(l_1l_2)^{1/2} \lesssim 0.5$ [or in real space, $(\rho_1/\rho_2)^{1/4} \times l_3'/(l_1'l_2')^{1/2} \lesssim 0.5$ from Eq. (A7.9)].

Practical Note: To simplify the application of the method when many calculations need to be made for a *single* sample (such as in a temperature-drift experiment), calculate the

multiplying factors to convert R_1 to ρ_1 and ρ_2 for several ratios of R_1/R_2, and plot these versus R_1/R_2 for easier reduction of the data. Nearly straight-line relations are usually obtained on a log–log plot.

Orthorhombic crystal systems

Procedure for determining ρ_1, ρ_2, *and* ρ_3:

With three unknown components of resistivity, the Montgomery method requires measurements on a *second* sample with its face cut normal to that of the first sample and also cut thin enough that the thin-sample condition is met [i.e., $l_3/(l_1 l_2)^{1/2} \lesssim 0.5$ as described above for the two-component case]. Then, the procedure for evaluating the data for the second sample face is the same as that for the *thin*-sample case given above, with corresponding new measured values assigned to l_1', l_2', and l_3'. This works because all the equations are independent of ρ_3 for the *thin*-sample case.

For *thicker* orthorhombic crystals [$l_3/(l_1 l_2)^{1/2} \gtrsim 0.5$], there appears to be no straightforward procedure for applying the Montgomery method unless one assumes a value for ρ_3 and uses an iterative approach (Montgomery 1971). Again, the best procedure in this case would be to mimic the thin-sample case by extending the electrode contacts along the edge of the sample perpendicular to the principal face.

References

Logan, B. F., Rice, S. O., and Wick, R. F. (1971). "Series for computing current flow in a rectangular block," *J. Appl. Phys.* **42**, 2975–2980.

Montgomery, H. C. (1971). "Method for measuring electrical resistivity of anisotropic materials," *J. Appl. Phys.* **42**, 2971–2975.

(ii) Sample-holder material properties (ref. Chapter 7)

A7.4 Sample-holder materials: Thermal contraction on cooling to liquid-helium and liquid-nitrogen temperatures (Sec. 7.3.2)

The total linear contraction from room temperature to the indicated temperature T is defined as

$$\Delta L/L_{293\text{K}-T} \equiv (L_{293\text{K}} - L_T)/L_{293\text{K}}.$$

The coefficient of linear expansion at room temperature is defined as

$$\alpha_{293\text{K}} \equiv (1/L)\, \mathrm{d}L/\mathrm{d}T.$$

Since the thermal expansion/contraction is approximately linear above room temperature, the total contraction from an upper reference temperature T_u above room temperature (such as soldering temperature) to a low temperature T can be determined approximately from

$$\Delta L/L_{T_u-T} = \Delta L/L_{293\text{K}-T} + (\alpha_{293\text{K}})\,(T_\text{u} - 293\ \text{K}).$$

Tabulated values are generally arranged within each material group by the magnitude of the thermal contraction to facilitate finding sample-holder materials with a thermal contraction which matches that of a given sample.

Additional thermal-expansion data for other materials and temperatures are tabulated in Appendix A6.4.

Thermal contraction of sample-holder materials

Material	$\Delta L/L_{293K-4K}$ [%]	$\Delta L/L_{293K-77K}$ [%]	α_{293K} [10^{-6} K^{-1}]
Metals			
Niobium	0.143 [c]	0.130 [m]	7.1 [s]
Titanium [c]	0.151	0.143 [m]	8.5
Iron [c]	0.198	0.190 [m]	11.5
Nickel [c]	0.224	0.212 [m]	12.5
Copper [b]	0.324	0.302 [m]	16.7
Silver [q]	0.412	0.370 [c]	18.5
Aluminum [c]	0.415	0.393 [m]	22.5
Alloys			
Fe–36Ni [f,m]	~0.037	0.038	3.0
Fe–9Ni [d]	0.195	0.188	11.5
Ti–6%Al-4%V [d]	0.173	0.163 [m]	8.0
Ti–5%Al–2.5%Sn [n]	0.20	0.17	8.3
Hastelloy C [t]	0.218	0.216	10.9 [u]
Inconel 718 [f]	0.24	0.22	13.0
Monel, S (67Ni–30Cu) [d]	0.25	0.24 [m]	14.5
SS 304 [r]	0.29	0.28 [b]	15.1
SS 304L [d]	0.31	0.28	15.5
SS 316 [r]	0.30	0.28 [b]	15.2
Cu–2%Be (UNS C17200 -TH 04) [c]	0.31	0.30	18.1
Brass 70/30 [d]	0.37	0.34 [m]	17.5
Bronze (Cu–5wt%Sn) [n]	0.33	0.29	15.0
Bronze (Cu–10wt%Sn) [n]	0.38	0.35	18.2
Bronze (Cu–13.5wt%Sn) [k]	0.40	0.36	18.8
Aluminum 2024-T86 [f]	0.396	0.374	21.5
Aluminum 7045-T73 [f]	0.419	0.394	23.5
Soft-Solder 50/50 [c]	0.514	0.480 [m]	25.5

Material	$\Delta L/L_{293K–4K}$ [%]	$\Delta L/L_{293K–77K}$ [%]	α_{293K} [10^{-6} K^{-1}]
Insulators			
Pyrex™ [j]	0.055	0.054	3.0
G-11 (warp) [a]	0.21	0.19	11
G-11 (normal) [a]	0.62	0.55	37
G-10CR (warp direction) [a]	0.24	0.21 [m]	12.5
G-10CR (normal direction) [a]	0.71	0.64 [m]	41
Phenolic, Cotton (warp) [f]	0.26	0.24 [m]	15
Phenolic, Cotton (normal) [f]	0.73	0.64 [m]	42
Stycast 2850 FT™ [s]	0.44	0.40	28
CTFE [c]	1.14	0.97 [m]	67
Epoxy [g]	1.16	1.03 [m]	66
Plexiglas™ [j]	1.22	1.06 [m]	75
Nylon™ [c]	1.39	1.26 [m]	80
TFE (Teflon™) [i]	2.14	1.94 [m]	250

[a] A. F. Clark, G. Fujii, and M.A. Ranney (1981), *IEEE Trans. Magn.* **MAG-17**, 2316–2319.
[b] T. A. Hahn (1970), *J. Appl. Phys.* **41**, 5096–5101.
[c] R. J. Corruccini and J. J. Gniewek (1961), *Thermal Expansion of Technical Solids at Low Temperatures.* Monograph 29, National Bureau of Standards, U.S. Government Printing Office, Washington, D.C.
[d] V. Arp, J. H. Wilson, L. Winrich, and P. Sikora, P. (1962), *Cryogenics* **2**, 230–235.
[f] A. F. Clark (1968), *Cryogenics* **8**, 282–289.
[g] K. Dahlerup–Peterson and A. Perrot (1979). *Properties of Organic Composite Materials at Cryogenic Temperatures*. ISR-BOM/79-39, CERN, Geneva, Switzerland.
[i] R. K. Kirby (1956), *J. Res. Natl. Bur. Stand.* **57**, 91–94.
[j] H. L. Laquer and E. L. Head (1952), *Low Temperature Thermal Expansion of Plastics*. AECU-2161, Technical Information Service Atomic Energy Commission., Oak Ridge, Tennessee.
[k] G. Rupp (1980), in *Multifilamentary 15 Superconductors,* eds. M. Suenaga and A. F. Clark, pp. 155–170, Plenum Press.
[l] D. S. Easton, D. M. Kroeger, W. Specking, and C. C.Koch, (1980), *J. Appl. Phys*. **51**, 2748–2757.
[m] A. F. Clark (1983), Chapter 3, in *Materials at Low Temperatures,* pp. 96–97, ASM International, Materials Park, Ohio.
[n] *Handbook on Materials for Superconducting Machinery* (1977), MCIC-HB-04. Battelle, Columbus, Ohio.
[o] Compilation by A. F. Clark (1983), Chapter 3 in *Materials at Low Temperatures,* pp. 96–97, ASM International, Materials Park, Ohio.

[p] N. J. Simon, E. S. Drexler, and R.P. Reed (1992), *Properties of Copper and Copper Alloys at Cryogenic Temperatures,* U.S. Government Printing Office, Washington, D.C.; N. Cheggour and D. P. Hampshire (2000), *Rev. Sci. Instrum.* **71**, 4521–4529.

[q] V. J. Johnson, ed, (1961), *Properties of Materials at Low Temperature, Phase 1*, U.S. Air Force.

[r] *Handbook on Materials for Superconducting Machinery* (1974, 1976), National Bureau of Standards, U.S. Government Printing Office, Washington, D.C.

[s] C. A. Swenson (1997), *Rev. Sci. Instrum.* **68**, 1312–1315.

[t] Y. S. Touloukian (1975), *Thermal Expansion*, **12**, 1248.

[u] R. Radebaugh et al. (2001), http://www.cryogenics.nist.gov/ and the references listed therein.

A7.5 Superconductor materials: Thermal contraction on cooling to liquid-helium and liquid-nitrogen temperatures (Sec. 7.3.2)

The total linear contraction from room temperature to the indicated temperature T is defined as

$$\Delta L/L_{293\text{K}-T} \equiv (L_{293\text{K}} - L_T)/L_{293\text{K}}.$$

The coefficient of linear expansion at room temperature is defined as

$$\alpha_{293\text{K}} \equiv (1/L)\, \mathrm{d}L/\mathrm{d}T.$$

Since the thermal expansion/contraction is approximately linear above room temperature, the total contraction from an upper reference temperature T_u above room temperature (such as soldering temperature) to a low temperature T can be determined approximately from

$$\Delta L/L_{T_u-T} = \Delta L/L_{293\text{K}-T} + (\alpha_{293\text{K}})\,(T_\text{u} - 293\ \text{K}).$$

Tabulated values are generally arranged within each material group by the magnitude of the thermal contraction.

Thermal contraction of superconductor materials

Material	$\Delta L/L_{293K-4K}$ [%]	$\Delta L/L_{293K-77K}$ [%]	α_{293K} [10^{-6} K^{-1}]
High-T_c *Superconductors*			
YBCO polycrystal [i]	0.23	0.21	11.5
YBCO *a*-axis [i]	0.13	0.12	7.4
YBCO *b*-axis [i]	0.18	0.16	9.6
YBCO *c*-axis [i]	0.38	0.34	17.7
YBCO *a,b*-plane avg. [i]	0.16	0.14	8.5
Bi-2212			
a,b-axes [o]	0.15	0.14	8.3
c-axis [o]	0.30	0.27	15.1
Ag [u]	0.41	0.37	18.5
Bi-2223/61%Ag alloy [a,b]		0.24	
Bi-2223 *a,b*-axes [o,p]		0.22	
Ag [q]	0.41	0.37	18.5
(Bi-2223) / 75vol%Ag wire [l]			
1st cool-down	0.22	0.23	16
2nd cool-down (difference due to Ag yielding)	0.29	0.30	13
Tl-2223			
Low-T_c *Superconductors*			
(N–67wt%Ti)/64vol%Cu wire [c]	0.26	0.25 [j]	12.5
Nb–67wt%Ti	0.13 [j,h]		5.8 [j]
Nb–45wt%Ti	0.19 [h]	0.17 [j]	8.2 [j]
Nb_3Sn wire (10vol%Nb_3Sn)	0.30 [g,m]	0.28 [g,m]	
Nb_3Sn wire (20vol%Nb_3Sn	0.28 [g,m]	0.26 [g,m]	
Nb_3Sn	~0.16 [j]	0.14 [j]	7.6 [d]
Bronze (Cu–13.5wt%Sn) [f]	0.40	0.36	18.8
Cu	0.32 [k]	0.30 [j]	16.7 [e,d]
Nb	0.14 [e]	0.13 [j]	7.3 [r]
Ta	0.14 [e]	0.13 [e]	6.3 [e,d]

[a] J. P. Voccio, O. O. Ige, S. J. Young, and C. C. Duchaine (2001), *IEEE Trans. Appl. Supercond.* **11**, 3070–3073.
[b] E. Harley (2004), American Superconductor Corp., personal communication.
[c] A. F. Clark (1968), *Cryogenics* **8**, 282–289.
[d] D. S. Easton, D. M. Kroeger, W. Specking, and C. C. Koch, (1980), *J. Appl. Phys*. **51**, 2748.

[e] R. J. Corruccini, and J. J. Gniewek (1961*) Thermal Expansion of Technical Solids at Low Temperatures.* Monograph 29, National Bureau of Standards, U.S. Government Printing Office, Washington, D.C.

[f] G. Rupp (1980), pp. 155–170 in *Multifilamentary 15 Superconductors,* eds. M. Suenaga and A. F. Clark), Plenum Press, New York.

[g] L. F. Goodrich, S. L. Bray, and T. C. Stauffer (1990), *Adv. Cryog. Eng. (Mater.)* **36A**, 117–124.

[h] F. J. Jelinek and E. W. Collings (1975), "Low-temperature thermal expansion and specific heat properties of structural materials," in *Materials Research in Support of Superconducting Machinery—IV,* eds. A. F. Clark, R. P. Reed, and E. C. Van Reuth. Fourth Semi-Annual Technical Report, National Bureau of Standards, U.S. Government Printing Office, Washington, D.C.

[i] Calculated from data by H. You, J. D. Axe, X. B. Kan, S. Hashimoto, S. C. Moss, J. Z. Liu, G. W. Crabtree, and D. J. Lam (1988), *Phys. Rev.* **B38**, 9213–9216.

[j] Compilation by A. F. Clark (1983), Chapter 3 in *Materials at Low Temperatures*, ASM International, Materials Park, Ohio.

[k] T. A. Hahn (1970), *J. Appl. Phys.* **41**, 5096–5101.

[l] N. Yamada, K. Nara, M. Okaji, T. Hikata, T. Kaneko, N. Sadakata (1998), *Cryogenics* **38**, 397–399.

[m] K. Tachikawa, K. Itoh, H. Wada, D. Gould, H. Jones, C. R. Walters, L. F. Goodrich, J. W. Ekin, and S. L. Bray (1989), *IEEE Trans. Magn.* **25,** 2368-2374.

[o] M. Okaji, K. Nara, H. Kato, K. Michishita, and Y. Kubo (1994), *Cryogenics* **34**, 163–165.

[p] S. Ochaia, K. Hayashi, and K. Osamura (1991), *Cryogenics* **31**, 954–961.

[q] R. J. Corruccini and J. J. Gniewek (1961), *Thermal Expansion of Technical Solids at Low Temperatures*, National Bureau of Standards Monograph 29, U.S. Government Printing Office, Washington, D.C.

[r] *CRC Handbook of Chemistry and Physics* (2001)*,* 82nd edition, CRC Press, Boca Raton, Florida.

A7.6 Thin-film substrate materials: Thermal conductivity and thermal contraction (Sec. 7.4.1 and Sec. 7.4.2)

Material	Thermal Conductivity			Thermal Expansion		
	λ (4K) [W/(m·K)]	λ (77K) [W/(m·K)]	λ (295K) [W/(m·K)]	$\Delta L/L$ (293K–4K) [%]	$\Delta L/L$ (293K–77K) [%]	α (293K) [10^{-6} K^{-1}]
Al N (‖ *a*-axis) [j]	—	—	—	—	0.032	3.7
(‖ *c*-axis) [j]					0.025	3.0
Sapphire (Al_2O_3) [l] (‖ *c*-axis)	451 [e]	10300 [e]		0.079	0.078	5.4 [j]
Beryllia	~1 [i]	~1000 [i]				
C (diamond)				0.024 [a]	0.024 [a]	1.0 [a]
$LaAlO_3$						12.6 [b]
MgO	82 [d]	507 [d]	61 [d]	0.139 [a]	0.137 [a]	10.2 [a]
$NdGaO_3$						7.8 [b]
Ni			90.7 [f]	0.224 [c]	0.212 [c]	13.4 [g]
Quartz (‖ optic axis)	420	32			0.104 [a]	7.5 [a]
Si			124 [m]	0.022 [a]	0.023 [a]	2.32 [a]
α-SiC (λ: crystal, ⊥ to *c*-axis)	27 [k]	4000 [k]	510 [k]	-	0.030 [j]	3.7 [j]
($\Delta L/L$: polycrystal avg.)						
$SrTiO_3$			60 [f]			11.1 [b]
Y-stabilized Zirconia (YSZ)						10.3 [b]
Cu (OFHC) (for reference)	630 [h]	544 [h]	397 [h]	0.324 [c]	0.302 [c]	16.7 [c]

[a] R. J. Corruccini and J. J. Gniewek (1961), *Thermal Expansion of Technical Solids at Low Temperatures*, National Bureau of Standards Monograph 29, U.S. Government Printing Office, Washington, D.C.

[b] Shinkosha Co., Ltd. Tokyo, Japan

[c] A. F. Clark (1983), Chapter 3 in *Materials At Low Temperatures*, ASM International, Materials Park, Ohio.

[d] Y.S. Touloukian and E. H. Buyco, E.H. (1970), *Specific Heat*, Vols. 1 and 2, Plenum Press, New York.

[e] R. Radebaugh et al. (2003), *http://ww*w.cryogenics.nist.gov/ and the references listed therein.

[f] Compiled by M. Paranthaman, Oak Ridge National Laboratory, Oak Ridge, Tennessee; and from J. Evetts, University of Cambridge, UK

[g] *CRC Handbook of Chemistry and Physics* (2001), 82nd edition, CRC Press, Boca Raton, Florida.

[h] Cryogenic Materials Properties Program CD, Release B-01 (June 2001), Cryogenic Information Center, 5445 Conestoga Ct., Ste. 2C, Boulder, CO 80301-2724, Ph. (303) 442-0425, Fax (303) 443-1821

[i] Lake Shore Cryotronics, Inc. (2002), *Temperature Measurement and Control* , Westerville, Ohio.

[j] Y. S. Touloukian (1977), *Thermal Expansion: nonmetallic solids*, Vol. 13, IFI/Plenum, New York.

[k] Y. S. Touloukian (1970), *Thermal Conductivity: metallic elements and alloys*, Vol. 2, IFI/Plenum, New York.

[l] For the thermal conductivity data, the heat flow is 60 degrees away from the hexagonal axis; values are thought to be accurate to within 10 % to 15 % at temperatures above 60 K, but highly sensitive to small physical and chemical variations below 60 K. Thermal linear-expansion data are parallel to the *c*-axis.

[m] *CRC Handbook of Chemistry and Physics* (2002), 83st edition, CRC Press, Boca Raton, Florida.

A7.7 Ultrasonic wire-bond material combinations (Sec. 7.4.3)

Substrate	Metal Film	Wire-bond lead Material	Wire-bond lead Diameter or Thickness Range [mm]
Glass	Aluminum	Aluminum wire	0.05 to 0.25
	Aluminum	Gold wire	0.08
	Nickel	Aluminum wire	0.05 to 0.5
	Nickel	Gold wire	0.05 to 0.25
	Copper	Aluminum wire	0.05 to 0.25
	Gold	Aluminum wire	0.05 to 0.25
	Gold	Gold wire	0.08
	Tantalum	Aluminum wire	0.05 to 0.5
	Chromel	Aluminum wire	0.05 to 0.25
	Chromel	Gold wire	0.08
	Nichrome	Aluminum wire	0.06 to 0.5
	Platinum	Aluminum wire	0.25
	Gold–Platinum	Aluminum wire	0.25
	Palladium	Aluminum wire	0.25
	Silver	Aluminum wire	0.25
	Copper on silver	Copper ribbon	0.7
Alumina	Molybdenum	Aluminum ribbon	0.08 to 0.13
	Gold–platinum	Aluminum wire	0.25
	Gold on molybdenum–lithium	Nickel ribbon	0.05
	Copper	Nickel ribbon	0.05
	Silver on molybdenum–manganese	Nickel ribbon	0.05
Silicon	Aluminum	Aluminum wire	0.25 to 0.5
	Aluminum	Gold wire	0.05
Quartz	Silver	Aluminum wire	0.25
Ceramic	Silver	Aluminum wire	0.25

From *Welding Handbook* (1991), 8th edition, Vol. 2, Chapter 25, pp. 784–812, American Welding Society, Miami, Florida; G. G. Harmon (1997), *Wire Bonding in Microelectronics: Materials, Processes, Reliability, and Yield*, p. 7, McGraw-Hill.

A8. Sample contacts (ref. Chapter 8)

A8.1 Overview of contacts for low-T_c and high-T_c superconductors. (Secs. 8.3 and 8.4)

Contact Type	Specific Contact Resistivity ρ_c * [$\Omega \cdot cm^2$]	Common Usage/Comments
Low-T_c Superconductors (copper sheathed)		
Cu / 63Sn–37Pb / Cu [a]	4×10^{-9}	Copper-to-copper joint soldered under light pressure
High-T_c Bi–Sr–Ca–Cu–O oxide superconductors		
Silver sheath/BSCCO interface [d]	$<<10^{-8}$	Copper connections to the silver sheath can be soldered with standard eutectic Pb–Sn solder and have ρ_c values comparable to those of the copper-to-copper joints listed above.
High-T_c Y–Ba–Cu–O oxide superconductors		
Silver or gold deposited on YBCO:		
In-situ [c] deposited; no anneal [b]	10^{-9} to 10^{-7}	Contacts to oxide superconductor films, typically for electronic applications
Ex-situ [c] deposited; oxygen annealed [e]	10^{-9} to 10^{-6}	Contacts for high current applications, including "coated conductors"
Ex-situ deposited; no oxygen anneal [f]	10^{-5} to 10^{-2}	Applications where oxygen annealing is precluded by other sensitive materials or processing steps. The lowest values of ρ_c obtained when the superconductor surface is ion milled or sputter etched just prior to contact deposition.
Soldered Y–Ba–Cu–O oxide superconductors		
Indium-solder connections to silver or gold pads deposited on YBCO	10^{-1} to 10^{-6}	High-current coated-conductor applications. The lowest values of ρ_c are obtained when the gold or silver pad thickness is at least 7 μm to 10 μm thick (see the subtopic on soldering in Sec. 8.3.3)
Indium solder applied directly on YBCO [g]	10^{-2} to 10^{-1}	Soldered voltage contacts for bulk oxide superconductors

* For low-T_c superconductors, the contact resistivity was measured at 4.2 K. For high-T_c superconductors, the contact resistivity does not appreciably change with temperature below T_c and thus applies to the entire temperature range from liquid-helium to liquid-nitrogen temperatures.

[a] L. F. Goodrich and J. W. Ekin (1981), *IEEE Trans. Magn*. **17**, 69–72.

[b] M. Lee, D. Lew, C–B. Eom, T. H. Geballe, and M. R. Beasley (1990), *Appl. Phys. Lett.* **57**, 1152–1154.

[c] "Ex-situ" and "in-situ" contacts refer to whether the superconductor surface is exposed to air before the noble-metal contact pad is deposited, as described in Sec. 8.4.2 on superconductor-film contact techniques.

[d] Y. S. Cha, M. T. Lanagan, K. E. Gray, V. Z. Jankus, and Y. Fang (1994), *Appl. Supercond.* **2**, 47–59.

[e] J. W. Ekin, T. M. Larson, N. F. Bergren, A. J. Nelson, A. B. Swartzlander, L. L. Kazmerski, A. J. Panson, and B. A. Blankenship, B. A. (1988), *Appl. Phys Lett.* **52**, 1819–1821.

[f] J. W. Ekin, A. J. Panson, and B. A. Blankenship (1988), *Appl. Phys. Lett.* **52**, 331–333.

[g] J. W. Ekin, unpublished data, National Institute of Standards and Technology, Boulder, Colorado.

A8.2 Contact methods for voltage and current connections to bare YBCO superconductors. (Secs. 8.3.1, 8.3.2, 8.3.3, and 8.4.2)

Contact methods are ordered within each category by the magnitude of contact resistivity ρ_c, with the best (lowest ρ_c) listed first.

Any of the *current* contact methods can also be used for *voltage* contacts, but they are more complex to fabricate than the simple techniques listed for voltage contacts.

Contact materials that do not work well with the oxide superconductors are included at the end of the table for pedagogical reasons (described in Sec. 8.3.3).

Contact Method	Procedure	ρ_c [a] $[\Omega\cdot cm^2]$	Comments
Voltage contacts			
In–3wt.%Ag solder	For these solders to wet YBCO surfaces, lightly scratch the sample surface under the molten solder with the soldering-iron tip, or use an ultrasonic soldering iron; see "Soldered…" and "Wetting…" in Sec. 8.3.2.	10^{-2}–10^{-1}	T_{melt} = 143 °C; eutectic
In–48wt.%Sn solder		"	T_{melt} = 118 °C; eutectic; beware that Sn dissolves thin silver or gold films
Spring contacts	Beryllium copper or other conducting spring stock is used to contact the sample; see "Pressure contacts" in Sec. 8.3.2.		Silver or gold pads deposited on the test sample lower the contact resistivity
Silver paint		10^{-1}–10^{0}	Weak connection, but sometimes needed for delicate samples; ρ_c can be improved by oxygen annealing; solvent carrier in paint can damage thin films
Current contacts			
In-situ gold or silver pad deposited on superconductor, no oxygen anneal	Descriptions of *in-situ* vs. *ex-situ* deposition techniques are given in Sec. 8.4.2.	10^{-9}–10^{-7}	Produces the lowest ρ_c In-situ contacts are mainly amenable to HTS *film* (not bulk) fabrication techniques Gold is more expensive than silver contact pads, but does not tarnish as readily

Ex-situ gold or silver pad deposited on superconductor, with oxygen annealing	See Sec. 8.4.2 and "Fabrication" in Sec. 8.3.3.	10^{-9}–10^{-6}	
Ex-situ gold or silver pad deposited on superconductor, no oxygen annealing	See Sec. 8.4.2 and "Fabrication" in Sec. 8.3.3.	10^{-6}–10^{-2}	Used for applications where oxygen annealing is not possible, or where very low ρ_c is not needed ρ_c depends on how well the surface is cleaned
Indium-solder connection to silver or gold pad	Make silver or gold pad thickness at least 7 μm to 10 μm. See "Soldering to noble-metal contact pads" in Sec. 8.3.3.	10^{-1}–10^{-6}	Used for connecting high-current bus bars or wires to the sample-contact pads ρ_c depends strongly on the soldering technique used (see text)
Failures			
Copper pad deposited on superconductor	Sputter deposited	10^{-2}	ρ_c no better than indium solder, and a lot more complex to fabricate.
Au–Cr pad deposited on superconductor	Sputter deposited	10^{-1}	Contact commonly used for semiconductors, but terrible for superconductors.
Pb–Sn solder		no bond	

[a] The contact resistivity does not appreciably change with temperature below T_c, so the same approximate ρ_c values apply at liquid-helium and liquid-nitrogen temperature.

A8.3 Optimum oxygen-annealing conditions for silver and gold contacts to Y-, Bi-, and Tl-based high-T_c *superconductors. (Sec. 8.3.3 and 8.4.2)*

Annealing times are about 30 min to 60 min (at full temperature) for contacts to bulk superconductors, 30 min or less for thin-film superconductors.

Contacts to Bulk High-T_c Superconductors	Annealing Temperature
Ag/YBCO [a]	500 °C in O_2
Au/YBCO [a]	600 °C in O_2
Ag/BiPbSrCaCuO	~400 °C in O_2
Ag/TlCaBaCuO	500 °C in O_2

Contacts to Film YBCO Superconductors	Annealing Temperature
Ag(<1μm)/YBCO film [b]	400 °C in O_2
Au(<1μm)/YBCO film [c]	450 °C to 500 °C in O_2

Annealing is carried out in oxygen at atmospheric pressure, flowing at a rate of about 2×10^{-6} m^3/s (~0.3 scfh, standard cubic feet per hour) by using a furnace such as that shown in Fig. 8.9.

For YBCO, the contacts were cooled in oxygen by ramping the furnace temperature down at a slow rate, ~2.5 °C/min for the bulk sintered superconductors used in these tests; rates for thin films should be kept below 50 °C/min to allow time for the crystal structure to take up oxygen as it cools and to minimize oxygen disorder. (Further information is given in B. H. Moeckly, D. K. Lathrop, and R. A. Buhrman, (1993), *Phys. Rev.* **B47**, 400–417.)

For silver-contact pads on films, the silver pad will "ball up" at oxygen annealing temperatures higher than about 400 °C if the pad is thin (<1 μm); see Fig. 8.13. For thick silver-contact pads (>>1 μm), the optimum annealing temperature can be slightly higher (A. Roshko, R. H. Ono, J. Beall, J. A. Moreland, A. J. Nelson, and S. E. Asher. (1991), *IEEE Trans. Magn.* **27**, 1616–1618).

[a] J. W. Ekin, T. M. Larson, N. F. Bergren, A. J. Nelson, A. B. Swartzlander, L. L. Kazmerski, A. J. Panson, and B. A. Blankenship (1988), *Appl. Phys Lett.* **52**, 1819–1821.

[b] J. W. Ekin, C. C. Clickner, S. E. Russek, and S. C. Sanders (1995), *IEEE Trans. Appl. Supercond.* **5**, 2400–2403.

[c] Y. Xu, J. W. Ekin, C. C Clickner, and R. L. Fiske (1998), *Adv. Cryog. Eng. (Mater.)* **44**, 381–388.

A8.4 Bulk resistivity of common solders, contact-pad materials, and matrix materials (Sec. 8.5.2)

The bulk resistivity values listed below are useful for estimating the effective contact resistivity in conjunction with Eq. (8.5).

Additional properties of solders are tabulated in Appendix A3.7.

Material	ρ_{4K} [μΩ·cm]	ρ_{77K} [μΩ·cm]	ρ_{295K} [μΩ·cm]
Solder (compositions in wt%)			
52In–48Sn [a] (eutectic) (T_{melt}=118 °C)	SC		18.8
97In–3Ag [a] (eutectic) (T_{melt}=143 °C)	0.02	1.8	9.7
90In–10Ag [a]	0.03	1.8	9.1
Indium [a] (T_{melt}=157 °C)	0.002	1.6	8.8
63Sn–37Pb [a] (standard eutectic soft-solder) (T_{melt}=183 °C)	SC	3.0	15
91Sn–9Zn [a] (T_{melt}=199 °C)	0.07	2.3	12.2
Contact Pad Material			
Silver (pure: evaporated, sputtered, or plasma-sprayed)	variable	0.27	1.6
Gold (pure: evaporated or sputtered)	variable	0.43	2.2
Low-T_c Superconductor Matrix Materials			
Copper	variable (~0.017 typical)	~0.2	1.7
Bronze (Cu–13wt%Sn)	~2	~2	
High-T_c Superconductor Matrix Materials			
Silver	variable	0.27	1.6
Silver dispersion strengthened with 1at%Mn [b]	2.2	2.7	4.0
Silver dispersion strengthened with 2at%Mn [b]	~4.1	~4.6	~6.0

SC ≡ Superconducting (see Appendix A3.9).

[a] C. Clickner (1999), unpublished data, National Institute of Standards and Technology, Boulder, Colorado.

[b] M. Putti, C. Ferdeghini, G. Grasso, A. Manca, and W. Goldacker, (2000), *Physica C* **341-348**, 2585-2586.

A8.5a Argon ion milling rates of elements* *(Sec. 8.4.2)*

Values of argon ion milling rates of elements are tabulated in nm/min, at a current density of 1 mA/cm^2, and incident argon ion energies of 200 eV and 500 eV.

Rates at other energies can be estimated from Fig. 8.11. An example is given in Sec. 8.4.2 under Cleaning etch.

Element	200 eV [nm/mm]	500 eV [nm/min]
Ag	100	220
Al	29	73
Au	71	170
Be	5.2	17
C	1.3	4.4
Co	26	55
Cr	33	58
Cu	53	110
Dy	58.0	110
Er	—	98
Fe	26	53
Gd	55.0	110
Ge	49	100
Hf	31	66
Ir	26	60
Mo	24	54
Nb	18	44
Ni	31	66
Os	20	51
Pd	60	130
Pt	39	88
Re	23	52
Rh	31	74
Ru	24	61
Si	16	38
Sm	51.0	110
Sn	85.0	180
Ta	20	42

Element	200 eV [nm/mm]	500 eV [nm/min]
Th	41	82
Ti	16	38
U	34	74
V	17	37
W	18	38
Y	45	96
Zr	27	62

* From a compilation by H. R. Kaufman and R. S. Robinson (1987), *Operation of Broad-Beam Sources.* Commonwealth Scientific Corp., Alexandria, Virginia, from data by G. K. Wehner et al. (1962), General Mills Report **2309**, General Mills Electronic Division, Minneapolis, Minnesota, published by P. R. Puckett, S. L. Michel, and W. E. Hughes, (1991), p. 760 in *Thin Film Processes II*, eds. J. O. Vossen and W. Kern, Academic Press, Boston.

A8.5b Argon ion milling rates of compounds* *(Sec. 8.4.2)*

Values of argon ion milling rates of compounds are tabulated in nm/min, at a current density of 1 mA/cm^2, and incident argon ion energies of 200 eV and 500 eV.

Rates at other energies can be estimated from Fig. 8.11. An example is given in Sec. 8.4.2 under Cleaning etch.

Compound	200 eV [nm/min]	500 eV [nm/min]
CdS [a]	110	230
GaAs (110) [a]	78	160
GaP (111) [a]	69	160
GaSb (111) [b]	90	190
InSb [a]	76	150
$LiNbO_3$ (Y-cut) [c]	—	40
MgO [e]	—	16
Mo_2C [a]	—	29
PbTe [a]	160	380
SiC (0001) [a]	—	35
SiO_2 [c]	—	40
$YBa_2Cu_3O_7$ [e]	—	45

***** From a compilation by H. R. Kaufman and R. S. Robinson (1987), *Operation of Broad-Beam Sources.* Commonwealth Scientific Corp., Alexandria, Virginia, published by P. R. Puckett, S. L. Michel, and W. E. Hughes (1991), p. 760 in *Thin Film Processes II*, eds. J. O. Vossen and W. Kern, Academic Press, Boston; and from J. W. Ekin (1992), unpublished data, National Institute of Standards and Technology, Boulder, Colorado.

[a] J. Comas, J. and C. B. Cooper (1966), *J. Appl. Phys.* **37**, 2820–2822.

[b] S. P. Wolsky, D. Shooter, and E. J. Zdanuk (1962), pp. 164–168 in *Transactions of the 9th National Vacuum Symposium,* Pergamon Press, New York

[c] H. L. Garvin (1971), *Bull. Am. Phys. Soc., Ser. II* **16**, 836.

[d] J. L. Vossen and E. B. Davidson (1972), *J. Electrochem. Soc.* **119**, 1708–1714.

[e] J. W. Ekin (1990), unpublished data, National Institute of Standards and Technology, Boulder, Colorado.

A10. Critical-current analysis parameters (ref. Chapter 10)

A10.1 Effective critical temperature $T_c^*(B)$ (Sec. 10.4.4)

Values of the effective critical temperature T_c^* as a function of magnetic field B are tabulated below. They were determined by linearly extrapolating the $I_c(T,B)$ curves of Figs. 10.17, 10.18, 10.19, and 10.21 to zero current.

The value of $T_c^*(B)$ at a given magnetic field B is useful when the critical current $I_c(T_1)$ is known at one temperature T_1 and we wish to determine its approximate value $I_c(T)$ at an arbitrary temperature T. For this purpose, a linear approximation of the $I_c(T)$ characteristic works fairly well for a number of conductors [Eq. (10.14) in Sec. 10.4.4]:

$$I_c(T)/I_c(T_1) = [T_c^*-T]/[T_c^*-T_1] \ .$$

This linear relationship between the critical current and temperature usually breaks down at high temperatures (within about 10 % of T_c^*) because of inhomogeneities in the superconductor, but the relationship is useful over most of the practical temperature range leading up to T_c^* (ref. Figs. 10.17, 10.18, 10.19, and 10.21).

For materials that cannot be modeled with a linear relationship, the temperature-transformation method described in Sec. 10.6.3 is much more general in nature and quite accurate for nearby transformations. A summary of the method is also given in Appendix A10.2b below under the subsection entitled Temperature dependence of the critical current.

Values of $T_c^*(B)$ at Various Magnetic Fields for Selected Superconductors

Magnetic Field B [T]	Nb–Ti [a] First number valid near T_c^*; the second for the range 4.0 K to 4.5 K [K]		Nb_3Sn [b] [K]	V_3Ga [d] [K]	YBCO [e] [K]
0	9.2	12.4			87
0.3	9.0	11.0			
1	8.66	9.78			
2	8.25	9.31	15.0		
3	7.89	8.77			
4	7.40	8.20	13.7	11.8	
5	7.07	7.54	13.1	11.4	
6	6.52	6.85	12.6		
7	6.14	6.16			
8	5.53	5.53	11.5	10.8	
9	5.16	5.01			
10	4.63	4.63	10.4	10.3	
12			9.5		

[a] For Nb–Ti, the first value of T_c^* is for use over the high-temperature regime where T approaches T_c^*. It is extrapolated from the slope of the data where I_c approaches zero. The second value of T_c^* is for use over the liquid-helium temperature range. It is extrapolated from data only between 4.0 K and 4.5 K. Note that because of curvature in the I_c vs. T plot *at low magnetic fields*, the second value of T_c^* (for use in the liquid-helium temperature range) can be significantly greater than the first (nominal) value. Data from L. F. Goodrich and T. C. Stauffer (2004), *Adv. in Cryog. Eng. (Mater.)* **50B**, 338–345 (the source data are plotted in Fig. 10.17 of this textbook).

[b] Extrapolated from data by L. F. Goodrich, L. T. Medina, and T. C. Stauffer (1998), *Adv. Cryog. Eng. (Mater.)* **44**, 873–880 (straight-line extrapolations are shown in Fig. 10.18 of this textbook).

[c] Extrapolated from data by S. A. Keys, N. Koizumi, and D. P. Hampshire (2002), Supercond. Sci. Technol. 15, 991-1010.

[d] Extrapolated from data by Y. Iwasa and B. Montgomery (1975), pp. 387–487 in *Applied Superconductivity,* Vol. **2,** ed. V. L. Newhouse, Academic Press, (straight-line extrapolations are shown in Fig. 10.19).

[e] Extrapolated from data by R. Feenstra and D. T. Verebelyi (1999), unpublished, Oak Ridge National Laboratory, Tennessee (the source data are plotted in Fig. 10.21).

A10.2a Scaling parameters for calculating the magnetic-field, strain, and temperature dependence of the critical current of low-T_c superconductors (Secs. 10.3, 10.5, 10.6, and 10.7)

The scaling-parameter values listed below can be used for technological purposes to analytically model and transform the critical current of multifilamentary low-T_c superconductors as a function of magnetic field, strain, and temperature. These parameters are used in conjunction with the scaling relations summarized in Appendix A10.2b. The scaling relations are listed in Appendix A10.2b in order of increasing complexity, starting with the simplest scaling laws (appropriate for fixed strain or temperature) and working to the most complete (the unified scaling law suitable for variable magnetic field, temperature, and strain). The relations are mutually consistent and build on each other, so it is worth utilizing the simplest relation for the task at hand.

Values of the scaling parameters tabulated here were determined from data correlations for specific classes of superconductors. They show good consistency (± 10 % to 20 %) within each class, where sufficient data exist for meaningful statistical correlations to be made (e.g., binary Nb_3Sn, V_3Ga, and, to some extent, Nb_3Al; see, for example, Figs. 10.30 and 10.31). These values will no doubt be refined and updated as more data are obtained for given classes of superconductors, such as specific types of ternary Nb_3Sn. To that end, these standard values and the accompanying scaling relations provide a basic *framework* for systematizing additional data as they become available.

This ongoing task is aided by the *separability* of this parameter set into magnetic field, strain, and temperature parameters. Defined in this way, the parameter values show good consistency and are easily updated. A significant advantage of the separable parameter set used here is the independence of strain and temperature parameters, which enables their values to be determined from separate strain and temperature experiments. This offers flexibility and considerable time savings. Also, since the parameters are not commingled, the entire set does not have to be redetermined every time additional new strain or temperature data become available for a particular conductor. (Further information on the practical use of this parameter set is given in Sec. 10.7.1 under the subheading Separable form, and in Sec. 10.7.4.)

If strain and/or temperature data are available for a specific conductor, scaling parameters tailored to that conductor can be determined with the robust methods given in Sec. 10.7.4 and substituted for the standard parameters given in the table below entitled Scaling Parameters. In this case, the values below are needed only to fill in missing gaps in the scaling-parameter set (see Sec. 10.7.4 for more details). These standard values also have predictive utility in the initial design stage of superconducting magnets.

Limitations:

(1) These parameter values are valid specifically for conductors with *solid filaments* (not tubular filaments, or bundles of filaments that fuse into a tubular structure after reaction).

(2) They also depend on *additive content* and *fabrication process* (e.g., bronze process vs. internal tin). The tabulated additive concentrations are not the starting weight percent of additive in the conductor before reaction; rather, they are the atomic percent actually measured in the Nb_3Sn reaction layer *after* fabrication, which can vary depending on the fabrication process. As more data become available, it is expected that consistent correlations of parameter values will be obtained for additional classes of conductors.

(3) The tabulated scaling parameters are for technological use over the *moderate intrinsic-strain range* ($-0.5\ \% < \varepsilon_0 < +0.4\ \%$), which is the range where most magnets are designed. For high compressive strains ($\varepsilon_0 < -0.5\ \%$), four more parameters are needed, as described in Secs. 10.5.6 and 10.7.3 and summarized below in Eqs. (A10.9)–(A10.11) and (A10.30)–(A10.32); these high-compression parameters may not be so consistent.

Examples:

Practical examples for utilizing these parameters with the scaling relations are given in the following sections:

- Magnetic-field modeling — Sec. 10.3.3
- Strain and magnetic-field modeling — Sec. 10.5.7
- Simplified strain transformations — Sec. 10.6.2
- Simplified strain-and-temperature transformations — Sec. 10.7.5

Temperature-scaling parameters

Values of the temperature-scaling parameters {for use with the temperature scaling law [Sec. 10.6.3 and Eq. (A10.12) below] and the unified strain-and-temperature scaling law [Sec. 10.7 and Eq. (A10.18)]} are available mainly for Nb_3Sn and not listed in the table below. The (dimensionless) temperature-scaling parameters v and w are nearly universal constants for the technological Nb_3Sn conductors evaluated thus far, including binary and ternary Nb_3Sn at both moderate and high intrinsic strains:

$v = 1.5$	for Nb_3Sn, as shown by Figs. 10.37 and 10.38
$w = 3.0$	for Nb_3Sn, as shown by Fig. 10.36.

Although not so nearly universal, the (dimensionless) temperature exponent η and the critical temperature at zero intrinsic strain $T_c^*(0)$ can be effectively approximated for nearby temperature transformations by

$\eta \approx 2.5$	for Nb_3Sn
$T_c^*(\varepsilon_0=0) \approx 17$ K	for Nb_3Sn.

With additional temperature correlations, values of these latter two parameters may become more standardized for individual classes of superconductors.

For Nb_3Sn, the scaling parameter $B^*_{c2}(T=0,\varepsilon_0=0)$ can be estimated by using Eq. (10.57) with the approximate values of $B^*_{c2}(4.2K,\varepsilon_0=0)$ given in the table below; that is,

$$B^*_{c2}(0,0) \approx B^*_{c2}(4.2K,0)\,[1-(4.2K/17.5K)^{\nu}]^{-1} \approx 1.14\,B^*_{c2}(4.2K,0).$$

Scaling Parameters [dimensionless, except for B^*_{c2}]:

Superconductor	Crystal Structure	Magnetic-Field Dependence of I_c			Strain Dependence of I_c ‡ * ($-0.5\% < \varepsilon_0 < +0.4\%$)			Ref.
		p †	q †	B^*_{c2} at 4.2K,ε_0=0 [T]	a^- (ε_0<0)	a^+ (ε_0>0)	s	
Strain-dependent Superconductors								
Nb_3Al (RHQT)	A15	0.5	~2.0	26	370		~2.5	a
V_3Ga	"	0.4	1.0	21	450	650	1.4	b
Nb_3Ge	"	0.6	1.9	25	500	—	~2	c
Nb_3Sn*	"	0.5	2.0	21	900	1250	1	d
Nb_3Sn +0.6at%Ti*	"	0.6	1.7	23	900	1250	1.1	e
Nb_3Sn +1.85at%Ti*	"	0.5	1.5	25	1100	1450	1.2	e,f
Nb_3Sn +0.6at%Ta*	"	0.5	1.4	24	900	1250	1.0	e
Nb_3Sn +2.2at%Ta*	"	0.5	1.4	24	1350	1800	~1	e,g
V_3Si	"	0.5	1.7	16	3500	—	~1	a
$PbMo_6S_8$	Chevrel	0.3	6	63	—	1900	~2	h
Strain-independent Superconductors								
NbN	B1	1.2	2.4	24	0	0	—	i
NbCN	"	1.4	2.5	17	—	0	—	j
$V_2(Hf,Zr)$	C15	0.7	0.6	20	—	0	—	k

† Values of p and q are effectively independent of temperature and strain (Sec. 10.7.1).

‡ The strain-parameter values listed are valid only for the moderate intrinsic-strain range ($-0.5\% < \varepsilon_0 < +0.4\%$). To model I_c at high-compressive strains ($\varepsilon_0 < -0.5\%$), additional parameters are needed, as described in Sec. 10.5.6 for the strain-scaling law and Sec. 10.7.3 for the unified strain-and-temperature scaling law.

* The strain parameters a^-, a^+, and s are applicable to *solid-filament* (not tubular-filament) superconductors. The strain-sensitivity parameter a is defined by Eq. (10.21) of Sec. 10.5.5 for a power-law exponent $u = 1.7$. [This value of u is found to hold experimentally for all the A15 and Chevrel-phase superconductors listed in the above table (see Sec. 10.5.5). It is also given by the model of Markiewicz with no adjustable parameters

(see Fig. 10.32).] The values of a^- and a^+ are dependent on the type and amount of *additives*, as shown for the various ternary Nb_3Sn materials listed in the table. Atomic percentages given are those measured in the Nb_3Sn layer *after* reaction. For example, 2.2at%Ta in the reaction layer was obtained with a starting filament alloy of Nb–7.5wt%Ta, but it can vary depending on conductor processing.

[a] Banno, N., Uglietti, D., Seeber, B., Takeuchi, T., and Flukiger, R. (2005), *Supercond. Sci. and Technol*. **18**, S338 – S343. RHQT ≡ rapid heating, quenching and transformation process.

[b] J. W. Ekin (1981), *IEEE Trans. Magn.* **MAG-17**, 658–661; D. G. Howe, T. L. Francavilla and D. U. Gubser (1977), *IEEE Trans. Magn.* **MAG-13**, 815–817; Furukawa Corp. (1984), personal communication.

[c] J. W. Ekin (1981), *IEEE Trans. Magn.* **MAG-17**, 658–661.

[d] J. W. Ekin (1980), *Cryogenics* **20**, 611–624.

[e] J. W. Ekin (1985), pp. 267–271 in *Proc. International Symposium of Flux Pinning and Electromagnetic Properties of Superconductors,* eds. K. Yamafuji and F. Irie, Matsukuma Press, Japan..

[f] Sample from G. Ozeryansky (1984), Intermagnetics General Corp.

[g] Sample from W. McDonald (1984), Teledyne Wah-Chang Corp.

[h] J. W. Ekin, T. Yamashita, and K. Hamasaki (1985), *IEEE Trans. Magn.,* **MAG-21**, 474–477.

[i] J. W. Ekin, J. R. Gavaler, and J. Greggi (1982), *Appl. Phys. Lett.* **41**, 996–998.

[j] J. W. Ekin, unpublished data, National Institute of Standards and Technology, Boulder, Colorado; sample from M. Dietrich (1984), Kernforschungszentrum Karlsruhe, Karlsruhe, Germany.

[k] H. Wada, H., K. Inoue, K. Tachikawa, and J. W. Ekin (1982), *Appl. Phys. Lett.* **40**, 844–846.

A10.2b Summary of scaling relations for utilizing the scaling parameters in Appendix A10.2a

The relations summarized here are based on consistent scaling data of the critical current as a function of magnetic field, strain, and temperature. Used in conjunction with the scaling parameters tabulated in Appendix A10.2a, they provide analytic expressions for modeling, interpolating, and predicting the critical current of most practical low-T_c superconductors as a function of magnetic field, strain, and temperature for technological applications. Further discussion and examples of the application of these scaling relations are given in the main text sections referred to in parentheses with each summary heading. The scaling relations are mutually consistent and listed progressively from the simplest to the most general. Again, use the simplest relation for the task at hand.

Because the parameter set used here is separable into temperature and strain parameters (see Sec. 10.7.1), the relations, when assembled, become the general unified scaling law described at the end of the list below. The separable nature of this parameter set also has the benefit that limited numbers of scaling parameters determined from early limited data (i.e., an incomplete set of values) are not a wasted effort. Rather, they build on each other and generally do not need to be refit later as more data become available. As refined parameter values are measured for an individual conductor, they can be substituted for the "standard" values listed in the Scaling Parameters table in Appendix 10.2a. This building process also parallels the way data are usually obtained for a given conductor (Sec. 10.7.4).

Magnetic-field interpolations (Secs. 10.3.2 and 10.3.3)

The dependence of the critical current I_c on magnetic field B is given by [ref. Eqs. (10.9)–(10.11)]

$$I_c(B) = k B^{-1} [B/B_{c2}^*]^p [1 - (B/B_{c2}^*)]^q, \qquad \text{(A10.1)}$$

where k is a proportionality constant and B_{c2}^* is the effective upper critical field. This is an empirical expression based on the general form of most pinning theories. Typical values of B_{c2}^* and the exponential constants p and q for most of the common high-field low-T_c superconductors are given in columns 3 to 5 of the Scaling Parameters table in A10.2a. Values of the parameters p and q tailored to a specific conductor can be obtained from a single $I_c(B)$ measurement at a fixed temperature and strain [preferably obtained at a temperature $T << T_c^*(0)$ to minimize the effects of B_{c2} inhomogeneity (Sec. 10.3.4), and at a strain not too far from $\varepsilon_0 \approx 0$ to avoid B_{c2} inhomogeneity effects as well as filament breakage at high tensile strains (Sec. 10.5.1)].

Strain dependence of the critical current (valid for fixed temperature $T << T_c$*; e.g., at 4.2 K in* Nb_3Sn*) (Secs. 10.5.4–10.5.7)*

The magnetic-field and strain dependence of the critical current of most low-T_c superconductors can be modeled at low temperatures with the strain scaling law [Eq. (10.18)]. The simplest parameterization of this law applies to the moderate intrinsic-strain range (–0.5 % < ε_0 < +0.4 %, assuming $\varepsilon_{irr} \geq$ +0.4 %), which is also the strain range where most (but not all) magnets are designed mainly because the critical currents are highest in this regime. [Extended-strain parameters covering the high compressive strain range (ε_0 < –0.5 %) are given in Secs. 10.5.6 and 10.7.3, and are summarized below in Eqs. (A10.9)–(A10.11) and (A10.30–A10.32).] This empirical scaling law is based on extensive correlations of strain data at 4.2 K in low-T_c superconductors, which show strain invariance of the shape of the pinning-force vs. magnetic-field characteristic (Sec. 10.5.4).

For the moderate strain range, the simplest and most consistent parameterization of the strain scaling law for technological purposes gives the following expression for the magnetic-field and strain dependence of the critical current $I_c(B,\varepsilon_0)$ [ref. Eqs. (10.20)–(10.22)]

$$I_c(B,\varepsilon_0) \;=\; g(0)\;\left[1 - a\,\left|\,\varepsilon_0\,\right|^{1.7}\right]^{s}\;B^{-1}\;\left[B/B^{*}_{c2}(\varepsilon_0)\right]^{p}\;\left\{1 - \left[B/B^{*}_{c2}(\varepsilon_0)\right]\right\}^{q}, \qquad \text{(A10.2)}$$

valid for fixed temperature $T << T_c$ (e.g., at 4.2 K in Nb_3Sn). Here, $g(0)$ is a proportionality constant and the scaling parameters p, q, a^- (for ε_0<0), a^+ (for ε_0>0), and s are tabulated in columns 3, 4, 6, 7, and 8, respectively, of the Scaling Parameters table in A10.2a. (The strain-sensitivity parameters a^- and a^+ are described more fully below.) The scaling parameter $B^{*}_{c2}(\varepsilon_0)$ is the strain-dependent effective upper critical field; values at 4.2 K are tabulated in column 5 of Table A10.2a.

The variable ε_0 is the *intrinsic* strain, defined as

$$\varepsilon_0 \equiv \varepsilon - \varepsilon_m, \qquad \text{(A10.3)}$$

where ε is the axial strain applied to the superconductor and ε_m is the axial strain at which I_c is maximum (e.g., Fig. 10.26). Negative values of ε_0 represent the compressive intrinsic strain in the superconductor, and positive values represent tensile intrinsic strain (Sec. 10.5.1). The upper strain limit for the validity of this strain scaling law is given by the irreversible strain limit ε_{0irr}, where the conductor is permanently damaged by axial strain. A typical value of ε_{0irr} in Nb_3Sn is about $\varepsilon_{0irr} \approx$ +0.4 %, but it can be more or less than this amount (Sec. 10.5.1). (Lower values of ε_{0irr} usually occur in conductors with larger filament diameters or fused filament clusters, whereas higher values of ε_{0irr} usually occur in conductors with small filament diameters, such as Nb_3Al or fine-filament Nb_3Sn conductors.)

Over the moderate intrinsic strain range (–0.5 % < ε_0 < ε_{0irr}), the effective upper critical field is well represented by a power law

$$\frac{B^*_{c2}(\varepsilon_0)}{B^*_{c2}(0)} = 1 - a\,|\,\varepsilon_0\,|^{1.7}, \qquad \text{(A10.4)}$$

where $B^*_{c2}(\varepsilon_0{=}0)$ is evaluated at the designated temperature T. This is an empirical parameterization that accurately and consistently represents the fundamental results of anharmonic strain theory over the moderate strain range (Sec. 10.5.5). Values of $B^*_{c2}(\varepsilon_0{=}0)$ at 4.2 K are listed in column 5 of Table A10.2a. For Nb_3Sn, values of $B^*_{c2}(\varepsilon_0{=}0)$ at other temperatures can be estimated from the 4.2 K values by using Eq. (10.57) [i.e., Eq. (A10.19) below] and the temperature-scaling parameter values listed just before Table A10.2a.

The parameter a in Eq. (A10.4) is the *intrinsic strain sensitivity* and is a simple quantitative index of the sensitivity of a given class of superconductors to axial strain. For compressive strains ($\varepsilon_0 < 0$), the strain sensitivity is denoted as a^-, with values listed in column 6 of Table A10.2a. For tensile strains ($\varepsilon_0 > 0$), the strain sensitivity is denoted a^+, with somewhat greater values listed in column 7 of Table A10.2a. (Sec. 10.5.5 gives a discussion of the fundamental origin of this difference.) The compressive parameter a^- (column 6) is usually the more important parameter from a technological standpoint, since it characterizes the strain sensitivity of a conductor over the moderate compressive strain range where most magnets are designed ($-0.5\ \% < \varepsilon_0 < 0\ \%$). Again, the tensile parameter a^+ is valid only up to the irreversible strain limit ε_{0irr} where damage occurs in the superconducting filaments.

Limitations:

(1) It bears reiterating that the strain-scaling parameters a^-, a^+, and s in the Table A10.2a apply to the most common types of conductors, *solid-filament* multifilamentary wires, not to other filament shapes such as wires with tubular filaments or fused tubular clusters, where the strain sensitivity is enhanced by three-dimensional strain effects.

(2) Occasionally, particular conductors need to be characterized by unsymmetrical values of the parameter s in Eq. (A10.2) [s^- for compressive intrinsic strain ($\varepsilon_0 < 0$) and s^+ for the tensile side ($\varepsilon_0 > 0$)]. Further data correlations are needed to see if such unsymmetrical values of s are "standard" for certain types of superconductors.

(3) For high-compressive strains ($\varepsilon_0 < -0.5\ \%$), a more general relationship must be used, given by Eqs. (10.23) and (10.24) in Sec. 10.5.6. This entails additional parameters that appear to be extrinsic in nature and, therefore, must be fitted on a conductor-by-conductor basis (Sec. 10.5.6).

<u>*Strain* transformation *method*</u> (Sec. 10.6.1)

The strain *transformation* method is a powerful technique for utilizing the strain scaling law to transform a single $I_c(B,\varepsilon_{01})$ curve obtained at a strain ε_{01} to a curve $I_c(B',\varepsilon_{02})$ valid at a

different strain ε_{02}, without the need to know the parameters p, q, $B^*_{c2}(0)$, or $g(0)$ in Eq. (A10.2). The derivation of this transformation method is given in Sec. (10.6.1).

The transformation is independent of the parameterization scheme; it is illustrated here with the separable parameter set employed above because of its practical utility, but it can be used with any of the alternative parameterization schemes that have been proposed for the prefactor term $g(\varepsilon)$ in the strain scaling law [Eq. (10.18)]. Again, the strain-transformation method is limited to transformations carried out at fixed temperatures $T << T_c$, such as 4.2 K in Nb_3Sn. (For combined strain and temperature transformations, see the unified-scaling transformation method summarized in the last subsection of this appendix.)

The application of the transformation consists of two steps. First, to obtain $I_c(B',\varepsilon_{02})$ when ε_{01} and ε_{02} fall within the moderate strain range ($-0.5\ \% < \varepsilon_0 < \varepsilon_{0irr}$), multiply the magnetic field data of the $I_c(B,\varepsilon_{01})$ data set by the constant β to obtain a new set of magnetic-field values B' [ref. Eq. (10.32)]

$$B' = \beta\, B. \tag{A10.5}$$

Second, multiply the critical current data of the $I_c(B,\varepsilon_{01})$ set by β^{s-1} to obtain new critical current values corresponding to the new magnetic-field data; that is, [ref. Eq. (10.33)]

$$I_c(B',\varepsilon_{02}) = \beta^{s-1}\ I_c(B,\varepsilon_{01}). \tag{A10.6}$$

The constant β in these two equations is given by [ref. Eq. (10.34)]

$$\beta \equiv \frac{B^*_{c2}(\varepsilon_{02})}{B^*_{c2}(\varepsilon_{01})} = \frac{1 - a\left|\varepsilon_{02}\right|^{1.7}}{1 - a\left|\varepsilon_{01}\right|^{1.7}}. \tag{A10.7}$$

(For an immediate clarification of this simple data-transformation procedure, please refer to the example given in Table 10.3 in Sec. 10.6.2.) Thus, all that's needed to carry out the transformation are the scaling parameters a and s. Again, values of s are listed in column 8 of Table A10.2a, and values of the strain-sensitivity parameter a are given in columns 6 and 7 of Table A10.2a (a^- for $\varepsilon_0 < 0$, and a^+ for $\varepsilon_0 > 0$).

For nearby transformations, this method is quite accurate. For example, when transforming from $\varepsilon_0 = -0.3$ % to 0 % in Nb_3Sn conductors, an error of 10 % in the value of a results in an error of less than 0.5 % in the transformed B values and effectively no error in the I_c values.

High compressive strains: For transformations involving high-compressive strains ($\varepsilon_0 < -0.5$ %), the magnetic-field transformation remains that given by Eq. (A10.5), but we use the more general transformation for the critical current [Eq. (10.30)]

$$I_c(B', \varepsilon_{02}) = \beta^{-1} \frac{g(\varepsilon_{02})}{g(\varepsilon_{01})} I_c(B, \varepsilon_1), \tag{A10.8}$$

where

$$\beta \equiv \frac{B^*_{c2}(\varepsilon_{02})}{B^*_{c2}(\varepsilon_{01})}.$$

The functions $B^*_{c2}(\varepsilon_0)$ and $g(\varepsilon_0)$ can be parameterized at high compressive strains by

$$\frac{B^*_{c2}(\varepsilon_0)}{B^*_{c2}(0)} = 1 - a\,|\,\varepsilon_0\,|^{1.7} + a_1\,|\,\varepsilon_0 - \varepsilon_0'\,|^{a_2}\, I(\varepsilon_0 < \varepsilon_0') \tag{A10.9}$$

and

$$\frac{g(\varepsilon_0)}{g(0)} = [1 - a\,|\,\varepsilon_0\,|^{1.7}]^s + g_1\,|\,\varepsilon_0 - 0.005\,|^{g_2}\, I(\varepsilon_0 < \varepsilon_0') \tag{A10.10}$$

with

$$I(\varepsilon_0 < -0.005) \equiv \begin{cases} 1 & \text{if } \varepsilon_0 < \varepsilon_0' \\ 0 & \text{if } \varepsilon_0 > \varepsilon_0' \end{cases}. \tag{A10.11}$$

Here, $I(\varepsilon_0 < \varepsilon_0')$ is an *indicator function*, which is zero except at high-compressive strains: $\varepsilon_0 < \varepsilon_0'$, with $\varepsilon_0' \approx -0.005$ for Nb_3Sn. Unlike transformations carried out over the intrinsic peak strain range, the extra parameters characterizing the extended strain range (a_1, a_2, g_1, and g_2) are probably extrinsic in nature and need to be determined on a conductor-to-conductor basis. The advantage of the parameterization given by Eqs. (A10.9)–A(10.10) is that the scaling parameters a and s characterizing the intrinsic peak region remain consistent and unaffected by those characterizing the extrinsic high compressive regime.

Temperature dependence of the critical current (valid for fixed strain) (Sec. 10.6.3)

The magnetic-field and temperature dependence of the critical current of most low-T_c superconductors can be modeled (at a fixed strain) with the temperature scaling law [Eq. (10.36)]. This empirical relation is based on correlations of temperature data at fixed strain, which show temperature invariance of the shape of the pinning force vs. magnetic-field characteristic (Sec. 10.6.3).

The simplest parameterization of the temperature scaling law for technological purposes is given by [ref. Eqs. (10.38)−(10.43)]

$$I_c(B,T) = h(0)\ [(1 - t^{\nu})]^{\eta}\ B^{-1}\ [B/B^*_{c2}(t)]^p\ \{1 - [B/B^*_{c2}(t)]\}^q, \tag{A10.12}$$

valid for fixed strain. Here, $h(0)$ is a proportionality constant, p and q are the scaling constants given in columns 3 and 4 of Table A10.2a, and ν and η are temperature-scaling constants listed for Nb_3Sn just before Table A10.2a.

The variable t is the *reduced* temperature, defined as

$$t \equiv T/T_c^*(\varepsilon_0), \qquad \text{(A10.13)}$$

where T is the temperature of the superconductor and $T_c^*(\varepsilon_0)$ is its effective critical temperature (at a fixed strain ε_0). When $t << 1$ and $|\varepsilon_0| \equiv |\varepsilon - \varepsilon_m| < \sim 0.4\%$, the better known *strain-free* value of T_c^* at $\varepsilon_0 = 0$ can be used (since the strain dependence of T_c^* is relatively gradual, as described for the unified-scaling relation below). For Nb_3Sn, the strain-free T_c^* is about 17 K, also listed with the temperature-scaling parameter values just before Table A10.2a.

The effective upper critical field in Eq. (A10.12) can be parameterized most simply by

$$B_{c2}^*(t) = B_{c2}^*(0)\,(1 - t^{\nu}), \qquad \text{(A10.14)}$$

where $B_{c2}^*(t=0)$ is evaluated at the designated strain ε_0. For Nb_3Sn, the strain-free value of B_{c2}^* (t=0) (i.e., at 0 K and at $\varepsilon_0 \equiv \varepsilon - \varepsilon_m = 0$) can be estimated from the values of $B_{c2}^*(4.2\text{K},\varepsilon_0=0)$ listed in column 5 of Table 10.2a by using the relation $B_{c2}^*(t=0,\varepsilon_0=0) \approx B_{c2}^*(4.2\text{K},\varepsilon_0=0)\,[1 - (4.2\text{K}/17\text{K})^{\nu}]^{-1} \approx 1.14\,B_{c2}^*(4.2\text{K},\varepsilon_0=0)$. (Here we have used the nearly universal value $\nu = 1.5$, which is appropriate for Nb_3Sn.) The strain-free B_{c2}^* also works for small values of intrinsic strain, since the strain dependence of B_{c2}^* is relatively gradual compared with its temperature dependence.

The temperature-scaling parameters are the least well characterized at present. As indicated in the material just before the Scaling Parameters table A10.2a, the value $\nu = 1.5$ is fairly well established for Nb_3Sn conductors, but the temperature-scaling parameter η is not yet, with values reported typically in the range 2 to 3.5 for different types of Nb_3Sn superconductors. More standard values of η are expected to be determined as data correlations become available for specific classes of superconductors. In the meantime, a nominal value of $\eta = 2.5$ can be used at least for estimation purposes. This nominal value of η also serves well for temperature *transformations*, particularly if they are nearby transformations, as described next.

Temperature transformation *method* (Sec. 10.6.3)

Similar to the strain transformation summarized earlier, the temperature transformation method is a greatly simplified technique for utilizing the temperature scaling law to transform a single $I_c(B,t_1)$ curve, obtained at a temperature t_1, to a curve $I_c(B',t_2)$ valid at a different temperature t_2, without the need to know the parameters p, q, $B_{c2}^*(t=0)$, or $h(0)$ in Eq. (A10.12).

The transformation is independent of the parameterization scheme. Again, it is illustrated here with the parameter set employed above because of its practical utility, but it can be used with any of the alternative parameterization schemes that have been proposed for the prefactor term $h(T)$ in the temperature scaling law [Eq. (10.36)] The temperature-transformation technique is limited to transformations carried out at a fixed strain; for combined strain and temperature transformations, see the unified scaling law summarized in the next subsection.

As for strain transformations, the application of the temperature transformation method consists of two steps. First, to obtain $I_c(B',t_2)$, multiply the magnetic-field data of the $I_c(B,t_1)$ data set by the constant β to obtain a new set of magnetic-field values B' [ref. Eq. (10.39)]

$$B' = \beta B. \tag{A10.15}$$

Second, multiply the critical-current data of the $I_c(B,t_1)$ set by $\beta^{\eta-1}$ to obtain values of the critical current corresponding to the new magnetic-field values; that is [ref. Eq. (10.41)]

$$I_c(B',t_2) = \beta^{\eta-1} I_c(B,t_1). \tag{A10.16}$$

The constant β is given by [ref. Eqs. (10.42) and (10.43)]

$$\beta \equiv \frac{B^*_{c2}(T_2)}{B^*_{c2}(T_1)} = \frac{1-(T_2/T_c^*)^{\nu}}{1-(T_1/T_c^*)^{\nu}}. \tag{A10.17}$$

(Again, for a clarification of this simple data-transformation procedure, please refer to the example given for strain in Table 10.3 in Sec. 10.6.2.) All that is needed to carry out the transformation are the scaling parameters T_c^*, ν, and η.

As noted above, data correlations of the temperature-scaling parameters have not yet been made for many of the different classes of technological superconductors. The value $\nu = 1.5$ is fairly well established for Nb_3Sn conductors and the strain-free T_c^* at $\varepsilon_0 = 0$ is about 17 K for Nb_3Sn, but the scaling parameter η is not so nearly universal, with values reported over the range 2 to 3.5 for a variety of Nb_3Sn conductors. A nominal value of $\eta = 2.5$ can be used for estimation purposes with most Nb_3Sn superconductors.

Nevertheless, this method is quite accurate if the transformations are nearby. For example, when making the very useful data transformation from 4.2 K to, say, 5.5 K in Nb_3Sn conductors, even a large error of 20 % in the value of η (which covers the range $2 < \eta < 3$) results in a difference of only about 3.5 % in the transformed I_c (and no error in B). For the same example, an error of 5 % in the parameter T_c^* results in a difference of only 1.2 % in the transformed I_c, and only 0.6 % in the transformed B.

Unified strain-and-temperature dependence of the critical current (Sec. 10.7)

The combined magnetic-field, temperature, and strain dependence of the critical current of most low-T_c superconductors can be modeled with the unified scaling law [Eq. (10.45)]. The simplest parameterization of this scaling law applies to the moderate intrinsic-strain range (–0.5 % < ε_0 < +0.4 %, assuming $\varepsilon_{irr} \geq$ +0.4 %), which is where most superconductor applications are designed (again, because in this regime the conductors are under the least stress and their critical currents are maximized). [Extended-strain parameters covering the high-compressive-strain range (ε_0 < –0.5 %) are discussed below with the unified-transformation method.] The unified scaling law is based on data in low-T_c superconductors showing shape invariance of the pinning-force vs. magnetic-field characteristic with respect to both strain and temperature simultaneously.

For the moderate intrinsic-strain range, the unified scaling law can be parameterized with the separable parameter set, giving the combined magnetic-field, temperature, and strain dependence of the critical current $I_c(B,T,\varepsilon_0)$ [ref. Eqs. (10.56)–(10.58)]

$$I_c(B,T,\varepsilon_0) = C\ B^{-1}\ (1 - a\,|\,\varepsilon_0\,|^{1.7})^{s}\ (1 - t^{\nu})^{\eta}\ b^{p}(1-b)^{q} \qquad \text{(A10.18)}$$

where

$$B_{c2}^{*}(t,\varepsilon_0) = B_{c2}^{*}(0,0)\,(1 - a\,|\,\varepsilon_0\,|^{1.7})\,(1 - t^{\nu}) \qquad \text{(A10.19)}$$

and

$$\frac{T_c^{*}(\varepsilon_0)}{T_c^{*}(0)} = \left(1 - a\left|\varepsilon_0\right|^{1.7}\right)^{\frac{1}{w}}. \qquad \text{(A10.20)}$$

Here, C is a proportionality constant and the variables are defined by:

$\varepsilon_0 \equiv \varepsilon - \varepsilon_m$ Intrinsic strain (where ε is the applied strain and ε_m is the applied strain at the peak, all in absolute units, not percent)

$b \equiv \dfrac{B}{B_{c2}^{*}(t,\varepsilon_0)}$ Reduced magnetic field

$t \equiv \dfrac{T}{T_c^{*}(\varepsilon_0)}.$ Reduced temperature

Equations (A10.18) through (A10.20) utilize the separable parameter set, mentioned in the introduction to this appendix, wherein the scaling parameters are separated into magnetic-field, strain, and temperature-scaling parameters with consistent, independent values that are easily updated as additional strain or temperature data become available for a given conductor. With this set, parameter values can also be determined from independent strain or temperature data [rather than from a lengthy, full matrix of combined $I_c(B,t,\varepsilon_0)$ data], which can save a month

or more of data acquisition per sample. Robust methods for determining values of the separable parameter set are described in detail in Sec. 10.7.4. Because this parameterization results in such consistent values, standard values of the parameters work for many purposes when values tailored to a particular conductor are not available. These parameters are discussed in the following paragraphs.

Magnetic-field scaling parameters. Standard values of the magnetic-field parameters B^*_{c2} (T=4.2K,ε_0=0), p and q are tabulated for most of the common low-T_c superconductors in columns 3 to 5 of the Scaling Parameters table in A10.2a. For Nb_3Sn, the parameter $B^*_{c2}(0,0)$ can be estimated from the measured values of $B^*_{c2}(4.2K,0)$ by using Eq. (A10.19); that is, $B^*_{c2}(0,0) \approx B^*_{c2}(4.2K,0)\,[1-(4.2K/17K)^{\nu}]^{-1} \approx 1.14\,B^*_{c2}(4.2K,0)$. Here, we have used $\nu = 1.5$ and $T^*_c(0) \approx 17$ K for technical Nb_3Sn conductors, as listed just before Table A10.2a.

Strain scaling parameters: Standard values of the *strain* parameters $a^-(\varepsilon_0<0)$, $a^+(\varepsilon_0>0)$, and s are tabulated in columns 6, 7, and 8, respectively, of Table A10.2a. The strain-sensitivity parameters a^- and a^+ are described more fully with the strain-scaling relation summarized above. The limitations of the validity of these standard strain-scaling parameter values are also summarized above (solid filaments, additive concentration dependence, and strain range). Note especially that they are limited to the moderate intrinsic strain range ($-0.5\ \% < \varepsilon_0 < +0.4\ \%$). The more general parameterization of the unified strain-and-temperature scaling law, valid for strains extending to high compression ($\varepsilon_0 < -0.5\%$), is given in Secs. 10.5.6 and 10.7.3, and is summarized in Eqs. (A10.30 – A10.32) below. As described in Sec. 10.5.6, this entails additional parameters that appear to be extrinsic in nature, and thus consistent parameter values cannot be tabulated; instead they must be fitted on a conductor-by-conductor basis.

Temperature scaling parameters. The temperature parameters ν and w have nearly universal values, at least for technical Nb_3Sn superconductors; values are listed for these two parameters just before Table A10.2a. The temperature parameters $T^*_c(0)$ and η are not yet well established. As noted for the temperature scaling law above, a value for $T^*_c(0)$ of about 17 K can be used for Nb_3Sn, but this would benefit from further data correlations for given classes of superconductors. Likewise, values of η have been reported anywhere from 2 to 3.5 for different types of Nb_3Sn superconductors, but a nominal value of $\eta = 2.5$ can at least be used for estimation purposes and serves well for the transformation technique to nearby strains and temperatures (described just below).

Extrinsic parameters. This leaves the parameters ε_m and C, which are highly variable extrinsic parameters that mainly depend, respectively, on conductor geometry and heat-treatment conditions. Therefore, they must be determined on a conductor-by-conductor basis. Often ε_m can be approximated from measurements on similar conductors, or determined for a specific

conductor from a single $I_c(\varepsilon)$ measurement at any fixed magnetic-field. The proportionality constant C can be determined from a single I_c measurement on the conductor in question (at any fixed magnetic field, temperature, and strain).

Unified strain-and-temperature transformation *method* (Sec. 10.7.5)

Similar to the transformations described above, the transformation method is a powerful technique for utilizing the unified scaling law to transform a single $I_c(B)$ curve measured at strain ε_{01} and temperature T_1, to another combination of strain ε_{02} and temperature T_2 without the need to know the parameters p, q, $B^*_{c2}(0)$, and C. The method is especially effective for nearby transformations, achieving high accuracy even with standard parameter values (see below). The transformation is independent of the parameterization scheme, but it is illustrated here with the separable parameter set because of its practical utility.

As shown in the example at the end of Sec. 10.7.5, the transformation is carried out in a spreadsheet program simply by multiplying a column of magnetic-field values and a column of corresponding critical-current values by two constant prefactors. That is, to transform a data set $I_c(B,T_1,\varepsilon_{01})$, which was obtained at temperature T_1 and strain ε_{01}, to a corresponding data set $I_c(B',T_2,\varepsilon_{02})$ valid at T_2 and ε_{02}, multiply the *magnetic-field* values in the first set by the constant β

$$B' = \{\beta\}\, B\,, \tag{A10.21}$$

and the *critical-current* values in the first set by the constant shown in brackets { }

$$I_c(B',T_2,\varepsilon_{02}) = \left\{ \beta^{-1}\, \frac{K(T_2,\varepsilon_{02})}{K(T_1,\varepsilon_{01})} \right\} I_c(B,T_1,\varepsilon_{01}), \tag{A10.22}$$

where

$$\beta \equiv \frac{B^*_{c2}(T_2,\varepsilon_{02})}{B^*_{c2}(T_1,\varepsilon_{01})}. \tag{A10.23}$$

For the common case where ε_{01} and ε_{02} fall within the moderate strain range ($-0.5\ \% < \varepsilon_0 < +0.4\ \%$), these two transformation constants {the terms in brackets in Eqs. (A10.21) and (A10.22)} can be evaluated with the separable parameter set as

$$\beta = \left(\frac{1-a\left|\varepsilon_{02}\right|^{1.7}}{1-a\left|\varepsilon_{01}\right|^{1.7}} \right) \left(\frac{1-t_2^{\nu}}{1-t_1^{\nu}} \right). \tag{A10.24}$$

and

$$\beta^{-1}\, \frac{K(T_2,\varepsilon_{02})}{K(T_1,\varepsilon_{01})} = \left(\frac{1-a\left|\varepsilon_{02}\right|^{1.7}}{1-a\left|\varepsilon_{01}\right|^{1.7}} \right)^{s-1} \left(\frac{1-t_2^{\nu}}{1-t_1^{\nu}} \right)^{\eta-1}, \tag{A10.25}$$

Again, the variables are defined by:

$\varepsilon_0 \equiv \varepsilon - \varepsilon_m$ Intrinsic strain (where ε is the applied strain and ε_m is the applied strain at the peak, all in absolute units, not percent)

$t \equiv \dfrac{T}{T_c^*(\varepsilon_0)}$ Reduced temperature

with

$$\frac{T_c^*(\varepsilon_0)}{T_c^*(0)} = \left(1 - a\left|\varepsilon_0\right|^{1.7}\right)^{\frac{1}{w}}. \tag{A10.26}$$

Thus, for the moderate strain range ($-0.5\ \% < \varepsilon_0 < +0.4\ \%$), the task of transforming both strain and temperature with Eqs. (10.21) and (10.22) is reduced to evaluating these two transformation constants from the scaling parameters: ν, w, η, s, a^-, a^+, $T_c^*(0)$, and ε_m. Again, the strain parameters are given in Table A10.2a and the temperature parameters are listed for Nb_3Sn just above the table. This leaves ε_m as the one extrinsic parameter that must be determined on a conductor-by-conductor basis from a single $J_c(\varepsilon)$ measurement at any fixed magnetic field and temperature, or it can be estimated from a single $J_c(\varepsilon)$ measurement on a similar conductor.

For transformations where either ε_{01} or ε_{02} fall in the high-compressive-strain range ($\varepsilon_0 < -0.5\ \%$), a more general form must be used for the two transformation constants because of the extrinsic nature of their strain dependence in this regime. The more general parameterization [which replaces Eq. (A10.24)] for the transformation constant β is

$$\beta = \frac{B_{c2}^*(0,\varepsilon_{02})}{B_{c2}^*(0,\varepsilon_{01})}\left(\frac{1-t_2^\nu}{1-t_1^\nu}\right), \tag{A10.27}$$

and the more general parameterization [which replaces Eq. (A10.25)] for the critical-current transformation factor is

$$\beta^{-1}\frac{K(T_2,\varepsilon_{02})}{K(T_1,\varepsilon_{01})} = \frac{g(\varepsilon_{02})}{g(\varepsilon_{01})}\left[\frac{B_{c2}^*(0,\varepsilon_{02})}{B_{c2}^*(0,\varepsilon_{01})}\right]^{-1}\left(\frac{1-t_2^\nu}{1-t_1^\nu}\right)^{\eta-1}, \tag{A10.28}$$

with

$$\frac{T_c^*(\varepsilon_0)}{T_c^*(0)} = \left(\frac{B_{c2}^*(0,\varepsilon_0)}{B_{c2}^*(0,0)}\right)^{\frac{1}{w}}. \tag{A10.29}$$

Any parameterization of $B^*_{c2}(0,\varepsilon_0)$ and $g(\varepsilon_0)$ will work with the general transformation factors given by Eqs. (A10.27)–(A10.29). The extended-range parameterizations discussed in Secs. 10.5.6 and 10.7.3 are suggested as a practical scheme that is easy to use because they preserve the consistency of the intrinsic parameter values a and s for the moderate strain range; that is,

$$\frac{B^*_{c2}(0,\varepsilon_0)}{B^*_{c2}(0,0)} = 1 - a\,|\varepsilon_0|^{1.7} + a_1\,|\varepsilon_0 - \varepsilon_0'|^{a_2}\, I(\varepsilon_0 < \varepsilon_0'), \tag{A10.30}$$

$$\frac{g(\varepsilon_0)}{C} = [1 - a\,|\varepsilon_0|^{1.7}]^s + g_1\,|\varepsilon_0 - \varepsilon_0'|^{g_2}\, I(\varepsilon_0 < \varepsilon_0'). \tag{A10.31}$$

Here, C is the same proportionality constant as in Eq. (A10.18), and the indicator function is defined as

$$I(\varepsilon_0 < \varepsilon_0') \equiv \begin{cases} 1 & \text{if } \varepsilon_0 < \varepsilon_0' \\ 0 & \text{if } \varepsilon_0 > \varepsilon_0' \end{cases}, \tag{A10.32}$$

with $\varepsilon_0' = -0.005$ for Nb_3Sn. [This function is readily programmed in spreadsheet programs with a conditional clause of the form: IF(ε_0<–0.5%, 1 if true, 0 if false).] Again, for the many applications at moderate intrinsic-strain levels, the high-compression term is not needed. This happens seamlessly with Eqs. (A10.30) and (A10.31) because the indicator function automatically drops the extra term for moderate strains, reducing these relations to the simpler power-law expressions.

The simplicity of this transformation procedure becomes readily clear by referring to the example given in Table 10.4 at the end of Sec. 10.7.5. The entire process can be carried out in a few minutes with a spreadsheet program. It is also quite accurate. For example, a relatively large error of 20 % in the temperature parameter η would result in an error in the I_c values of only about 3.5 % when transforming from the canonical temperature of 4.2 K to a difficult-to-measure temperature, such as 5.5 K. Likewise, when transforming from, say, $\varepsilon_0 = -0.3$ % to 0 % in Nb_3Sn conductors, a relatively large error of 10% in the value of the strain sensitivity parameter a would result in an error of less than 0.5% in the transformed B values and negligible error in the transformed I_c values. Again, with this method there is no need to determine the shape of the I_c–B curve, and it is independent of the extrapolation method used to determine B^*_{c2}. The method, given in general form by Eqs. (A10.21) through (A10.23), *relies only on the unified scaling law,* Eq. (10.45), not on the separable parameter set used to illustrate it here. *Thus, it*

would readily work with any other parameterization of the prefactor $K(T,\varepsilon_0)$ *in the unified scaling law, Eq. (10.45).*